NASA CR - 72790
GE - 70 SD 4282

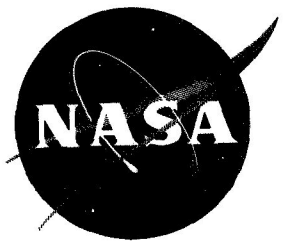

AN EXPERIMENTAL LIQUID METAL SLIP RING TO TRANSFER POWER BETWEEN ROTATING SATELLITE PARTS

by

S. M. Weinberger

GENERAL ELECTRIC COMPANY
SPACE SYSTEMS

Prepared for

NATIONAL AERONAUTICS & SPACE ADMINISTRATION

NASA Lewis Research Center

CONTRACT NAS 3-11538

Robert R. Lovell, Project Manager

NOTICE

This report was prepared as an account of Government-sponsored work. Neither the United States, nor the National Aeronautics and Space Administration (NASA), nor any person acting on behalf of NASA:

A.) Makes any warranty or representation, expressed or implied, with respect to the accuracy, completeness, or usefulness of the information contained in this report, or that the use of any information, apparatus, method, or process disclosed in this report may not infringe privately-owned rights; or

B.) Assumes any liabilities with respect to the use of, or for damages resulting from the use of, any information, apparatus, method, or process disclosed in this report.

As used above, "person acting on behalf of NASA" includes any employee or contractor of NASA, or employee of such contractor, to the extent that such employee or contractor of NASA or employee of such contractor prepares, disseminates, or provides access to any information pursuant to his employment or contract with NASA, or his employment with such contractor.

Requests for copies of this report should be referred to:

National Aeronautics and Space Administration
Scientific and Technical Information Facility
P. O. Box 33
College Park, Md. 20740

NASA CR - 72790
GE - 70 SD 4282

FINAL REPORT

AN EXPERIMENTAL LIQUID METAL SLIP RING TO TRANSFER POWER BETWEEN ROTATING SATELLITE PARTS

by

S. M. Weinberger

GENERAL ELECTRIC COMPANY
SPACE SYSTEMS
Valley Forge Space Center
P. O. Box 8555
Philadelphia, Pa. 19101

Prepared for

NATIONAL AERONAUTICS & SPACE ADMINISTRATION

August 1970

CONTRACT NAS 3-11538

NASA Lewis Research Center

Cleveland, Ohio

Robert R. Lovell, Project Manager
Spacecraft Technology Division

FORWARD

The work described herein was done at the Space Systems Operation, General Electric Company, under NASA Contract NAS 3-11538 with Mr. Robert R. Lovell, Spacecraft Technology Division, NASA Lewis Research Center, as Project Manager.

The author wishes to acknowledge the efforts of Peter Ring, Metallurgist, Space Systems Operation for his contributions to Section 3, Materials Selection.

TABLE OF CONTENTS

TABLE OF CONTENTS (cont'd)

TABLES

FIGURES

FIGURES (Continued)

ABSTRACT

An engineering model liquid metal slip ring was developed to transfer electrical power across a rotating joint in a satellite. The slip ring was operated at 100 amps DC at voltages up to 3000 volts at rotational speeds of 1 revolution per day, in air and vacuum environments. The liquid metal was gallium; the electrode materials were tungsten, tantalum, and molybdenum; and the insulation was Delrin. A contamination of gallium was observed and efforts made to identify it.

1.0 SUMMARY

A program was undertaken to develop an engineering model liquid metal slip ring to transfer electrical power across a rotating joint in a satellite. The program consisted of three major tasks: material selection and experiments, engineering test model design and fabrication, and engineering test model testing and evaluation. During the material selection and experiment phase, candidate liquid metal, electrode and insulation materials were selected and tested. Gallium was selected as the liquid metal, and tungsten, tantalum, molybdenum, and graphite were selected as the electrode materials. Noryl, Teflon, and Delrin were chosen as the insulation materials. Selection was based on the functional requirements of the slip ring, the inherent properties of the materials, their compatibility with each other, and their suitability for ground and space operation.

An experimental program was run to evaluate the materials and their compatibility with each other. Low electrical resistance was achieved by the removal of the electrode surface oxide. There was no gallium attack upon the electrodes as determined by metallographic and spectrographic analyses. The electrical noise was negligible, the capillary retaining force was stable, and the freezing of gallium resulted in no deleterious effects. Delrin and Teflon insulations showed no attack by gallium.

An engineering test model slip ring was designed, fabricated and tested. It was operated at 100 amps DC at voltages up to 3000 volts between rings at rotational speeds of 1 revolution per day in air and vacuum environments. In the engineering test model, the electrodes were fabricated of tungsten, tantalum, and molybdenum and the liquid metal was gallium. A gallium contamination was observed in the slip ring and efforts were made to identify

it by means of spectrographic, x-ray diffraction, and infrared analyses. The tests showed no evidence of electrode material in the gallium. The contamination could not be identified.

2.0 INTRODUCTION

A program was established to develop an experimental liquid metal slip ring to transfer electrical power between rotating satellite parts. The slip ring was to be capable of carrying 100 amps per ring at voltages up to 3000 volts between rings at a nominal rotational speed of one revolution per day and be operational both on the ground and in space. The liquid metal was to be either gallium or alloys of gallium and it was to be retained in the slip ring by capillary forces.

A number of potential problem areas were identified as requiring investigation before the experimental slip ring could be designed. These included:

Reaction of gallium with electrode and insulation material.

Utilization of capillary forces, contact angle, surface tension, and the stability of liquid metal-solid interface.

Other technical areas were identified as requiring investigation included definition of critical design, launch and operational conditions, and the capability to operate in zero gravity and vacuum conditions for five to ten years without degradation of performance.

In order to solve these problems, a program with three major tasks was undertaken. These tasks were:

Task 1. Material Selection and Experiments
Task 2. Engineering Test Model Design and Fabrication
Task 3. Engineering Test Model Testing and Evaluation

Task 1, Material Selection and Experiments, consisted of selecting candidate liquid metal, electrode and insulating materials and testing them to determine their performance characteristics. Task 2, Engineering Test Model Design and Fabrication, was the effort to provide a test bed to verify the slip ring design concepts. Task 3, Engineering Test Model Testing and Evaluation, entailed the test effort performed to determine the operational characteristics and to demonstrate the validity of the liquid metal slip ring design concept. In addition to these tasks, a study was made of the gallium contamination which was observed in the experimental slip ring.

3.0 MATERIAL SELECTION

The first major task in the overall development of the liquid metal slip ring was the selection of the materials that would be used and to define the experimental program that would test the functional characteristics of these materials. There are three major categories of materials involved in the slip ring: the liquid metal, electrode material and insulation. At this point in the program, structural materials, wiring, bearings, etc., were not considered to be critical to the performance of the slip ring. The selection of materials had to be considered not only on the basis of their individual properties but also on their interactions with each other in the final component.

Based on pre-proposal and proposal efforts, it appeared that the selection of materials would start with the identification of the liquid metal to be used and that the primary candidate for this liquid metal would be gallium or alloys of gallium. Gallium is not a widely used material and its characteristics have been studied principally from a scientific point of view rather than as a practical engineering material. This necessitated a thorough understanding of the possible problem areas, a careful selection of the materials that will be used with it, and an experimental evaluation program.

As part of the material selection phase, the critical material areas were identified, parameters of material selection established, a literature search performed, and candidate materials defined.

In the three categories of materials considered, liquid metals, electrodes and insulators, the basic important parameters of these materials were their inherent electrical, physical, chemical and metallurgical properties; their compatiblity with each other and with ground and space operating environments; and their functioning together so as to obtain an optimum liquid metal slip ring.

3.1 GENERAL CONSIDERATIONS OF GALLIUM-ELECTRODE INTERACTIONS

The interactions of gallium and electrode material were extensively examined from chemical and metallurgical points of view based on theoretical considerations. In addition, a comprehensive literature search was made to obtain specific information as well as data concerning the possible reactions between gallium and candidate electrode materials.

Generally, gallium-electrode reactions can occur in a number of forms:

Solution attack - electrode attacked by gallium yielding a liquid phase.

Alloy attack - electrode attacked by gallium yielding solid phases composed of solid solutions and intermetallic compounds.

Intergranular attack - preferential attack occurring at grain boundaries.

Electrical effects - electrolytic transport of electrode material from one electrode to another.

Corrosion - chemical reaction that results in the formation of intermetallic compounds.

Erosion - wearing away of electrode material by relative motion between electrode and gallium.

The solution, alloy, intergranular and electrical forms of attack seemed the most likely to occur and were given the most attention with the greatest emphasis placed on solution and alloy. Electrical effects were considered as potential problems; however, since no information was found in the literature concerning the behavior of gallium in this respect and these effects, if they exist, would show in experimental results.

The gallium-electrode reactions are influenced by two phenomena: the concentration gradient and the thermal gradient. A concentration gradient is established when any reaction products varies spatially between the unreacted electrode material and the unreacted gallium. Thermal gradients which can be caused by a variety of reasons, such as current flow, can cause increased localized reaction rates because of convection effecting the gallium-electrode interface. Concentration and thermal gradient transfer were thought not to be a problem in the systems under consideration, particularly since the attempt is not to limit attack but to eliminate attack.

The basic corrosion phenomena has been well studied and the importance of impurities documented and will not be re-elaborated. The corrosion mechanisms that could occur in this program were greatly simplified by the fact that the specimens as well as the slip ring system were constructed from single metals and tested under static or near-static conditions.

3.1.1 Solution Attack

3.1.1.1 Dissolution of Base Metal

In systems containing a single alloy, the most direct reactions can occur by dissolution of the base metal,(electrode) in the liquid metal environment. The rate determining factor for the transfer of material from the solid to the dissolved state is controlled by the rate at which the solute moves by diffusion through a surface film into the bulk of the fluid. A second mechanism is termed "solution rate limited", which postulates that the diffusion step is slow compared with the initial rate of solution. Unless a passivating film can be developed at the liquid-solid interface (deposition of reaction product films), one can expect a relatively rapid rate of corrosion that is temperature dependent. Factors such as the presence of impurities in the liquid metal, and the formation of compounds with the alloy can have a marked effect on the reaction rate since they provide mechanisms for sustaining the reactions beyond saturation of the liquid metal by the dissolving element. As an example, in alkali metals, the dissolution rate of some metals is known to be dependent upon the oxygen content of the liquid metal.

3.1.1.2 Solution Criteria

Liquid metal theory is at present only poorly understood and attempts to apply conventional solution theory reveal many exceptions to the rule. Hildebrand[1] has attempted to apply internal pressure and potential theory to liquid metal and although some indications of mutual solubility can be obtained, no dependable correlation was produced which would even semi-reliably predict the behavior of one metal dissolved in another, the most useful indication of behavior, see Table 1, is provided by a function termed solubility parameter (δ) derived from the energy of vaporization (E^V), (taken as a measure of internal pressure and closeness of packing), and atomic volume (V) expressed as:

$$\delta = \left(\frac{\Delta E^V}{V} \right)^{1/2}$$

The internal pressure theory appears to break down largely due to the formation of intermediate compounds which indicate a strong interaction between unlike atoms relatable to differences in electro-negativity. Thus, slight differences in solubility parameters should result in high mutual solubility and this can be shown to occur in several instances, but the converse does not hold, many metals with large differences in solubility parameters do form homogeneous liquid phases. So while some indications of behavior can be obtained from thermodynamics, reliable prediction of metal solubility awaits better understanding of liquid metal theory.

Metal	Atomic Radius	Electro-chemical Potential	Valency	Melting Point °C	Crystal Structure	Approximate Liquid Solubility at 80°C (at %) in Gallium	Electro-negativity	Heat of Vaporization kg-cal/g-atom	Solubility Parameters at 25°C $(cal/cm^3)^{\frac{1}{2}}$	Surface Tension dyne/cm (25°C)	Free Energy of Oxide Formation K cal/gram Atom of O_2
Ga	1.41	+0.52	3	29.8	Cubic		1.6	1.34	74	735	Ga_2O_3 - 80
In	1.66	+0.340	3	156	Tetragonal	65%	1.7	0.78	60	630*	In_2O_3 - 73
Sn	1.62	+0.1406	4(2)	231	Tetragonal	25%	1.8	1.72	65	620	SnO_2 - 62
Zn	1.38	+0.7628	2	419	Close packed hexagonal	8%	1.6	1.76	58	822	ZnO - 75
Al	1.43	+1.67	3	660	Face centered cubic	6%	1.5	2.55	86	914	Al_2O_3 - 125
Mg	1.60	+2.37	2	650	Close packed hexagonal	4%	1.2	2.14	50	677	MgO - 135
Ag	1.44	-0.799	1	960	Face centered cubic	4%	1.9	2.70	82	934	Ag_2O - 2
Cd	1.54	+0.4020	2	320	Close packed hexagonal	2%	1.7	1.46	45	606	CdO - 55
Ni	1.24	+0.23	2	1453	Face centered cubic	1%	1.8	4.21	124	1640	NiO - 50
Cu	1.28	-0.522	2	1083	Face centered cubic	1%	1.9	3.11	107	1269	Cu_2O - 35
Au	1.44	-1.42	1	1063	Face centered cubic	1/2%	2.4	3.03	93	1134	Au_2O_3 +39
Be	1.12		2	1277	Close packed hexagonal	(see text)	1.5	2.8	129	1620*	BeO - 137
V	1.34	+0.255	5	1900	Body centered cubic		1.6	4.2	119	1528	V_2O_3 - 93
Fe	1.26	+0.441	3	1536	Body centered cubic	No liquid solubility given 1.2% solid solubility	1.8	3.67	117	1731	Fe_3O_4 - 61
Hf	1.50		4	2222	Close packed hexagonal		1.3	5.2	112	1510*	HfO_2 - 126
Ti	1.47	+1.75	4	1668	Close packed hexagonal		1.5	3.7	94	1208*	TiO - 117
Zr	1.60		4	1852	Close packed hexagonal		1.4	4.0	94	1380*	ZrO_2 - 124
Pt	1.38		4	1769	Body centered cubic		2.2	5.2	121	1820	PtO - 10
Ta	1.46		5	2996	Body centered cubic	0.01% wt. at 450°C solid solubility	1.5	6.8	136	2330*	Ta_2O_5 - 90
Nb	1.46		5	2415	Body centered cubic		1.6	6.4	127	2030*	NbO - 90
Mo	1.39	-0.01	6	2610	Body centered cubic		1.8	6.6	128	2240*	MoO_2 - 60
Re	1.37		7	3180	Close packed hexagonal		1.9	7.9	146	2480*	ReO_2 - 45
W	1.39	-0.485	6	3410	Body centered cubic	0.001-0.008% at 815°C	1.7	8.05	145	2680*	WO_2 - 62
C	0.914		4	3727 (gas)	Hexagonal		2.5				

*Estimated

Elements are ranked where possible in order of decreasing solubility in gallium

TABLE I

METAL PROPERTIES CONSIDERED POTENTIALLY RELEVANT TO ATTACK BY LIQUID GALLIUM

3.1.2 Alloy Attack

3.1.2.1 Alloy Formation

The aforegoing has been primarily concerned with solution attack likely to be one of the most severe corrosion mechanisms in liquid gallium. Formation of solid solutions or direct alloy attack is probably less of a problem, but it is interesting to relate the solid solution to the liquid solution. Hildebrand[1] has attempted to apply liquid solution theory to solid solution and possibly some relationship can be established in the other direction by applying the semi-empirical rules produced by Hume-Rothery. This is valid if we accept the tenet that short range order exists in a liquid and a crystal-like lattice is retained in which rapid thermal motion of the molecules has blurred and distorted the regularity of the crystal lattice.

3.1.2.2 Factors Affecting Alloying and Solid Solution Formation

Based upon the Hume-Rothery rules, there are a number of factors which can effect the solid solution formation of intermetallic compounds:

1. Size Factor

The size factor principle simply states that if the atomic diameters of two metals differ by less than 15 percent, the size factor is favorable and formation of a solid solution is possible in terms of size. In point of fact, this is a basic general rule but problems are encountered when applying it to gallium since interatomic distances in the gallium crystal are of two values because of an orthorhombic crystal structure.

2. Crystal Structure

From the aspects of crystal structure, complete solid solubility never occurs unless both metals have the same crystal structure. However, this factor by no means prevents alloying but does limit the solubility.

3. Electrochemical Series

The greater the separation of two metals in the electrochemical series, the greater is the tendency towards restricted solid solution ranges and the formation of intermetallic compounds.

4. Valency

Relative valency is also very significant. Metals with lower valencies tend to dissolve metals of high valencies. A higher valency metal will generally be a poor solvent for a lower valency metal. Theoretically, the electrode material selected for the slip ring should be a metal with high valency compared to gallium.

5. Melting Point

Solubility is greater in those metals for which the melting point is lower.

3.1.3 Electrode Material Preference

It would seem, therefore, from alloying theory alone, that by selecting a metal with an atomic diameter greater than 3.2A^{o} or less than 2.4A^{o} (that is differing from the lattice parameter of gallium, taken as 2.82A^{o} by more than 15%), a potential widely different from the potential of gallium (+0.52V) and a valency other than three, then this element should

(from solid solution considerations only) be resistant to attack. It is not difficult to test this theory. Table 1 lists a series of metals whose behavior in gallium has been studied. Atomic radius, considered one of the major factors in substitutional alloying does show some slight significance when alloys subject to attack are graded by relative solubility (Table 1). There appears, however, to be no significance whatsoever in atomic radius as applied to the metals resistant to gallium attack; W, Mo, Nb, Zr and Ti all have atomic radii well within the range suitable for alloying. Of course, this poor correlation hardly is surprising, atomic radii and size factor only become important in the precise crystal lattice of a solid solution, liquid solutions with their vague expanded lattice could be expected to accommodate differences in atomic size. Other factors mentioned at the start of this discussion would be expected to hold greater significance. For example, crystal type and interatomic binding forces. In fact, Table 1 does suggest that some basis for selection exists in consideration of crystal lattice, valency and melting point. The closely related heats of vaporization already have been discussed and their importance expressed in liquid solution theory in terms of solubility parameters. Close packed structures, fcc, cph, appear more susceptible to attack than body centered cubic structures. Note: Indium has a distorted face centered tetragonal structure, closely related to the face centered cubic. Higher valency metals are resistant to attack. All parameters interact, of course, but selection of a metal with the preferred parameters should result in an acceptable electrode material. For example, consideration of melting point alone would not indicate that λ iron (that is, fcc stainless steel) was any

less acceptable than α iron (pure iron, bcc low carbon steel, or a ferritic stainless steel) yet considerations of the crystal structure indicate that this is in fact so.

A selection made on the basis of the above factors gives the following materials in order of preference:

Carbon

Tungsten

Rhenium

Molybdenum

Niobium

Tantalum

Vanadium

α Iron

Hafnium

Titanium

Zirconium

Platinum

It should be noted that the materials towards the lower end of the list are given poor ratings in the Liquid Metals Handbook. Unfortunately, the precise conditions of test are not given and have not yet been obtained; of course, these materials are not expected to be as resistant as tungsten or rhenium, nevertheless, appreciable resistance would be expected. Although some conclusions have been reached, the data is largely empirical and exceptions are very prone to occur (consider bcc platinum and vanadium). It is therefore necessary to evaluate existing data on gallium attack and examine corrosion rates cited by other workers in this field.

A quite comprehensive literature survey was made to correlate data on gallium attack. Unfortunately, results are often vague and contradictory, often expressed merely as "poor resistance", "good resistance", etc. In addition, researchers have normally been concerned with gallium at fairly high temperatures of testing. At the comparatively low temperatures we are concerned with, a wide range of materials are probably suitable. However, literature (particularly references 2, 3, 4 and 5) does show graphite, tungsten, tantalum, molybdenum and columbium to be resistant to gallium in the temperature range we are considering.

Evaluation of materials then from both theory, literature and equilibrium diagrams indicate that the following materials would be suitable for the present application:

Prime	Carbon	
	Tungsten	
	Rhenium	Anticipated decreasing resistance to attack.
	Molybdenum	
	Niobium	
	Tantalum	
Secondary	Vanadium	
	α Iron	
	Hafnium	Anticipated decreasing resistance to attack.
	Titanium	
	Zirconium	
	Platinum	

In selecting materials to be tested, it seemed sensible to choose not only materials with optimum potential for gallium resistance, but also some materials apparently less suitable in this category yet advantageous in other ways. For example, fabrication, availability, expense should be considered. Low carbon steel or ferritic stainless steel, for instance, may be adequate at the low temperatures with which we are concerned. The six selected materials based on these criteria would be:

Graphite

Tungsten

Rhenium

Molybdenum

Ferritic iron

Titanium

Note: There are indications in the literature that beryllium would be resistant to gallium. Beryllium from theoretical standpoints does not appear especially promising, but Hansen, equilibrium diagram data, states that "at 600°C, Be dissolves in gallium to the extent of 4 ppm. However, gallium diffuses into the Be to form a reaction zone, probably a protective compound". The final rationale and selection of materials is discussed in Sections 3.2, Liquid Metal, and 3.3, Electrode Material.

3.1.4 Resistance of Metallic Oxide to Gallium Attack

Up to this point, we have considered electrode materials solely as a function of the resistance of the metal itself, another approach is feasible: consideration of the stability of the metal oxide film and its resistance to gallium. A completely new spectra of elements then becomes available. The uncertainty of this method of protection, particularly in a

non-oxygen environment renders this approach questionable. It is perhaps more relevant, at least in the case of corrosion tests to take the negative approach and determine whether non-adherent oxide films are likely to form on the selected electrode materials. Along with the oxide films should be considered other films: carbides, nitrides, sulphides. If we take the most common surface film, oxide, which has been found to be particularly serious in alkali metal systems, then if the film is tenacious, attack is retarded. If, however, the film is removed either by its own lack of adherence or by a fluxing action of the liquid, metal or other oxides, then a continuous attack mechanism exists which would not be indicated by previous crystallographic considerations. The situation in fact becomes somewhat complex, depending on the free energies of formation which show that oxide films cannot be relied on as protective mechanisms, at least from a straightforward consideration of thermodynamics, and oxide stability. Al_2O_3 has a free energy of formation of -125 KCal/gram-atom compared to gallium -80 Kcal/gram-atom, aluminum oxide would therefore be expected to form in preference to Ga_2O_3. Approximate free energies of formation at 25^oC for the most stable oxides of certain metals are shown in Table 1.

3.1.5 Consideration of Wetting Characteristics

All solid-liquid systems showing either intermetallic compound formation or solubility of the liquid in the solid show wetting, i.e., low contact angle tending to zero. Liquid-solid metal systems which are essentially non-reactive at the temperature of testing do not wet, i.e., the contact angle approaches 180^o. Systems showing restricted solubility of the solid in the liquid fall in between the above categories some limited wetting takes place, with a contact angle $> 0^o < 180^o$.

It is clear from this, that formation of a transition phase either solid solution or intermetallic reduces solid-liquid interfacial tension, in other words, "corrosion" is accompanied by wetting. Unfortunately, this cannot be used as a simple guideline in the choice of materials. A metal which is wetted by gallium is not necessarily corroded by it. However, it seems reasonable to assume that in the absence of wetting, corrosion will not take place since oxide-free gallium does not wet any surface until the onset of alloying or chemical reaction.

This approach is valid not only for general solution or corrosion but also intergranular penetration since a low-interfacial tension facilitates the spread of the liquid metal around the solid metal grains.

In the choice of electrode material, therefore, it is reasonable to select a metal which is not wetted by gallium, i.e., has a high contact angle where contact angle is given by:

$$\theta = \cos^{-1} \left(\frac{\sigma SG - \sigma LS}{\sigma LG} \right)$$

θ = contact angle

σSG = solid-gas interfacial tension

σSL = solid-liquid interfacial tension

σLG = liquid-gas interfacial tension

Unfortunately, values for the magnitude of the above forces for liquid gallium/solid metal/gas systems are not readily available to enable precise calculation of contact angles* but an indication of the

---

* Recent work by A. V. Grosse (J. Inorg Nucl Chem. 1962 Vol. 24) indicates that values for surface tension can be obtained by a relationship between surface tension (σ), surface energy (σA) of a liquid metal, and its critical temperature (Tc) and atomic volume (V_A). The relationship is expressed as:

$$\sigma A^{\circ} = \sigma : V_A \, 2/3 = 0.64 \text{ (ergs/gramme atom}^{2/3}\text{/Tc (in}^{\circ}\text{K)}$$

contact angle in several systems can be obtained since from the equation above, it is seen that for a given solid, a high contact angle is favored by a high solid-liquid interfacial tension (σLS) and by a high liquid/gas tension (σLG).

Values for σLG are available from the literature and σLS values have been found to be of the same order of magnitude to liquid metal gas tension (Ref. 14, p. 401). Both these values increase progressively in relation to increase in melting point (Ref. 14, p. 403); however, the value σLS above refers to a solid metal in contact with its own liquid metal. The interfacial tension between a solid and a liquid can be considered as a measure of the thermodynamic disparity between the two phases. The smaller this difference, the lower the magnitude of the interfacial tension. In other words, the interfacial tension will be a minimum for a solid metal in contact with its own liquid, similarly, in metals with low mutual solubility, the interfacial energy will tend towards maximum.

Thus, we have a further indication that high melting point metals are preferable in the selection of electrode materials. It must be admitted that up to this time, the contribution of affect of interfacial chemical reactions, adsorbed gases and film formation have been ignored. It is very possible in this type of work to obtain practically a value for contact angle which in fact represents a value for the liquid metal-oxide, potentially far different from the liquid metal-solid metal contact angle.

There are two considerations here: in vacuum, where the slip ring assembly will be employed, an oxide film on the electrode material may well be removed either by abrasion, heating in a controlled atmosphere, or in the case of adsorbed gases, by outgassing. In the absence of oxygen, replenishment cannot take place, wetting may then occur. However, in such circumstances removal of the gallium oxide film is also likely and as was pointed out previously, in the absence of the gallium oxide, the solid metal is not wetted unless some form of alloying occurs.

It is obviously preferable, however, to evaluate a system on the basis of liquid metal-solid metal interfacial tension excluding all oxides, since this is the more stable state for our application.

The affect of interfacial reactions has another interesting facet which can be discussed only briefly here. We have established that from the aspect of corrosion, non-wetting is preferable. Should it be discovered, however, that wetting is advantageous for another reason, e.g., interface resistivity, then it is probable that a small percentage addition of another element to the gallium would produce a transition zone and facilitate wetting. For example, Kurkjian and Kingery (1955) showed that small additions of chromium and titanium to a liquid nickel solid Al_2O_3 system significantly lowered the interfacial tension even though chromium and nickel have higher surface tensions. It is thought that this decrease in tension is the result of solute atom (M) transfer from the bulk of the liquid to the interface with the formation of M-O bonds.

$$xM + yO = MxOy - \Delta Pmo$$

and

$$-\Delta Fmo = RT \ln K$$

K being equal to $\frac{MxOy}{(M)^x (O)^y}$

The free energy change for this chemisorption being directly related to the standard free energies for formation of the oxides. Materials forming oxides more stable than the solvent (in the case of nickel) are adsorbed at the interface and lower the tension. Of particular interest in this respect is the work performed by A. J. Neval, General Electric (Ref. 2), on mercury where addition of titanium and magnesium resulted in greatly reduced rates of attack even on low carbon steel.

3.2 LIQUID METAL

The primary candidate liquid metal was pure gallium because of its low vapor pressure, approximately 10^{-36} mmHg, and its low melting temperature, 29.8°C. Mercury, which is a more common material than gallium and less costly, is unsatisfactory because of its higher vapor pressure, 10^{-3} mmHg, which would result in excessive evaporation in a space environment of the magnitude of 1000 grams per square centimeter of exposed surface per year.

Consideration was given to the use of alloys of gallium, such as gallium-indium, gallium-indium-tin, and gallium-lead-bismuth, which have lower melting temperatures than pure gallium. However, these alloys are much more complex metallurgically and did not present any apparent advantage over gallium.

Gallium is available in varying degrees of purity ranging from 99.9% to 99.9999% pure. Because of the relatively small price differential and the advantages of having the highest purity possible, the 99.9999%, "Semiconductor Grade" was used. The data in Table 2 was given by Alcoa for the impurity content of this grade of gallium. Table 3 lists the general physical properties of gallium with mercury as a comparison.

TABLE 2.

IMPURITIES IN 99.9999% PURE GALLIUM

Impurity	Maximum Amount (ppm, by spectrographic methods)
Silver	.01
Aluminum	.3
Calcium	.3
Cadmium	.3
Chromium	(5)
Copper	.03
Iron	.1
Mercury	.3
Magnesium	.003 (estimated)
Manganese	.03
Molybdenum	(.5)
Nickel	(3.0)
Lead	.3
Silicon	.1
Tin	.3
Titanium	(3.0)
Vanadium	(.5)
Zinc	(1.0)
Sodium	.03

Values in parentheses based on tests run in 1959; other values based on newer test techniques.

TABLE 3.

PHYSICAL PROPERTIES OF GALLIUM & MERCURY

	Gallium			Mercury
Atomic number	31			80
Atomic weight	69.7			200.6
Melting point	29.8°C (85.6°F)			-38.9°C
Boiling point	2403°C			357°C
Specific gravity (g/ml)				
Solid	5.904 (29.6°C)			
Liquid	6.095 (29.8°C)			13.6
	5.095 (301°C)			
Expansion of solidification	3.2%			
Volume coefficient of thermal expansion				
Solid (0 to 30°C)	5.8×10^{-5}			
Liquid (100°C)	12.0×10^{-5}			
Vapor pressure (mmHg)				
30°C	$\approx 10^{-36}$			$\approx 10^{-3}$
600°C	4.4×10^{-9}			
800°C	5.9×10^{-6}			
Viscosity (centipoises)	1.6 (97.7°C)			1.5
Surface tension (dynes/cm)	735			470
Volume resistivity (microhms-cm)				
Liquid	25.2 (0°C) 25.6 (20°C) 26.0 (40°C)			94.1 (0°C)
Solid	C-axis	A-axis	B-axis	
0°C	48.0	15.4	7.2	
29.7°C	54.3	17.4	8.1	
Crystal structure	Orthohombic			
Specific heat (cal/g°C)				
0 to 24°C (solid)	0.089			
12.5 to 200°C (liquid)	0.095			
Heat of fusion (cal/g)	19.2			
Gallium purity available	99.9 to 99.9999%			
Toxicity	Nontoxic			

The major disadvantage of gallium is that it is a relatively reactive material, especially at high (several hundred degrees centigrade) temperatures. This means that care must be exercised in selecting the materials that will be in contact with it. Fortunately, the slip ring will operate at lower temperatures where the rate of reaction is substantially less and can be accommodated. Two basic problems result from gallium attack: the first is the destruction of the material from gross attack, and the second, more important, even slight amounts of dissolved foreign material in gallium can result in a substantial increase in the melting temperature. This has serious implications since a 5-year life is desired on the slip rings and the increase in melting temperature can cause the slip ring to freeze up, lock, and prevent rotation.

3.3 ELECTRODE MATERIAL

The selection of electrode material for the liquid metal slip ring is very critical since the electrodes perform two basic functions; containing the gallium and providing a path for current flow. The electrode material must be chemically and metallurgically compatible with gallium and must have a low electrical interface resistance with gallium. The wetting characteristics of the electrode with gallium must not change with time since this will effect the retaining forces of the gallium.

There are two categories of electrode materials, non-reactive and reactive with gallium. Non-reactive materials do not readily react with gallium, have a high electrical interface resistance, and are not wet by gallium. By contrast, reactive materials have a low electrical interface resistance and are wetted by gallium. Typical non-reactive materials are

graphite, carbon, and the refractory metals such as tungsten, tantalum, and molybdenum; typical reactive materials are copper, nickel and titanium.

It should be noted that the non-wetting and high interface resistance characteristics of the non-reactive materials of the refractory metals group is dependent upon the surface oxide which is present on the metal. When this oxide is removed from an area, the material becomes wetted in this area and the electrical interface resistance becomes lower by an order of magnitude or more.

In an electrode-gallium system, there are actually two possible conditions for both the electrode and gallium interface surfaces; these are: electrode surfaces oxidized and non-oxidized, and gallium surfaces oxidized and non-oxidized. Clean surfaces of both refractory metals and gallium tend to become oxidized very rapidly unless they are maintained in an inert environment. It may be difficult to ascertain the exact surface conditions which exist unless positive measures are undertaken that will assure that the desired surface conditions exist.

In the selection of electrode material, there are other criteria to be considered; these include such factors as fabrication, cost, and availability. The refractory metals are comparatively hard to fabricate and tend to be expensive. They are, however, relatively easy to procure. Rhenium, which ranks high in its resistance to gallium attack, is quite expensive and available in only small size pieces.

During the material selection phase, the General Electric Company was directed to limit its efforts to the investigation of the non-wetting electrode materials. Based on such factors as compatibility

with gallium, availability, cost and adaptability to the design and fabrication of an engineering test model slip ring, the following electrode materials were therefore selected:

Graphite

Tungsten

Molybdenum

Niobium

Tantalum

Beryllium

Vendors were contacted to determine the characteristics, size, cost and availability of the various materials selected. On the basis of this, specific vendors and materials were chosen, these are enumerated in Table 4.

3.4 INSULATION

The use of dielectric materials is required to contain the gallium in both solid and liquid form and to provide electrical insulation between electrodes. The material must operate in a vacuum at 800C and must withstand non-operating temperature excursions from -50°C to 120°C. It must withstand long-term dielectric stresses of from 30 to 3000 volts at 80°C. It should not be wetted by (have a small contact angle in contact with) the liquid gallium.

A listing of pertinent properties of various candidate insulating materials is given in Table 5. If these materials are ranked in order of (1) superior electrical properties, (2) superior mechanical properties, (3) vacuum weight loss, and (4) thermal stability, (5) manufactureability, (6) availability, the following list could be established:

TABLE 4.

MATERIAL SELECTION

Material	Vendor	Designation and Nominal Composition
Graphite	Poco Graphite, Garland, Texas	Grade - AXF 5Q Total Impurity - 5ppm Iron, Silicon, Aluminum Magnesium
Tungsten	General Electric Co. Cleveland, Ohio	GE-15, 99.95% Pure, Annealed Impurities - ppm Al-< 6, Cr-4, Mn< 6, Zr< 3 Ca-< 3, Ni-10, Mg< 3, Interstial Si-< 7, Cu-5, Sn< 6, C< 10 Mo-40, Na-4, Pb< 6, O-15 Fe-20, K-3, Co< 3, H-1 Ti< 6, N-1
Molybdenum	General Electric Co. Cleveland, Ohio	GE-100, 99.95% Pure, Annealed Impurities - ppm Al-10, Ni-10, Mn-10, Zr-< 10 Ca-30, Cu-12, Mg-< 10, Interstial Si-17, W-100, Sn-10, C-< 10 Fe-40, Na-8, Pb-< 10, O-20 Cr-10, K-3, Co-< 8, H-2 Ti-< 10, N-5
Niobium	Kawecki-Berylco New York, N.Y.	99.9% Pure, Metallurgical Grade Impurities - % Ta - .05, Zr - .001, C < .0025 Si - .001, Mo - .001, H < .001 Fe - .003, W < .01, N < .002 Ti - < .001, B < .001, O < .01
Tantalum	Kawecki-Berylco New York, N.Y.	99.9% Pure, Metallurgical Grade Impurities - % Cb - .006, W - .0025, H - .0002 Si - .003, Zr - .0005, N - .0025 Fe - .002, Mo - .005 Ti - .001, C - .0025
Beryllium	Kawecki-Berylco New York, N.Y.	Grade HP 20 Composition % Be - 98.0, Si - 0.08, Mg - .08 Al - 0.15, BeO - 2, Others - .04 Fe - 0.18, C - 0.15

TABLE 5.

PROPERTY COMPARISON CHART FOR CANDIDATE SLIP RING INSULATING MATERIALS

Property	Units	ASTM Test Method	Temp. °C	LEXAN	TEFLON 1	Zytel 101		Zytel 31		PPO	Delrin	NORYL	TEFLON 15% Glass	TEFLON FEP
						Dry	Equil. at 50% RH	Dry	Equil. at 50% RH					
ELECTRICAL:		D149-61	-51											
		D149-61	25	700	600	620	620	620	620		650	1100		600
Dielectric Strength	Volts/mil	D149-61	80						356					
		D149-61	120						196					
Volume Resistivity	Ohm-Cm	D257-61	-51	10^{17}	10^{18}		10^{15}		10^{15}					10^{17}
		D257-61	25	$2.1x10^{16}$	↕	$9x10^{14}$	$9x10^{14}$		$7x10^{14}$	10^{17}	10^{15}	$1x10^{16}$	10^{13}	↕
		D257-61	80	$2.8x10^{15}$			$1x10^{11}$		$8x10^{10}$			$2x10^{15}$		
		D257-61	120	$2.7x10^{14}$	10^{18}		$3x10^{8}$		$2x10^{8}$					10^{17}
Surface Resistivity	Ohms/Sq.cm^2	D257-61	-51		10^{16}									10^{16}
		D257-61	25		↕						10^{15}	$1x10^{17}$	10^{18}	↕
		D257-61	80									$3x10^{16}$		
		D257-61	120		10^{16}									10^{16}
MECHANICAL:														
Tensile Ultimate	psi	D638	25	9500	2500-3500	11800	11200	8500	7100		10000		2800-3600	3000
Tensile Yield	psi	D638	25	8500		11800	8500	8500	7100	10500		9600		1700
Tensile @ Prop Limit	psi	D638	25	3500										
Tensile Modulus	psi	D882-61T	-51		94000	470000	500000	320000	370000	410000				94000
		D882-61T	25	345000	59000	410000	205000	280000	160000	390000	520000	355000		63000
		D882-61T	80	304000		140000	80000	70000	70000	380000	240000	290000		
		D882-61T	120	300000	13400	60000	60000	50000	60000	350000	100000			10800
Elongation	%	D638	25	110	350	60	300	85	220	25	25	20	325	300
PHYSICAL:														
Density	gm/cl	D792		1.20	2.1-2.3	1.14		1.08		1.06	1.42	1.06	2.22	2.15
Coeff. Therm. Exp.	in/in/°F	D696			$7.5x10^{-5}$	$5x10^{-5}$		$6x10^{-5}$		$2.9x10^{-5}$	$5.5x10^{-5}$	$4.1x10^{-5}$	$8.4x10^{-5}$	$9.0x10^{-5}$
Coeff. Moist. Exp.	in/in-%H_2O			0.0015	0	0.0025		0.0020		0	0.004			0
Vacuum Wt. Loss	Total/cond. Wt % in 24 hrs @ 10^{-6} torr		125	0.06/0.02	0.10/0.03		3.58/0.21		1.85/ 0.42	0.09/ 0.02	0.56/ 0.06			0.02/ 0.01
Gallium Wettability					Does not wet		Wets		Wets	Wets		Wets		Wets

Order of Preference	Material
1	LEXAN Polycarbonate
2	NORYL Mod. Polyphenylene Oxide
3	Zytel 101 Polyamide (Nylon 66)
4	Teflon 1 Polytetrafluoroethylene
5	Delrin 150 Polyacetal
6	TEFLON FEP
7	PPO Polyphenylene Oxide
8	Zytel 31 Polyamide (Nylon 610)

If gallium non-wettability is an added requirement, Teflon 1 is the only candidate insulating material. This is based on experiments with sheets of these plastics. The experiment, which was done on a clean bench, consisted of placing droplets of gallium on the solvent (ethanol) cleaned surface of the plastics and visually observing the wetting action. A slight degree of adherence was observed at room temperature on those plastics that are considered to be wettable by the gallium. This was evidenced by a momentary retention of portions of the liquid ball at discrete locations on the plastic surface as the drop was "rolled" over the surface with a glass eyedropper. The plastics (with the exception of Teflon TFE) were wetted when the end of the eyedropper was immersed in the droplet to the plastic surface and then rubbed on the plastic. If gallium wets the plastic, it could conceivably migrate on the plastic surface affecting the surface resistivity and the electric breakdown voltage. These effects should be established by test. It is noted that these results conflict with Quinlan and Vroman (TIS #DF 62SL103, "Current Collectors - Liquid Metals") who state that Nylon is not wetted in gallium. The discrepancy might be accounted for by the rubbing action at the immersed surface which Quinlan did not do.

3.5 GALLIUM-ELECTRODE TEST CONSIDERATIONS

3.5.1 Gallium-Electrode Corrosion Testing

A study was made to define the testing procedure that would be followed to determine the characteristics of gallium and electrode materials. This procedure and the background philosophy is as follows:

Materials will be selected. Specimens will be cut from sheet or bar stock, depending on availability; (all specimens of all materials shall have been formed in the same manner, i.e., rolled, drawn, or extruded) at this time,sheet appears preferable since the actual slip ring prototype will probably employ sheet. If sheet is used rolling directions will be the same for all specimens.

Tentative Specimen Size - 3/4" x 3/4" x 1/16"

Specimen size is very largely dictated by metallographic preparation requirements which conflict with weighing requirements, that is, appreciable volume but small surface area for a metallographic specimen and large surface area to volume ratio for weighings.

Identification - All specimens will be lettered and numbered using a "vibratool", such as tungsten - W_1, W_2, W_3 and this identification preserved throughout.

Annealing - All specimens will be annealed. The purpose of annealing is two-fold:

(1) All specimens will after annealing be as near as possible in the same conditions irrespective of slight variations in manufacturing procedures.

(2) Within the limits of this project's budget, stress corrosion tests, unfortunately, cannot be performed. Therefore, stress affects will be avoided both in experimental cells and in the prototype slip ring. Note: All metal components of the slip ring must be annealed after any forming or machining operation.

Surface Preparation - Specimens will be mounted in epoxy resin in the conventional metallographic manner and ground on 120, 220 grit paper. Half the number will then be further ground on 320, 400 grit paper and finally polished. Stress induced during each step in this procedure is minimal and removed by the succeeding step.

Polishing will be mechanical 6 micron diamond or alumina.

Electrochemical methods have been considered but are thought to introduce too many variables.

Mount Removal - The mounting plastic will be removed and the electrodes cleaned in acetone.

Weighing - After cleaning specimens will be weighed on a Mettler semimicro balance accurate to $\pm$ 0.3 mgs.

Cell Setup - The electrodes will be arranged as shown in Figure 1. It seems reasonable to array several cells representing similar conditions in one assembly.

An individual cell will consist of two identical plates of the electrode metal (3/4" x 3/4" x 1/16") clamped together with a 0.050" thick insulating material as separator. Current will be introduced via the clamps as shown in Figure 1. Voltage drop across the cell will be measured through a separate set of clamps to avoid erroneous readings. The insulating material will be cut in the form of a square U, the separation between the

TEST ARRANGEMENT
SIX SAMPLE PACKAGE

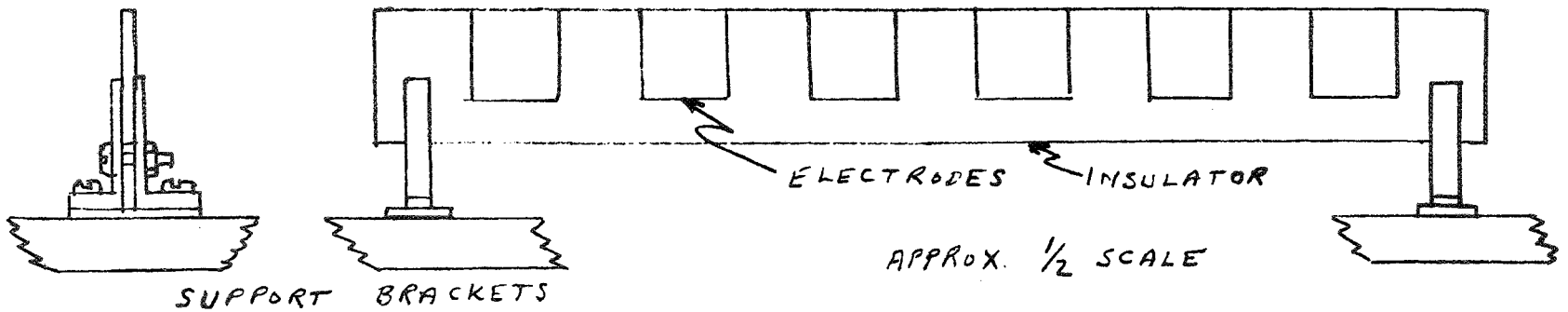

CLAMPING BRACKETS AND ELECTRICAL WIRING SHOWN BELOW

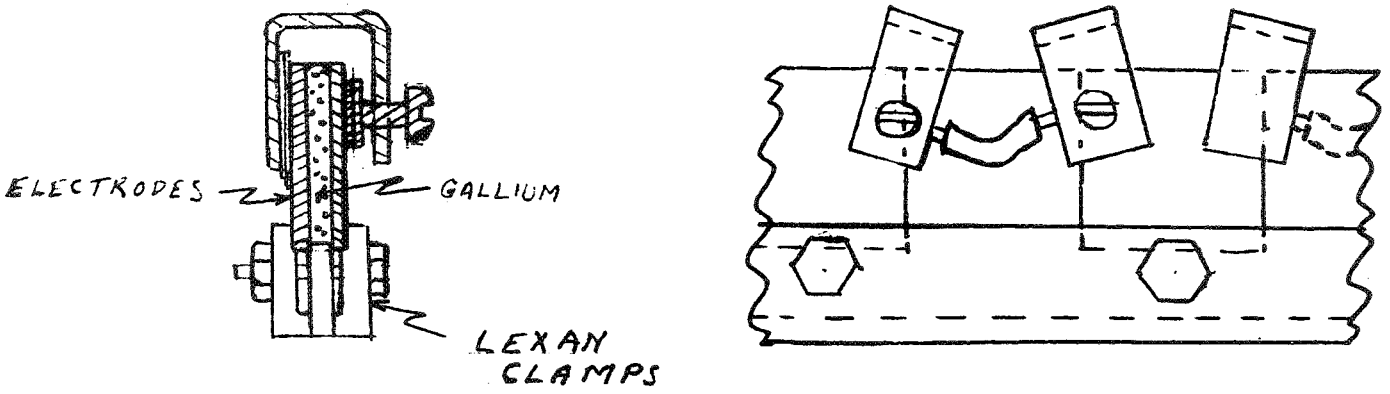

FIGURE 1

7-21-69

two plates. Teflon being the first choice insulator. Clamping of the plates to the Teflon prevents gallium leakage, since the electrodes have flat, ground surfaces.

Process - Disconnect current supply, extract gallium if liquid by pipette and submit for analysis. If solid, it will have to peeled off. Disassemble. Treat each cell individually as follows: Remove adhering gallium. This is a relatively unknown area. In some cases, it is hoped gallium will not adhere at all, in others blowing with inert gas under pressure will, it is hoped, remove loosely adherent gallium. Strongly adherent gallium, i.e., an alloy layer, will not be removed until after the first weighing. Then by peeling or by dissolution in KoH or, if necessary, by raising the temperature and removing with a soft cloth. The electrode should then be reweighed.

Visual & Metallographic Examination - All specimens low power (30X) examination. Highly polished specimens (200X) and greater. All specimens will be photographed. Items of special interest, e.g., localized attack, intergranular corrosion, etc., will be photographed at various magnifications.

Sectioning and Examination - All specimens from the maximum exposure series will in addition to the above be sectioned and examined microscopically. Section location and method will be determined by the results of the exposued surface microscopical examination.

Potential Problem Areas

(1) Weighings - In view of the requirement to detect very low corrosion rates, hence over a three of four month period very small weight changes, the specimen area is critical; ideally specimens should have as large a surface area to volume ratio as possible. However, this is in contradiction to the requirements

for metallography. At the present time a compromise is being made using specimens 1/16" thick, that is, thicker than optimum for weighing purposes but thinner than optimum for metallography.

(2) Gallium removal from electrodes without causing erroneous weight change. This area has already been discussed and methods for gallium removal described. However, it still remains a potential source of trouble.

(3) Preparation of refractory metal specimens.

3.5.2 Gallium Liquid Metal Corrosion Tests

Corrosion or attack by liquid metals can involve any of the following reactions:

(1) Dissolutive Corrosion

(a.) Dissolution of solid metal by liquid metal.

(b.) Alloying of liquid metal with solid metal (includes diffusion and formation of intermetallics).

(c.) Mass transfer (ion).

(d.) Temperature gradient mass transfer.

(2) Interstitial Alloying

(a.) Liquid metal impurities.

(b.) Solid metal impurities*.

(3) Stress Corrosion

From the above reactions, it can be seen that liquid metal attack involves more than simple alloying; however, alloying is certainly a large part of the reaction and a consideration of the parameters relative to alloying is important.

---

* Presence of O, N or C greatly increase attack by molten Li.

1. Substitutional Alloying

Necessary conditions

a.) Atomic radii should not differ by greater than 15%.

b.) Metals should have similar crystal structures.

c.) Metals should have similar low melting points.

2. Interstitial Alloying

The formation of a solid solution takes place among large atomic radii transition metals when the ratio of the interstitial atom to that of the solvent is less than 0.59.

None of the above parameters take into consideration the affect of surface film which may, at the temperatures we are considering, be a prime protective mechanism on one hand; yet, a serious impediment to current flow on the other.

Corrosion Tests

The corrosion test results will be influenced by the following:

1. Chemical composition - gallium and electrodes.
2. Specimen size and shape.
3. Fabrication and metal history.
4. Surface treatment and finish.
5. Number of specimens tested.
6. Duration.

In addition, other parameters will be introduced.

1. Current density.
2. Polarity
3. Temperature.

Consideration of the Possible Types of Attack

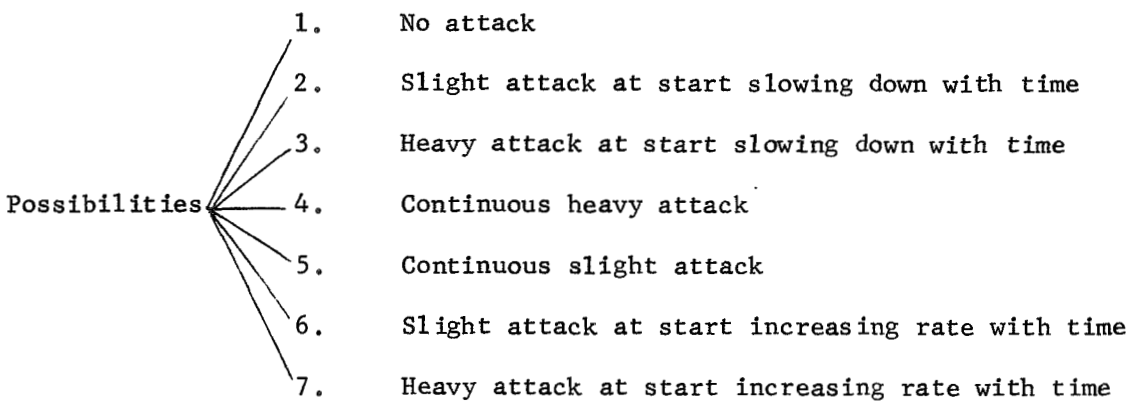

Appearance of Attack

Attack may be manifested by:

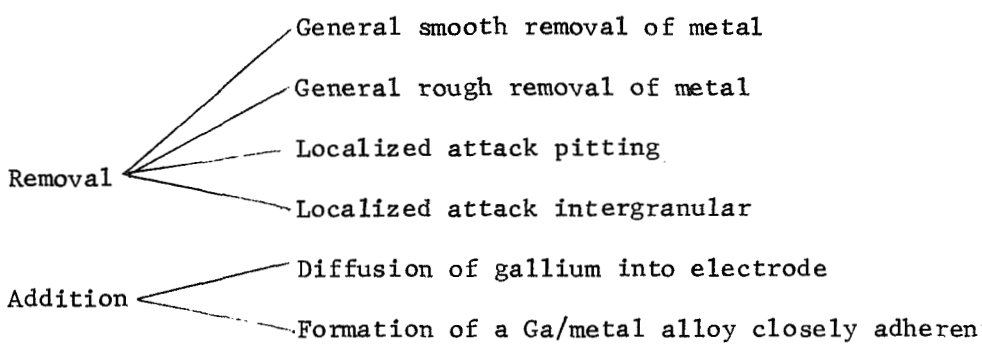

From observation of the previous possibilities, it is obvious that several methods of attack detection are necessary and complementary. That is weighings, metallographic examination, visual examination, and analysis. One method alone is not sufficient. For example, analysis at intervals during test, while at first sight ideal, would in fact give no information concerning buildup of alloy films at the liquid metal/electrode surface. It is also clear that in view of the likelihood of change in attack rate, a minimum of five weighings are necessary to obtain a clear picture of electrode metal behavior. Points requiring further clarification are the terms "slight" and "heavy" attack for while it is conceivable that

an electrode could happily survive a rate of attack up to two mils/year, the liquid alloy could not. The quantities of liquid gallium to be employed are small and would soon become saturated with the electrode metal resulting in a corresponding increase in fusion point and possibly solidification of the alloy. In fact, it is considered that an attack rate of 0.00005 in/year could be disastrous over a period of five years.

Corrosion Cell Concepts

Basically an individual corrosion cell will consist of two identical strips of metal exposed to liquid gallium. Electrode separation should be as close as possible to 0.050" with little excess gallium round the back sides of the plates. This is to ensure a reasonable correlation with actual slip ring conditions. Several concepts have been considered, each having various advantages but when the essential requirements of the cell are considered, one of the simplest cell designs appears most suitable.

Cell Requirements

1. Simple assembly and disassembly.
2. Open to atmosphere.
3. Size and shape chosen to employ minimum quantity of gallium.
4. Well-defined limits to the area of electrode exposed to gallium.
5. As little interference as possible by liquid metal container.

4.0 EXPERIMENTS

Experiments were run to determine the characteristics of gallium-electrode systems. These experiments were run for various conditions of electrode material, electrode surface finish, current, temperature, and time periods under both air and vacuum conditions. Some of the parameters

which were investigated included electrical, metallurgical and chemical characteristics of the gallium-electrode system. These tests have been grouped as short-term experiments and long-term experiments. In addition, miscellaneous tests were run. These were contact angle tests, freezing, noise and oxide stability investigations.

The test vehicle for the short-term and long-term experiments was the test cell. The basic test cell consisted of two electrodes separated by gallium; the electrodes consisting of different materials which had been selected under the first phase of this task. In order to better determine the effects of the gallium upon the electrode material, electrodes of two surface finishes were used, 8 and 32 microinches. The electrodes were approximately 3/4" x 3/4" x .06" thick and were separated by approximately .04" of gallium. In order to be able to attain accurate electrode weight changes, no mechanical connections were made to the electrodes. Electrical connections were made to the electrodes through copper plates placed in back of, and in contact with, the electrodes. The mechanical pressure between the copper back-up plates and the electrodes is not critical as long as there is electrical conductivity between the back-up plates and the electrodes. This is easily achieved because of the asperities on both the electrode and copper surfaces causing high localized pressures and good electrical contact. There were 13 test racks. Each test rack consisted of 12 cells and each test cell had thermocouple leads and voltage leads attached (see Figure 2). The cell resistance was determined by measuring the voltage drop from electrode to electrode with a known current flowing.

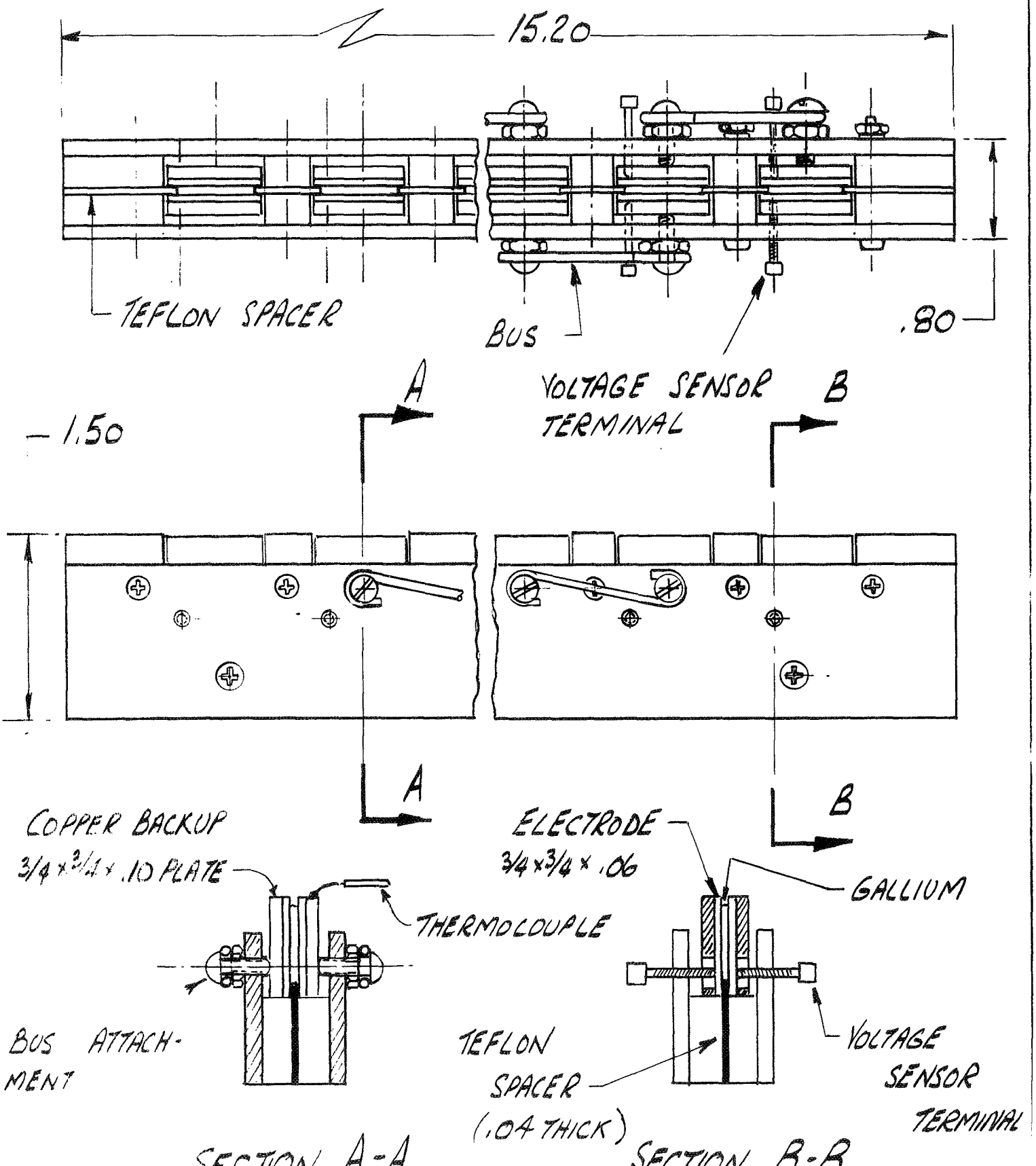

TEST RACK

FIGURE 2

The voltage drop was measured with a six-place DC digital voltmeter and current was measured with a precision laboratory DC ammeter having an accuracy of .05%. The DC current was supplied by a laboratory power supply.

The experiments consisted of setting up test cells in racks and running them for varying periods of time under varying conditions of current at ambient temperatures.

4.1 SHORT-TERM EXPERIMENTS

4.1.1 Electrical Tests

When the electrodes were put under test, two phenomena were noted: first, the electrical resistance, electrode-to-electrode, was higher than anticipated based upon on pre-proposal investigations; and second, the electrical resistance was not constant. This variable resistance took two forms. There was a short-term variation and long-term variation. The short-term variations were rather abrupt changes in resistance that took place over a period of minutes to hours and appeared as an abrupt change followed by another change bringing the resistance back to close to its original value. The other resistance change was a long-term slow increase in resistance.

These effects were attributed to the oxide film that is inherent on the surface of the refractory metals. This oxide is a thin, high resistivity layer which forms almost instantly when the pure metal is exposed to air. This theory was strengthened by the observation that the resistance was a function of current magnitude and polarity. It was then decided to break down the oxide electrically by fritting. This method consisted of applying a voltage across the electrode that will result in a voltage gradient of approximately 10^6 volts/cm. Since the oxide film thickness is of the order of 10^{-6} cm, the voltage required to produce this gradient

is small, of the order of magnitude of 1 volt. The results of fritting tests on tantalum and tungsten electrodes with surface oxides are shown in Figure 3 and cross-plotted in Figures 4 and 5. As the voltage was increased, the current initially increased proportionately, indicating constant resistance. At approximately 0.5 volts on the tantalum electrodes and 0.1 volts on the tungsten, an increase in voltage was accompanied by a decrease in resistance. This decrease in resistance continued until the limit of the power supply being used, 100 amps, was reached, when the test was stopped. A rerun of this test showed that the electrode resistance was constant at all currents up to 100 amps; the magnitude of the resistance at all currents being that of the 100 amp magnitude. It should be noted that although the initial resistance of the tantalum and tungsten electrodes differed by an order of magnitude, the electrode resistance after the application of 100 amps was almost the same. An explanation of these results is that the oxide film on the electrodes remains intact until the critical fritting voltage gradient is attained. When this happens, the oxide film is punctured through, reducing the resistance. Further increases in current enlarges the "hole" in the film, causing further reductions in resistance. The fritting procedure was successful in that it reduced the resistance by an order of magnitude and demonstrated that if the oxide layer were removed, there would be a substantial reduction in resistance achieved.

Figure 6 illustrates assembled test cells in partially assembled and wired test racks. Figure 7 shows test racks undergoing preliminary air tests on a laminar flow bench with power supply and electrical monitoring equipment. The test equipment and power supply are further illustrated in Fig. 8. The automatic data acquisition system can be seen in Fig. 9.

VOLTAGE - CURRENT CHARACTERISTICS

TUNGSTEN + TANTALUM ELECTRODES WITH SURFACE OXIDE

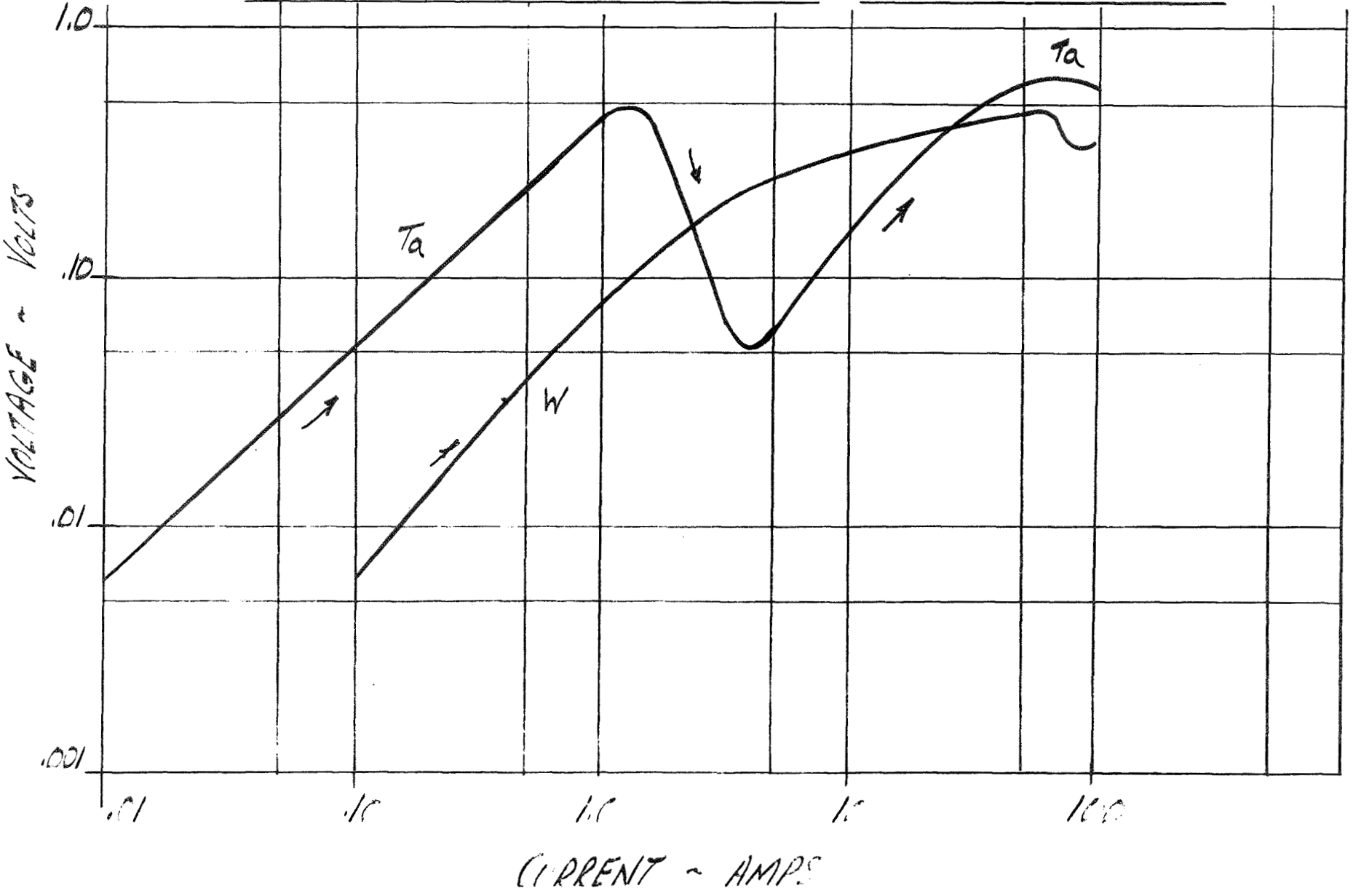

FIGURE 3

VOLTAGE ~ RESISTANCE CHARACTERISTICS

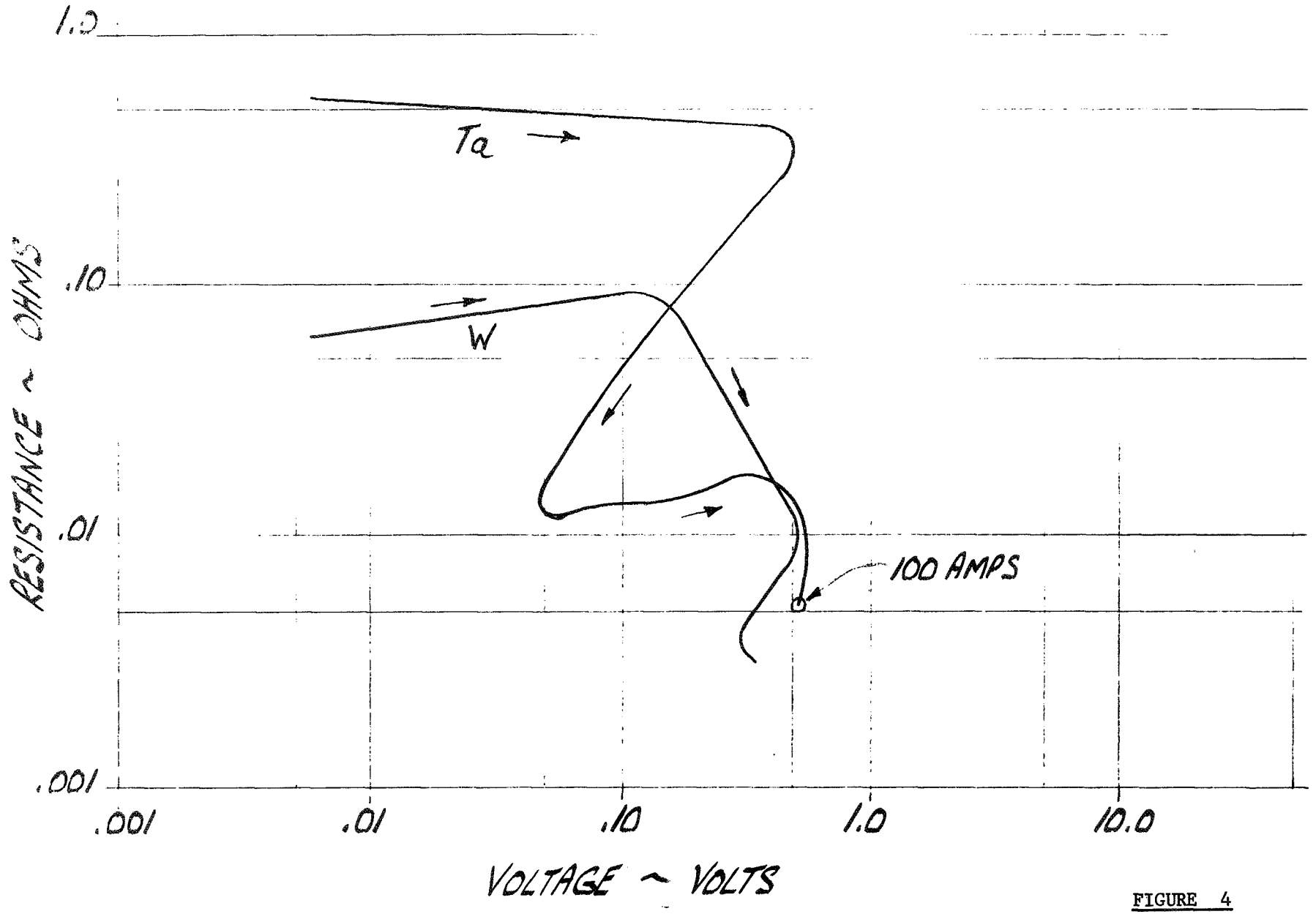

FIGURE 4

CURRENT ~ RESISTANCE CHARACTERISTICS

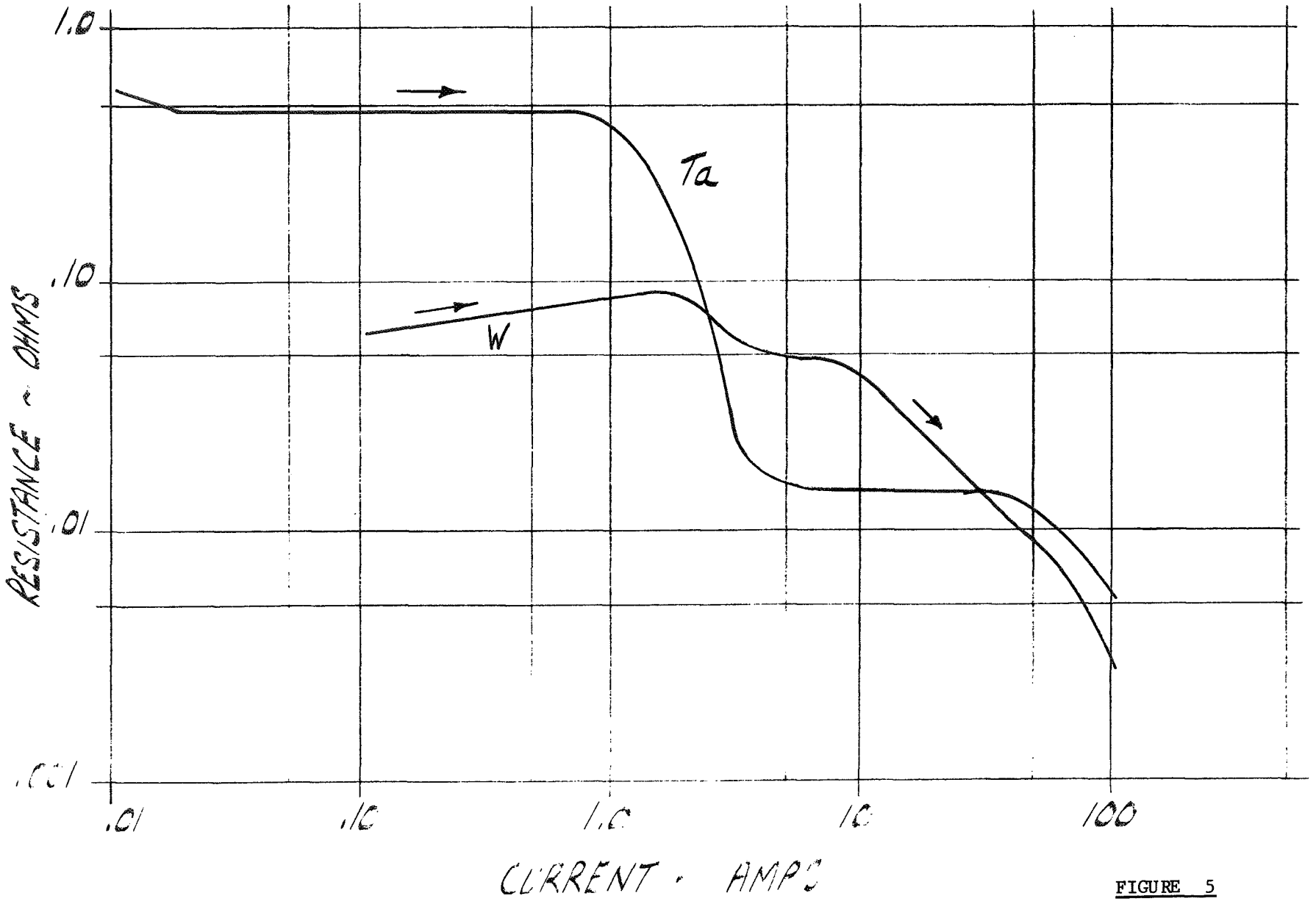

FIGURE 5

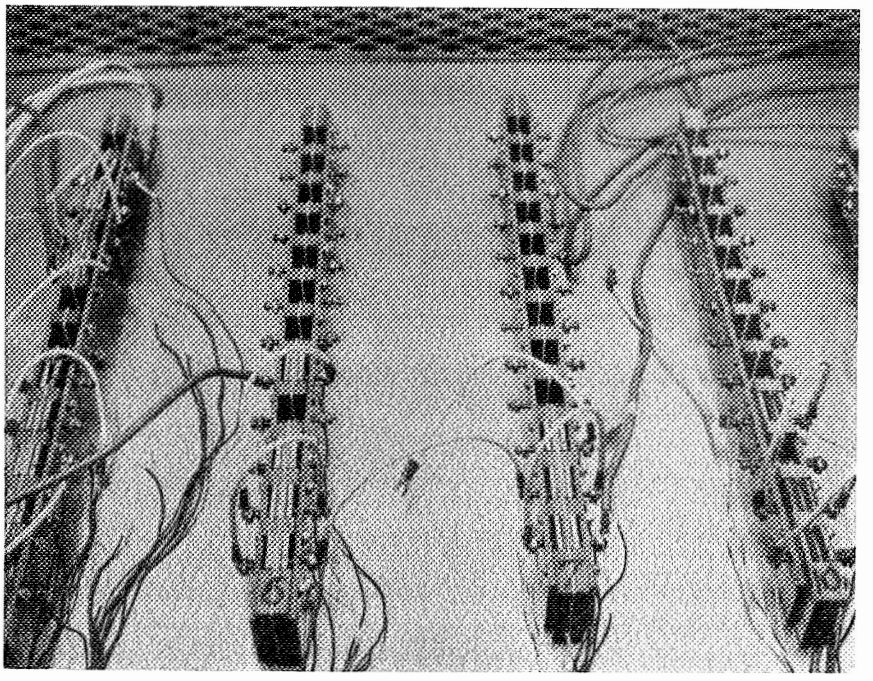

Figure 6. Test Cells Partially Assembled & Wired

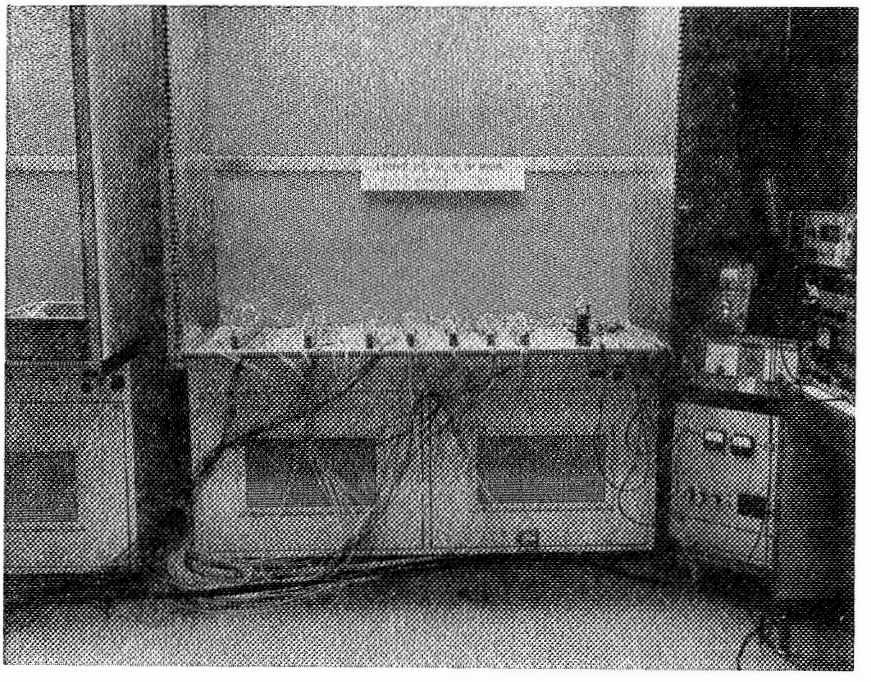

Figure 7. Preliminary Air Tests

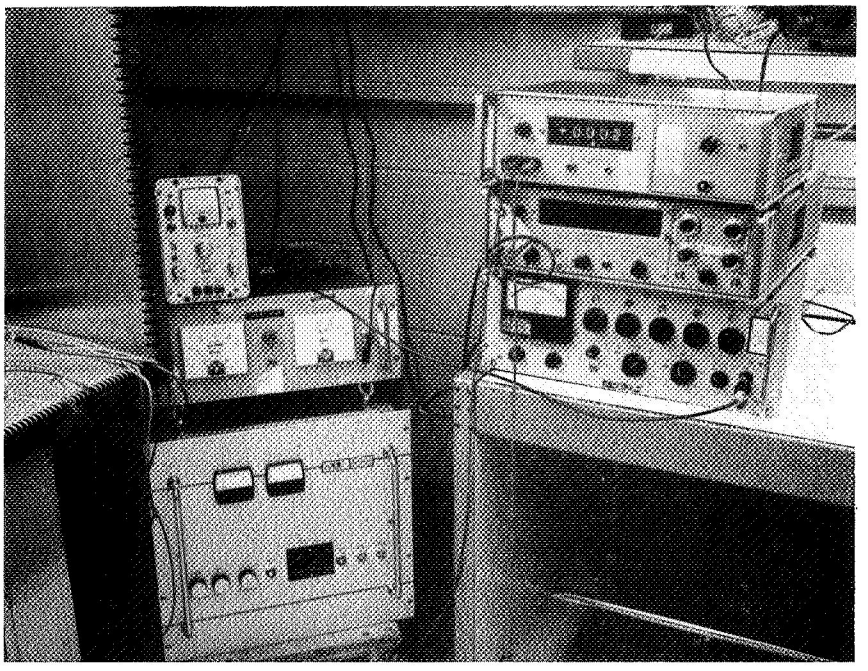

Figure 8. Electrical Test Equipment and Power Supply

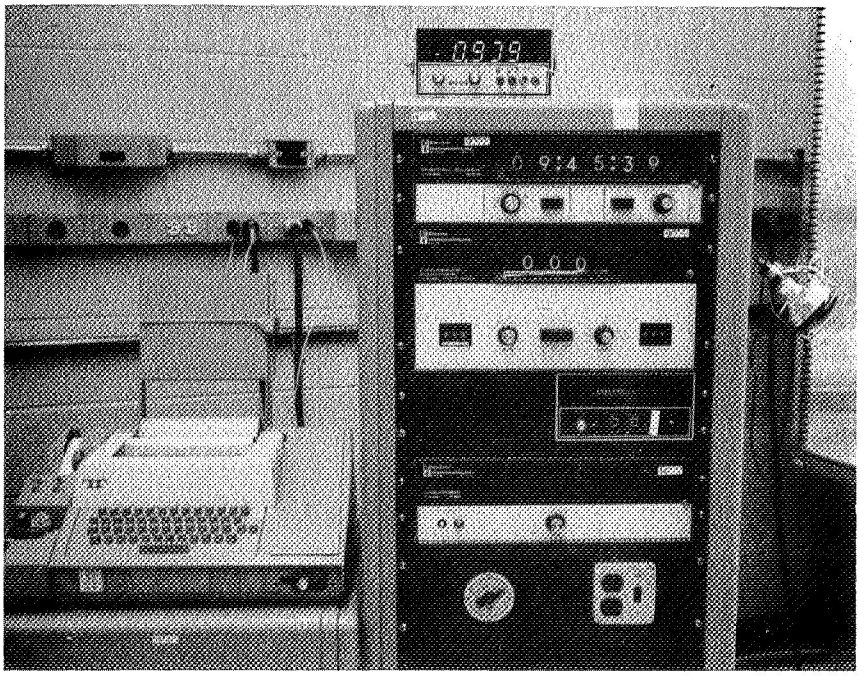

Figure 9. Automatic Data Acquisition System

4.1.2 Oxide Removal

The investigations of fritting indicated that the electrical interface resistance between gallium and the refractory metals was very largely influenced by the presence of an oxide layer on the electrode surface. If the layer is removed, even in a limited area, the interface resistance drops dramatically by several orders of magnitude. The fritting technique accomplishes this but it had the disadvantage of affecting only a very limited surface area of the electrode, perhaps in the magnitude of .01" in diameter. There was concern about relying upon this small area for electrical conduction for a period of years since an increase in resistance was experimentally observed over a period of weeks. This increase in resistance may be a result of the fritted area of the electrode becoming slowly reoxidized. The source of oxygen for the reoxidation could be dissolved oxygen in the liquid gallium.

A much more satisfactory approach would be to remove the oxide from the entire surface of the electrode. There are a number of techniques which can be used for the removal of the surface oxide. These include chemical attack, mechanical abrasion, and heating the electrode material to a temperature sufficient to vaporize the oxide. The mechanical abrasion technique was tried and found to be a successful approach. The abrasion approach consisted of rubbing the electrode surface with emery cloth while keeping the electrode surface covered with a layer of gallium. The electrode surface was covered with gallium in order to prevent the reoxidation of the surface by re-exposure to oxygen. The effectiveness of this technique was verified by removing the oxide from two electrodes, placing them in a test cell with gallium, and measuring the electrical resistance. The

electrode-to-electrode resistance was found to be in the micro-ohm range which indicated successful oxide removal. However, the abrasion technique has two major disadvantages. First, it is very time consuming and would be difficult to implement on the engineering test model which had large curved electrode surfaces. Secondly, after abrading the electrode, it might be difficult to determine if there were an attack by gallium, and it would be impossible to measure any small changes in electrode weight as a result of attack. A further disadvantage of abrading is that a rough surface is more susceptible to chemical attack than a smooth one; abrasion could therefore lead to accelerated attack by gallium.

The most applicable technique would be the removal of oxide by heating the electrodes to temperatures sufficient to vaporize the oxide; the oxides of tungsten, molybdenum and tantalum vaporize at 1000°C. The heating must be done in a controlled atmosphere; for tungsten and molybdenum, this atmosphere could be hydrogen, for tantalum which cannot be exposed to hydrogen at 1000°C because of hydrogen embrittlement, a vacuum furnace must be used. After the removal of surface oxide by furnace heating, the reformation of oxide on the electrode surface must be prevented when the electrodes are exposed to air again. This can be accomplished by having the electrodes in trays and after heating, flooding the trays with gallium to a sufficient depth to completely cover the electrode surfaces with a thin adhering film of gallium which will prevent reoxidation.

The specific procedure for oxide removal by the vaporization technique is as follows:

(1) The electrodes are cleaned, degreased, and placed in trays of 300 series stainless steel.

(2) The trays of electrodes are then heated in a furnace for 1 hour at temperature.

Material	Temperature °C	Furnace Atmosphere
Tungsten	1000	Hydrogen
Molybdenum	1000	Hydrogen
Tantalum	1000	Vacuum

(3) The electrodes are furnace cooled to 150°C. The furnace immediately is flooded with argon to prevent oxidation of the electrodes during gallium flooding.

(4) The trays are flooded with gallium to sufficient depth to completely cover that part of the electrode surface that was to be wetted.

(5) The furnace is cooled to room temperature and the trays removed.

Visual examination of the electrode surfaces showed them to be at least 90% wetted by the gallium. There did not appear to be any observable difference in the ability to wet electrodes of molybdenum, tantalum, or tungsten. The gallium on the surface of the electrodes did not appear highly oxidized.

4.1.3 Summary

Tungsten, molybdenum and tantalum have an inherent oxide film on their surfaces which results in excessively high electrode-to-electrode electrical resistance through gallium. The surface oxide can be removed by a number of methods, such as abrasion, chemical and heating. The technique most applicable to the liquid metal slip ring electrodes is by heating. The tungsten and molybdenum electrodes are heated to 1000°C in hydrogen and the tantalum is heated to 1000°C in a vacuum environment. This causes the oxide to volatilize. To prevent reoxidation, the furnace is flooded with argon and the electrode surfaces immediately wetted with gallium. This technique of oxide removal reduced the electrode-to-electrode resistance for one half square inch electrodes from initial values ranging from 0.01 to 1 ohm to less than 10×10^{-6} ohms.

4.2 LONG-TERM EVALUATION TESTS

4.2.1 Long-Term Evaluation Tests

As part of the long-term evaluation tests, test cells containing electrodes of various materials were run for an extended period of time to determine the combined effects of current, elevated temperature and vacuum upon the electrical, mechanical, metallurgical, and chemical characteristics of gallium and the electrode materials.

The test consisted of placing a rack of test cells in a vacuum chamber and continuously monitoring electrode resistance and temperature in order to detect any significant changes. The vacuum chamber was a diffusion pump chamber capable of maintaining a vacuum of 10^{-6} torr. The test cells were connected in series to a DC power supply that provided the 20 amp test current. The electrical resistance of each test cell was determined by measuring the voltage drop across it with a six-place digital voltmeter. Temperature was measured using copper-constantin thermocouples on each test cell. The current was measured with a precision laboratory DC ammeter having an accuracy of .05%. Table 6 summarizes the test conditions.

TABLE 6. TEST CONDITIONS

Environment	Material	Surface Finish (micro-inches)	Current (amps)	Ambient Temp. (^{o}C)	Number of Cells
Vacuum (10^{-6} torr)	Tungsten*	8	20	80	3
	Tantalum*	8	20	80	3
	Molybdenum*	8	20	80	3
	Graphite	8	20	80	3
	Delrin insulation	---	--	80	---

* Oxide removed by heating to 1000^{o}C in controlled atmosphere furnace.

Although electrodes with a 32 micro-inch finish might better approximate the surface finish anticipated on the engineering test model, the 8 micro-inch finish was necessitated for metallurgical study and examination. Photomicrographs of 32 micro-inch surfaces are not satisfactory and it is also more difficult to discern pitting, corrosion, or intergranular attack on 32 micro-inch finishes.

Prior to running in vacuum and in order to be assured of the integrity of the test equipment in vacuum, the test cells were first run in air at 2 amps and 20 amps. The proper functioning of the test racks and voltage and temperature sensors was assured.

Table 7 shows the electrical resistance characteristics in air and vacuum for currents of 2 amps and 20 amps. The resistance values of the tantalum, molybdenum, and tungsten electrodes were quite low being in the micro-ohm range; however, the graphite electrodes showed very much higher resistance values, in the milli-ohm range. The theoretical electrode-to-electrode resistances based on electrode and gallium resistivity and geometry of the test cells are as follows:

Tantalum	2.0×10^{-6} ohms
Molybdenum	1.3×10^{-6} ohms
Tungsten	1.3×10^{-6} ohms
Graphite	240×10^{-6} ohms

The measured resistance of the refractory metals is very nearly that of the theoretical value; however, the measured resistance of graphite is much higher than the theoretical. No obvious explanation has been found for this difference in resistance. The graphite electrodes could have a surface oxide, such as carbon oxide, and such effects as the gallium wetting charac-

teristics or absorbed water on the graphite surface may also be the cause of the high electrical resistance. The high electrical resistance of graphite resulted in I^2R losses of approximately 2 watts to 4 watts for each cell at 20 amps. In vacuum, this caused a localized excessive heating and in order to prevent a failure of the entire test rack, the graphite electrodes were removed from test by shorting them out.

The test results in Table 7 show a difference in electrical resistance, especially in the case of molybdenum electrodes between air and vacuum. The reason for this is probably a result of a slight zero-offset of the digital voltmeter used to measure the cell voltage drop. The cell voltage drop at 20 amps is of the magnitude of .1 to .2 milli-volts. A small meter zero-offset can effect the apparent reading magnitude quite substantially. It is believed that all electrodes had resistances of 10 micro-ohms or less.

TABLE 7. ELECTRODE RESISTANCE
(Micro-ohms)

Environment:	Air	Air	Vacuum
Current (amps):	2	20	20
Cell Material			
Ta	0	0	0
Ta	20	3	3
Ta	0	3	0
Graphite	5800	5700	removed
Graphite	9000	8000	from
Graphite	5100	4900	Test
Mo	40	60	4
Mo	20	40	0
Mo	10	30	2
W	10	2	0
W	10	10	5
W	20	10	0

Typical results from the long-term vacuum evaluation tests are given in Table 8. In these tests, the graphite electrodes had been removed from test by shorting them out; however, they were not physically removed from the test rack and their thermocouples were left in place. The electrical resistance of the test cells was less than 10 micro-ohms for all electrodes; the magnitude of the resistance remained constant, within the limits of instrumentation accuracy. The apparent poor correlation between resistance and temperature is probably due to joint resistance between leads and electrodes. As stated earlier, all electrical connections were mechanical because of the difficulty in obtaining good braze, weld or solder connections to the test electrodes. This is substantiated by the fact that the total input voltage to the test rack, which has all the cells and electrical connections in series, is approximately 0.5 volts. The voltage drop across the individual cells is of the order of .1 millivolts. Thus, the total input power to the test rack is 10 watts (0.5 volts x 20 amps) or about 1 watt per cell. The electrode-to-electrode power loss is (0.1×10^{-3} volts x 20 amps) or 2 milliwatts. A 2 milliwatt power dissipation per cell should not produce a significant temperature rise in a vacuum; however, 1 watt per cell would produce an appreciable temperature rise.

TABLE 8. LONG-TERM EVALUATION TEST RESULTS

Cell No.	Electrode Material	Date 3/10/70 Electrical Resistance (micro-ohms)	Date 3/10/70 Temp. (°F)	Date 4/8/70 Electrical Resistance (micro-ohms)	Date 4/8/70 Temp. (°F)	Date 4/28/70 Electrical Resistance (micro-ohms)	Date 4/28/70 Temp. (°F)
1	Ta	1	180	4	98	4	97
2	Ta	.5	180	.5	217	.5	212
3	Ta	.5	187	.5	221	.5	218
4	Graphite	--	167	--	194	--	196
5	Graphite	--	---	--	96	--	97
6	Graphite	--	170	--	193	--	198
7	Mo	7	181	5	206	5	211
8	Mo	.5	183	.5	206	.5	40
9	Mo	3	179	2	206	2	214
10	W	.5	181	.2	201	1	210
11	W	2	179	0	197	0	204
12	W	--	175	--	187	--	198
Platen Temperature			130		151		151

Current	20 amps dc
Environment	vacuum — 10^{-6} torr
Electrode cross-section area to current flow	.5 square inches (approx.)
Voltage drop across entire test rack	.5 volts (approx.)

During the running of the long-term evaluation tests, there was no evidence of electrode or insulation attack or of significant quantities of gallium contamination. The surface of the gallium in some of the test cells had a light grey appearance which was ascribed to oxidation. However, the quantity of this contamination was small and did not appear to increase during either the air exposure portion of the tests or in vacuum; in other cells, the gallium appeared bright throughout the entire test cycle.

A number of important results were obtained from the long-term evaluation tests of the electrodes and the Post-Test Evaluation, Section 4.2.2. These include the following:

(1) The electrical resistance of test cells using electrodes of tungsten, molybdenum and tantalum is about 10×10^{-6} ohms. This is comparable to the bulk resistance of the materials and demonstrates the ability to remove electrode surface oxides.

(2) There is no indication of an increase in electrical resistance with time in vacuum and based on limited testing in air. This shows that there is little or no restoration of the electrode surface oxide.

(3) There is no gross attack by gallium on the Delrin and Teflon insulation that was used in the test rack.

4.2.2 Post-Test Evaluation

At the completion of the long-term evaluation tests of the electrodes in vacuum, a post-test evaluation was made. First, visual observations were made of the gallium and electrodes in the test racks prior to their disassembly. There was no evidence of attack on the electrodes, the gallium in some of the cells appears lightly oxidized while in others, there was more, but not extensive, oxidation. The oxidation had the characteristic light

grey color. In five of the eleven test cells, during the vacuum test, gallium had formed a bubble, perhaps due to the expansion of entrapped gas. Where the bubble contacted the copper back-up plates, a crystal developed. A typical cell with a bubble is shown in Figure 10. It was also noticed that the bubble of gallium tends to be on one side of each cell. It was not random, but was always on to the same electrode, the cathode. There is no explanation for this preferential location of the gallium bubble. From previous tests, it was observed that this bubble appeared only when the test rack was under vacuum; when air was allowed in the bell jar, the bubble collapsed.

The gallium metal from each cell was analyzed by means of emission spectrography at LeRC. While additional trace elements were found, none of the electrode materials were found in the gallium. The spectrographic results are presented in Table 9.

TABLE 9.
SPECTROGRAPHIC ANALYSIS OF GALLIUM FROM TEST RACK ELECTRODE

Electrode Mat'l	Ga	Cu	Ag	Al	Si	P_b	S_n	M_g
Ta	S	M	T	T	T	-	-	-
Ta	S	M	T	T	T	-	-	-
Ta	S	M	T	-	-	T	T	-
Graphite	S	T	T	-	-	T	-	T
Graphite	S	T	T	-	-	-	-	-
Mo	S	T	T	-	-	T	-	T
Mo	S	T	T	-	-	T	-	T
Mo	S	T	T	-	-	T	-	T
W	S	T	T	-	-	-	-	T
W	S	T	T	-	-	-	-	T
W	S	T	T	-	-	-	-	T

S = strong indication
M = moderate indication
T = trace indication
- = no indication

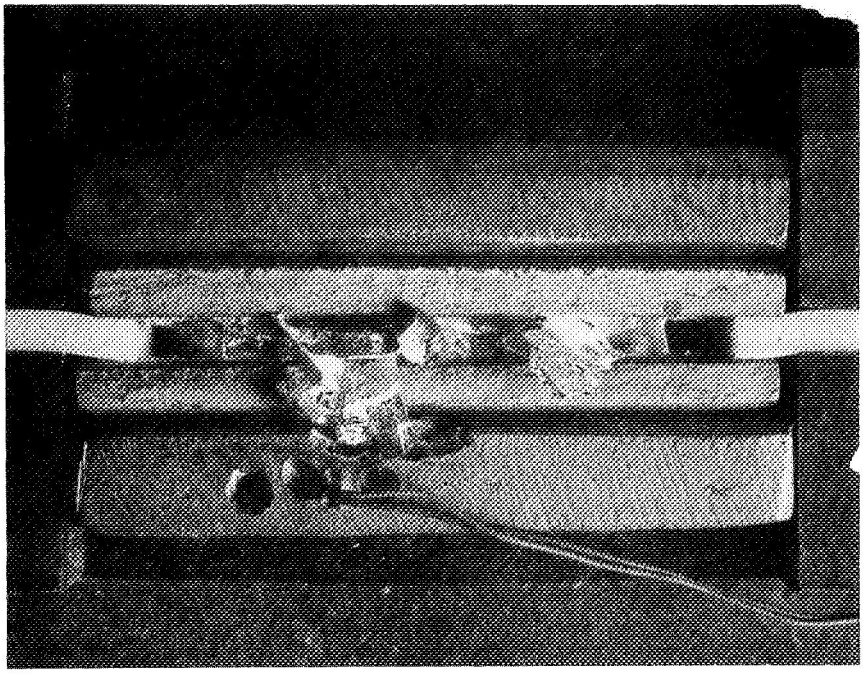

Tantalum Electrodes

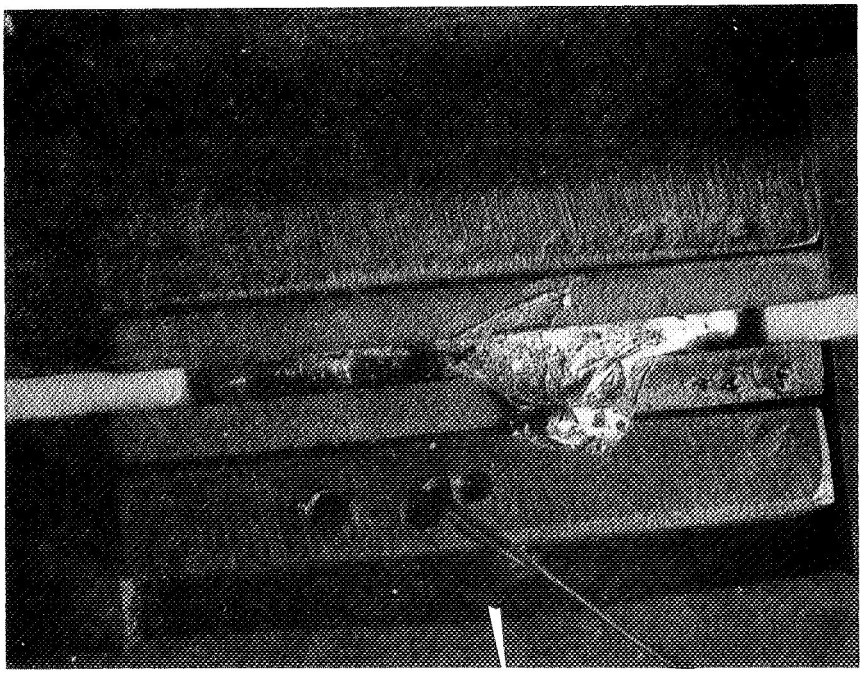

Tungsten Electrodes

Figure 10. Test Cells Showing Gallium Attack on Copper

Subsequent to the removal of the gallium from the test cells and their disassembly, each electrode was examined in detail by the use of a metallograph at approximately 5X and 200X. They were photographed at these magnifications, the 200X photograph being made of a specifically selected area for comparison to similar photographs made prior to test exposure. Photographs of one cell of each material are shown in Figures 11 through 16. The pre-test photographs show the 8 microinch surface; the post exposure photographs show the same surface after having the gallium removed by wiping with a soft tissue. There is some residual gallium present on the photographed surface. The differences observed are due to this residual gallium and were not found to be attack, crevices or pits.

In none of the electrodes was there any indication of attack, pitting, or corrosion. Each electrode was then placed in an acid bath, hydrofluoric for molybdenum and tungsten, and nitric for tantalum, to remove the last traces of gallium from the surface. After drying, the electrodes were weighed and compared to the initial weights. This information is tabulated in Table 10. Weight loss was observed in every case. After completion of photography, one of the tungsten electrodes was sectioned and polished to determine if attack had occurred. These sections are shown in Figures 17 and 18. No pitting or attack is discernible.

None of the observations made, visual, microscopic, or chemical, reveal any attack of the electrode materials by the liquid gallium at the test conditions.

The weight loss of the electrodes is not easily explained. It is possible that the electrodes were attacked in the acid etching bath that was used to remove the last traces of gallium before reweighing. The

(a)

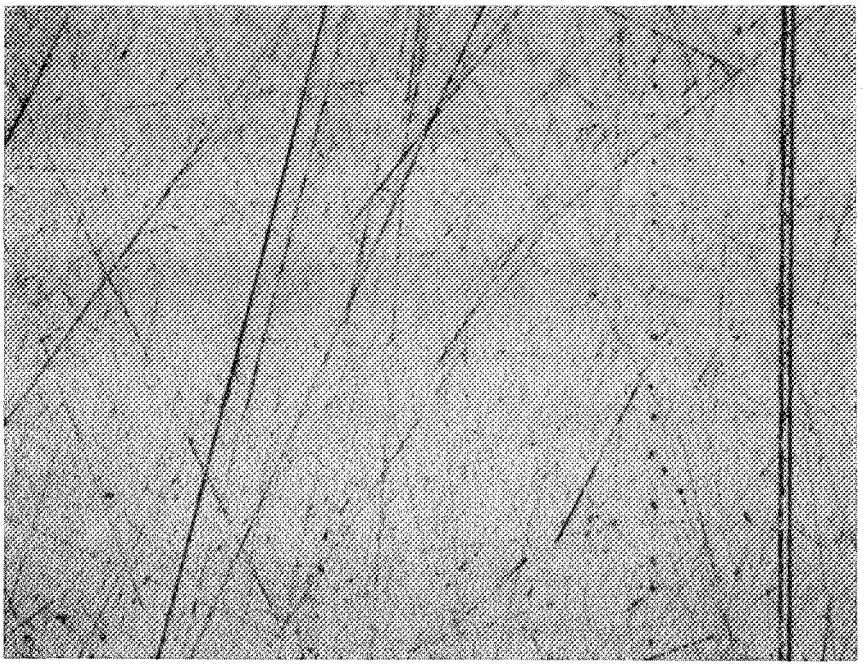

(b)

Figure 11. Photomicrographs of Tantalum Electrode 200X

(a) Initial (b) After long term evaluation test

(a)

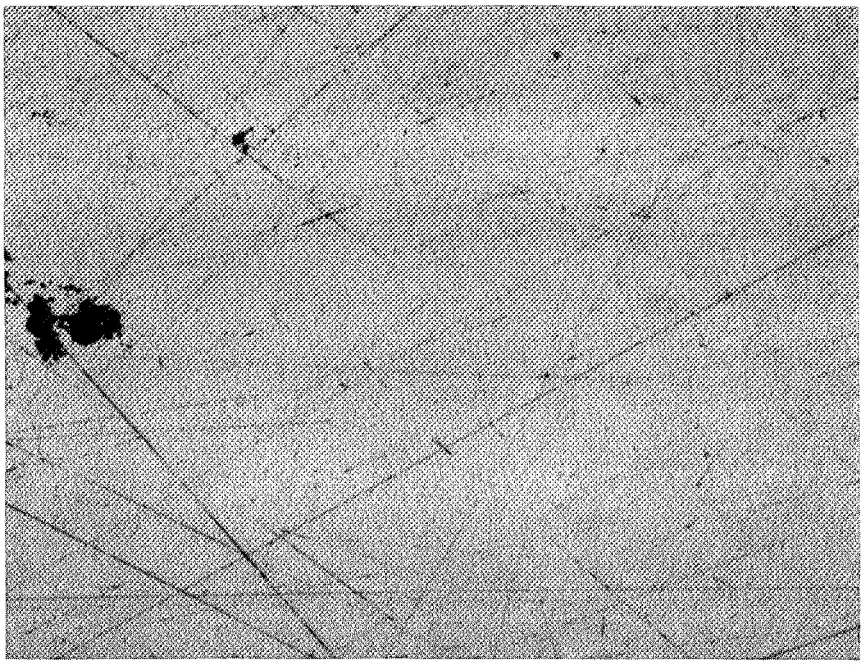

(b)

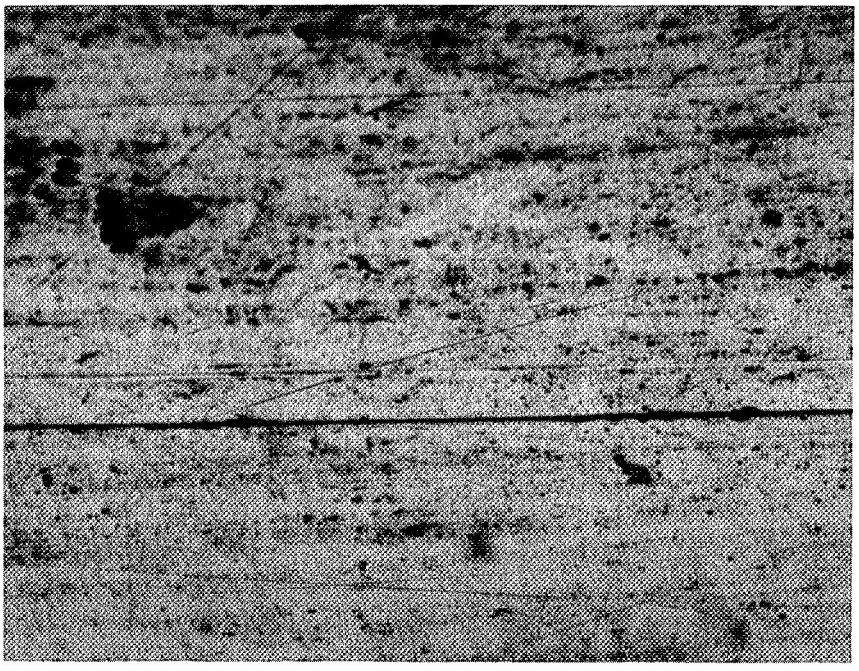

Figure 12. Photomicrographs of Tantalum Electrode (200X)

(a) Initial (b) After long term evaluation test

(a)

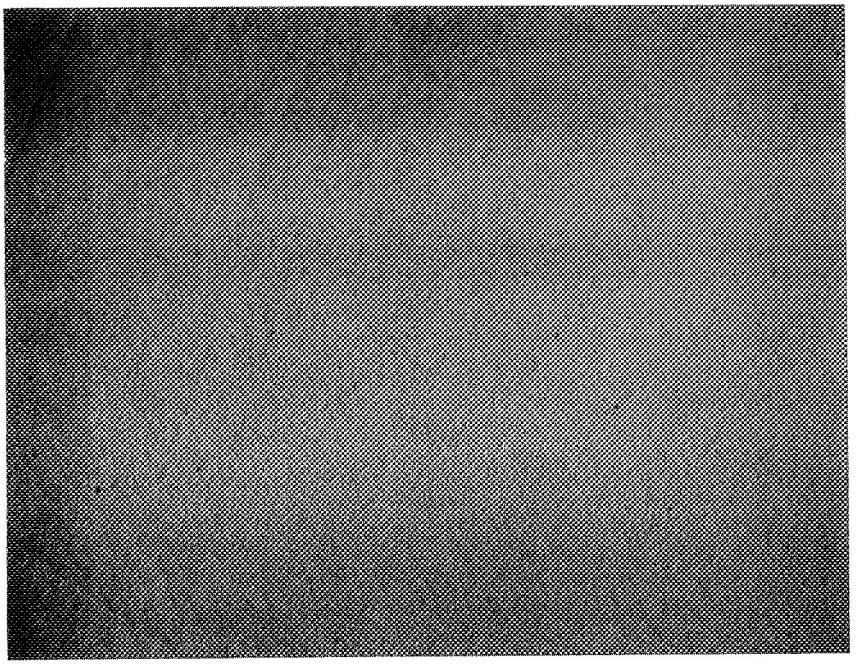

(b)

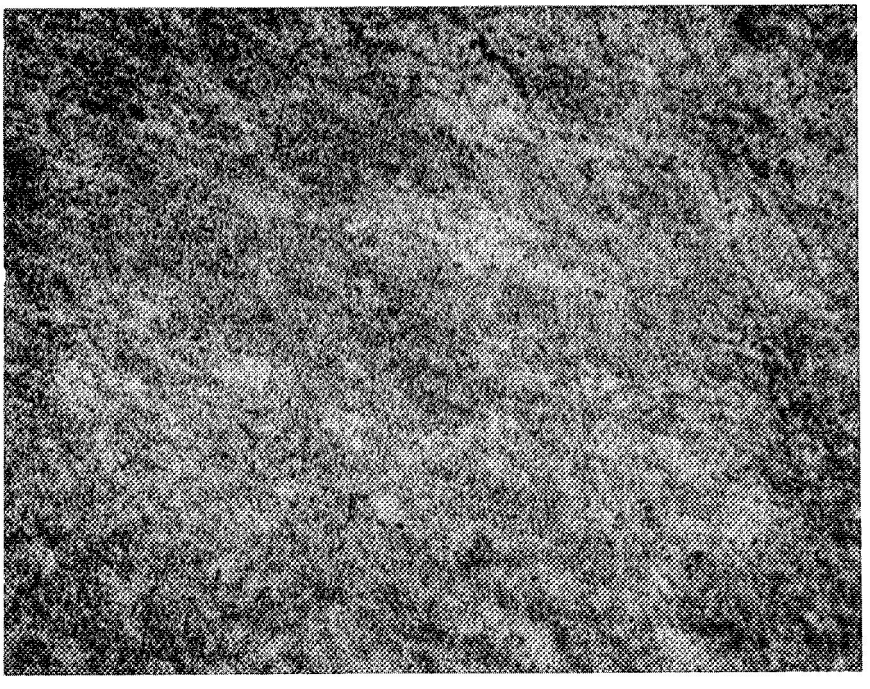

Figure 13. Photomicrographs of Molybdenum Electrode (200X)

(a) Initial (b) After long term evaluation test

(a)

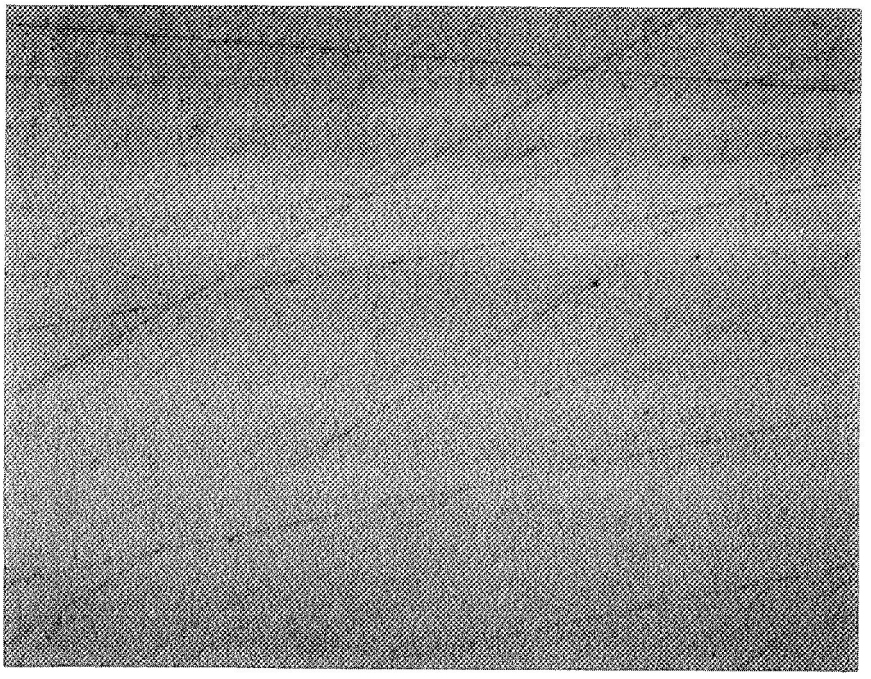

(b)

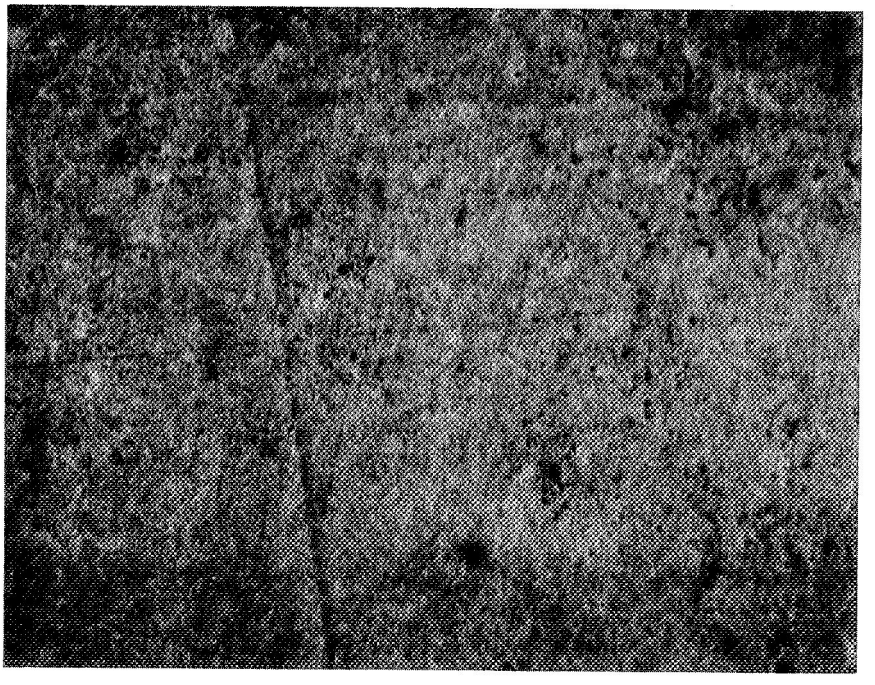

Figure 14. Photomicrographs of Molybdenum Electrode (200X)
(a) Initial (b) After long term evaluation test

(a)

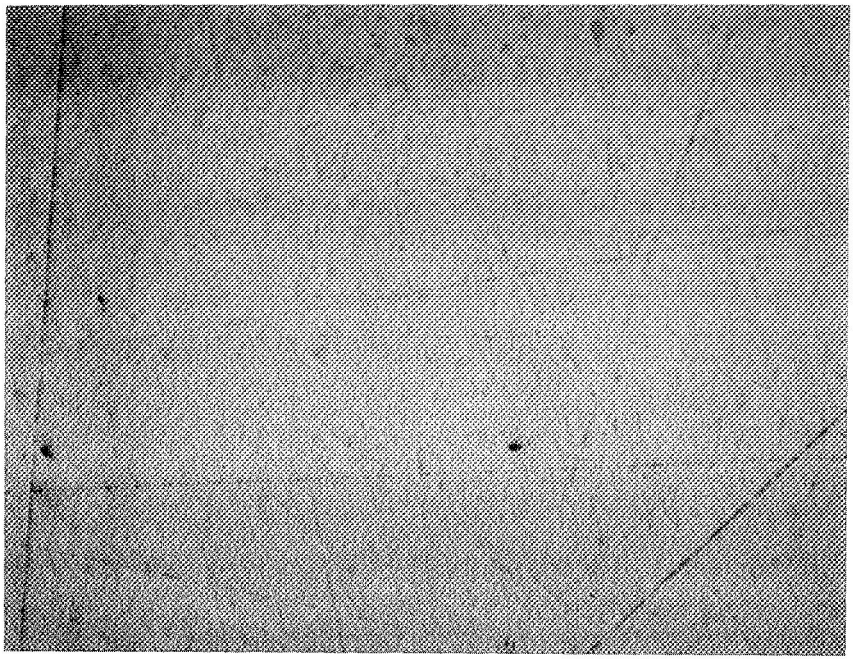

(b)

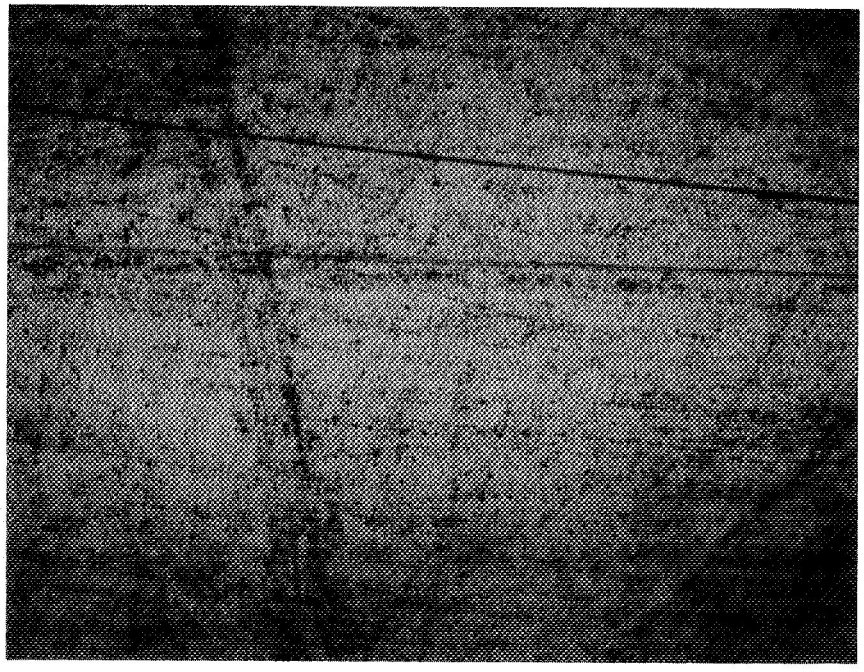

Figure 15. Photomicrographs of Tungsten Electrode (200X)
(a) Initial (b) After long term evaluation test

(a)

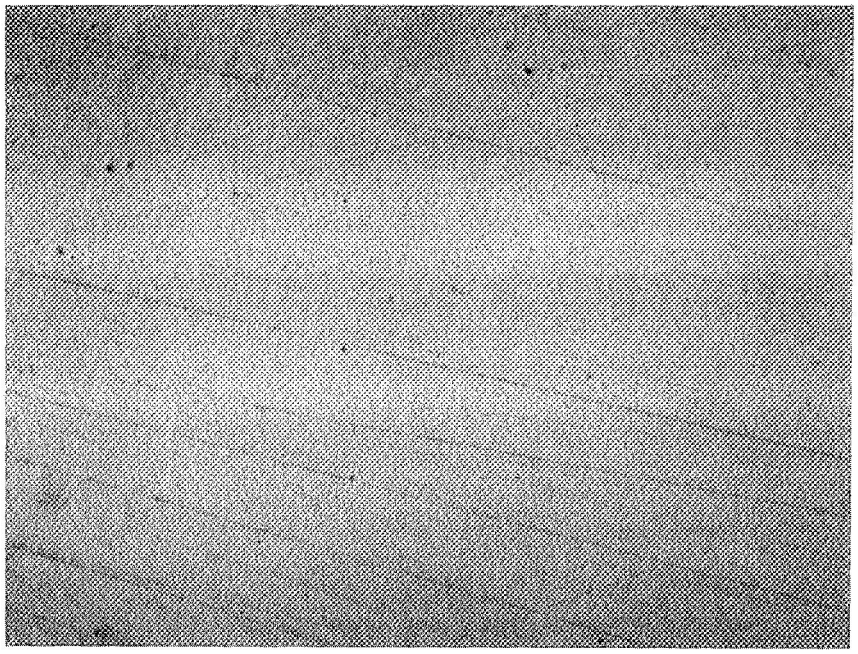

(b)

Figure 16. Photomicrograph of Tungsten Electrode (200X)
(a) Initial (b) After long term evaluation test

(a)

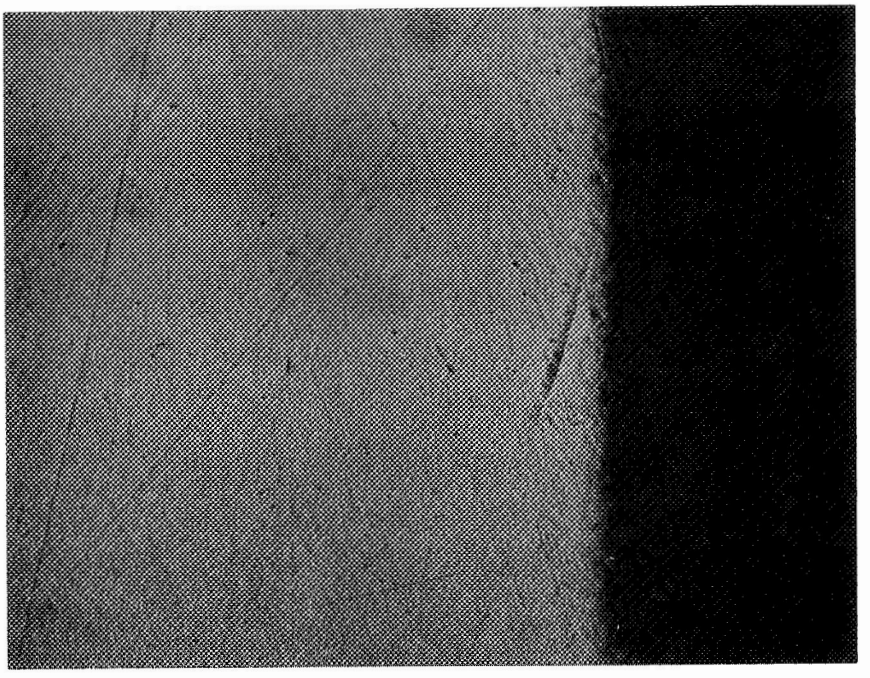

(b)

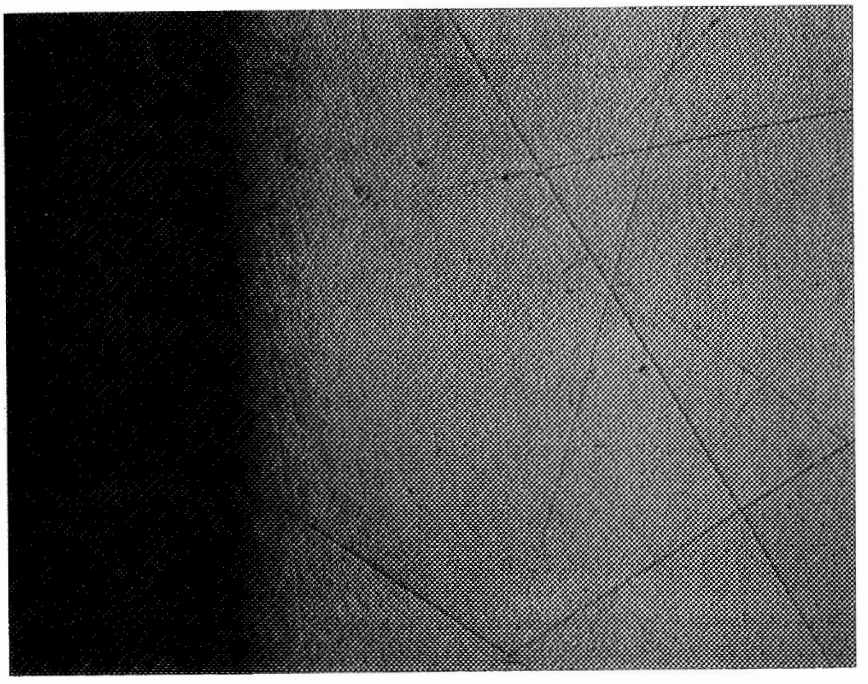

Figure 17 . Section of Tungsten Electrode, Unetched. (200X)

(a) Side unexposed to gallium.
(b) Side exposed to gallium.

(a)

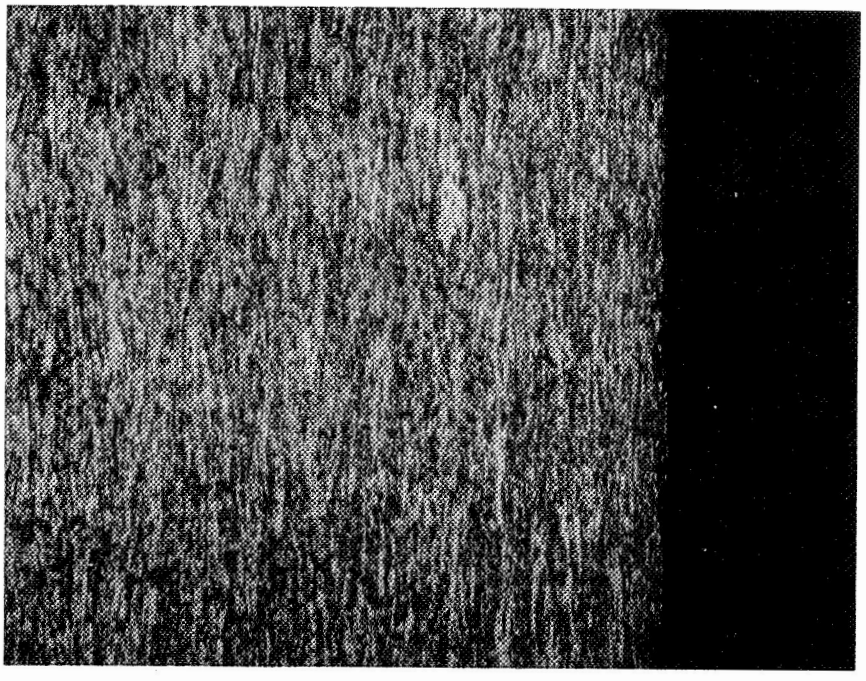

(b)

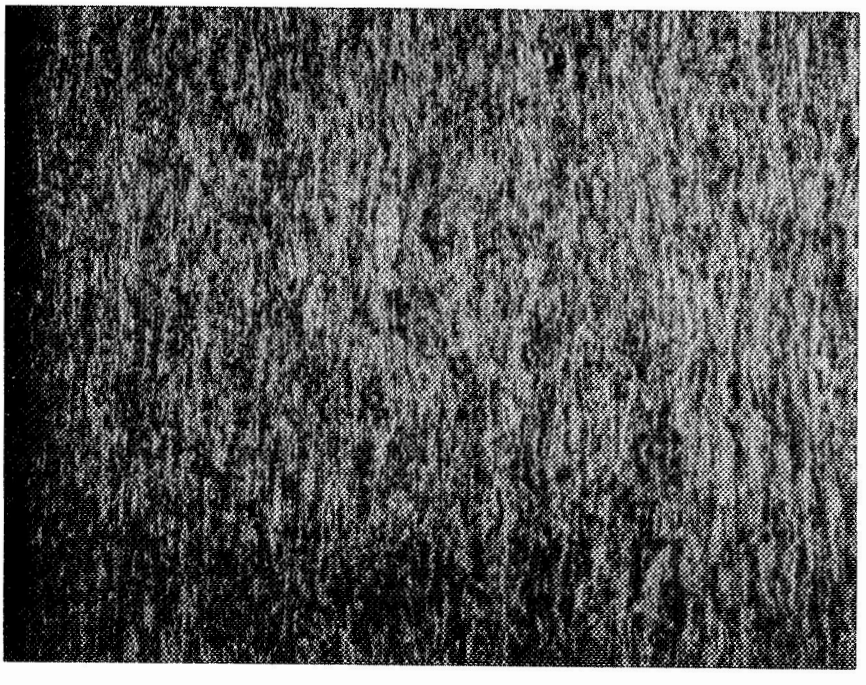

Figure 18. Section of Tungsten Electrode after Etching (200X).

(a) Side unexposed to gallium.
(b) Side exposed to gallium.

graphite electrode weight information is not reported since it was learned that the graphite electrodes were dressed to fit the test fixture after their weight was determined. However, its surface appeared unaffected by the gallium. The attack of the copper back-up electrodes by the gallium resulting in crystal growth is expected and predicted by the phase diagram.

Attack of the electrodes themselves cannot be detected by microscopic examination of the surfaces. The representative photomicrographs and cross-section confirm this. Therefore, the original analysis that showed that these materials are not subject to attack by gallium even after the removal of surface oxides have been substantiated by test.

TABLE 10.

WEIGHT CHANGE OF ELECTRODES

Material	Initial (grams)	Final (grams)	Change (grams)
Tungsten	10.1736	10.1678	-.0058
		10.3318	
	10.6075	10.6020	-.0055
	10.5082	10.5011	-.0071
	9.9975	9.9911	-.0064
	10.4441	10.4375	-.0066
Molybdenum	5.9758	5.9730	-.0028
	6.0288	6.0255	-.0033
	6.1204	6.1148	-.0036
	6.1395	6.1362	-.0033
	6.0490	6.0473	-.0027
	6.0666	6.0645	-.0021
Tantalum	9.1421	9.1399	-.0022
	9.1100	9.1059	-.0041
	9.0761	9.0717	-.0044
	8.8068	8.8030	-.0038
	9.1382	9.1355	-.0027
	9.2337	9.2289	-.0048

4.3 MISCELLANEOUS TESTS

4.3.1 Contact Angle Tests

Since capillary forces will be utilized to retain the gallium between the electrodes of a slip ring, the contact angle between the gallium and the electrode is an important parameter. The capillary depression for a non-wetting system, or capillary rise for a wetting system, is a measure of the retaining forces that will be exerted. For two parallel plates, the capillary depression in a non-wetting system is:

$$h = \frac{2 \sigma \cos \theta}{g \rho r}$$

where: h = head of fluid, cm.

σ = surface tension, dynes/cm.

θ = contact angle

g = acceleration of gravity

ρ = density of fluid, grams/cc

r = one-half plate separation, cm.

The contact angle, θ, shown in Figure 19, is the angle that the fluid makes with the material; it is greater than 90^{o} for non-wetted systems and less than 90^{o} for wetted systems. If the contact angle approaches 90^{o}, the capillary force approaches zero.

The contact angle can be measured using the sessile drop technique as described in "Physical Chemistry of Surfaces" by Arthur Adamson. This method consists of putting a small drop of the liquid metal on the electrode surface and measuring the angle which the side of the drop makes with the surface. This angle can be measured using a microscope with a calibrated reticle.

There are a number of important parameters which influence the apparent contact angle between the gallium and the electrode materials. These parameters include surface roughness, oxides and contaminants on the surface of the gallium, oxides and contaminants on the surface of the electrode material and hysteresis effects.

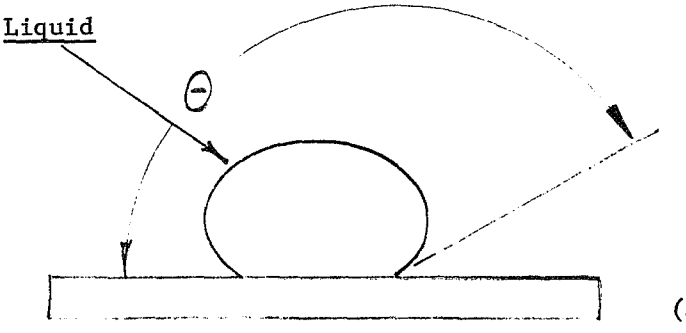

Contact Angle
$\theta > 90^{o}$

(a) Non-wetting Surface

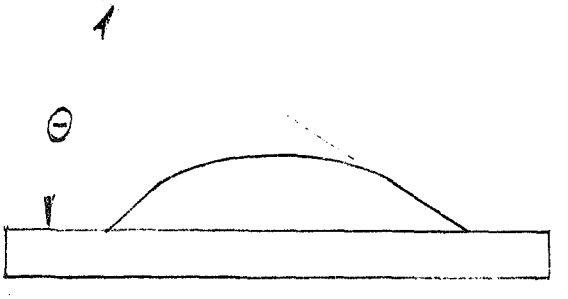

Contact Angle
$\theta < 90^{o}$

(b) Wetting Surface

Figure 19. Contact Angle Determination

The effects of roughness have been treated by a number of writers. If two contact angles are considered: θ_t , the true contact angle and θ_r , the contact angle of a rough surface,

$$\cos \theta_r = r \cos \theta_t$$

where r is the ratio of actual to projected surface area. As the surface becomes more rough, the ratio, r , increases (Reference: "Physical Chemistry of Surfaces", 2nd Edition, A. W. Adamson, p. 358). When the contact angle, θ , is less than 90^o as for wetted surfaces, the effect of roughness is to decrease the contact angle. When the contact angle is greater than 90^o, as for non-wetted surfaces, the contact angle is increased. Thus, the effect of roughness is to increase the capillary forces. Tests were run on 32 micro-inch finish electrodes; this finish selected as being typical of that which would be attained on the engineering test model. As a first order approximation, electrode surface roughness is not expected to alter the contact angle characteristics appreciably for the range of roughness expected between the test sample surfaces and engineering model electrode surfaces. If there is any difference in roughness, the engineering test model electrodes would probably be rougher than 32 micro-inch; this would result in greater capillary forces. Contact angle tests could have been run on the 8 micro-inch electrodes; however, these were made primary for metallurgical tests and it was not thought desirable to subject them to excessive handling.

The contact angle characteristics will be greatly influenced by the surface conditions of both the gallium and electrode surfaces. The surface of the electrode is oxidized; in addition, it may contain absorbed water vapor and oxygen. Gallium oxidizes very rapidly so that its surface is

probably oxidized; the oxide also might be hydrated, depending upon its exposure to water vapor. It is difficult to quantitize these effects, but gross tests show that both moderately oxidized and "fresh" gallium will wet electrode surfaces from which the oxide has been removed, and that neither moderately oxidized or clean gallium will wet oxidized electrodes.

Tests were run in air at room temperature, pressure and humidity to determine the contact angle of gallium and various electrode materials. Prior to testing, the electrode surfaces were cleaned with ethanol. The test consisted of placing a drop of gallium having a diameter between 1/8" and 1/4" on the electrodes. The electrodes had a 32 micro-inch finish and the temperature of the electrodes and gallium were held between 30°C and 40°C. The results were as follows:

Material	Contact Angle, degrees
Tungsten	135 ± 5
Tantalum	135 ± 5
Molybdenum	135 ± 5
Graphite	135 ± 5
Beryllium	125 ± 5

These angles were obtained by visually measuring the angle of contact with a microscope having an angularly calibrated reticle. During these tests, the gallium was in a liquid condition since the temperature of the electrodes and gallium were deliberately kept above the melting temperature of the gallium.

4.3.2 Freezing Tests

When gallium freezes, it undergoes a rather large volumetric expansion, approximately 3.2%. This expansion presented a concern relating to the design of the engineering model slip ring. It wasn't known whether the freezing of the gallium would impart large axial forces through the rotating center electrode and cause a failure in the support bearings. It also wasn't known whether the radial forces in the outer electrode caused by the expansion of the gallium would be sufficient to fracture it. No design calculations could be done to determine the magnitude of the expected forces since there is very little data on the mechanical properties of pure gallium. A test was therefore undertaken to determine whether this problem actually existed.

A solid beryllium outer electrode with a center electrode externally supported was filled to the nominal depth of gallium that it would have when properly filled for operation. This was approximately 0.3". The gallium was frozen and the resulting displacement of the center electrode was measured with dial indicators around its periphery. The axial displacement of the center electrode was measured to be less than 0.0005 inch. This is less than the thermal expansion of the gallium and is of such magnitude as can easily be accommodated by the mechanical compliance of the mechanical elements of the slip ring. Also, there was no evidence of mechanical failure of fracture of the outer electrode. Therefore, no deleterious effects could be anticipated in the ETM caused by the freezing of gallium.

4.3.3 Noise Tests

Tests were run to determine whether electrical noise is developed in the gallium-electrode junction of the test cells. A preliminary analysis did not indicate that there was any significant source of electrical noise expected in the electrode-liquid metal system; however, it was necessary to verify this by test. The noise test consisted of three basic measurements: a coarse measurement of cell voltage using an oscilloscope, a measurement using EMC-10 and EMC-25 receivers, and a measurement of the noise generated by the power supply. Tests were run on a total of three test cells, one each of tungsten, tantalum, and molybdenum electrodes which had their surface oxides removed by heating to 1000^{o}C in a controlled atmosphere furnace.

A Tektronic 547 oscilloscope with a high gain differential amplifier was connected across the individual cells of tungsten, tantalum, and molybdenum running with 5 amps at room temperature. No noise was observed. This coarse measurement showed that the noise level was below the 100 microvolt level and indicated that there was no severe noise problem.

A more sensitive noise test was run on a tantalum cell first using an EMC-25 receiver. Three readings were taken, apparent cell noise, receiver noise, and power supply noise. The power supply noise was determined by measuring the output across a 0.1 ohm resistor with 5 amps DC flowing. The results of these tests are given in Table 11.

TABLE 11. NOISE MEASUREMENTS

Frequency Band	Cell Noise Signal (micro-volts)	Receiver Noise (micro-volts)	Power Supply Noise (micro-volts)
14 - 30 kHz	.2	.018	.2
30 - 60	.04	.03	.05
60 - 128	.024	.018	.03
120-260	.02	.018	.026
250 - 520	.019	.017	.027
.5 - 1.1 mHz	.031	.026	.034
1.1 - 2.4	.028	.023	.031
2.3 - 5.3	.018	.016	.055
5.0 - 11.4	.026	.02	.06
11.0 - 25.0	.016	.015	.054
25.0 - 50.0	.044	.043	.045
50 - 100	.062	.062	----
100 - 200	.1	.1	----
200 - 500	.063	.063	----
500 - 1000	.15	.15	----

After completion of the test using the EMC-25 receiver, a run was made with the EMC-10 receiver. The EMC-10 covers the frequency spectrum from 30 Hz. to 50 kHz. Since there was no appreciable noise recorded at the high end of the spectrum, 14 kHz to 1000 mHz, the lower end of the spectrum was scanned to determine if any noise was generated in the test cell. This scanning indicated that all the noise present was generated in the power supply and there was no noise directly attributable to the test cell.

The results of the noise tests show that the noise generated by the power supply is the major source of the system noise level. The level of noise generated by the test cell is negligible. The noise produced by other electrode materials is the same as that of tantalum as determined by oscillographic observations.

Figure 20 shows the noise measuring equipment with Fairchild EMC-10 and 25 receivers.

4.3.4 Stability of Oxide

The operational slip ring was intended to utilize the non-wetting properties of the oxidized refractory metals and gallium to retain the gallium under orbital conditions due to the capillary forces. There is, however, no metallurgical data concerning the stability of the oxide surface film in vacuum at nominal temperatures. It was thought that the film would be stable at 80°C in vacuum; there was, however, no substantiating data and since oxide can actually be removed in vacuum at high temperature, there did appear to be valid reason for performing an evaluation test.

The test cell electrodes of tungsten, tantalum, and molybdenum had their oxide removed by heating them to 1000°C in a controlled atmosphere and then flooding the surface with gallium. The gallium was then removed from the periphery of the electrodes by treating the tungsten and molybdenum electrodes with hydrofluoric acid and the tantalum with hydrochloric acid. The removal of the gallium from the electrode edge re-exposed this surface to air and caused it to re-oxidize.

The electrodes of tungsten, tantalum, molybdenum and in addition, graphite, were assembled in a test rack and filled with gallium. The test rack was laid on its side so that the interface between the gallium and the electrode could be observed for changes while under vacuum. The loss of the surface oxide would also result in a loss in the capillary forces retaining the gallium and the gallium would spill out.

The test rack was laid on its side on a platform in a vacuum chamber, as shown in Figure 21. The platform was heated to approximately 80°C and a vacuum of 10^{-6} torr was maintained. There was no current in the electrodes during this test. The test conditions were maintained for four months.

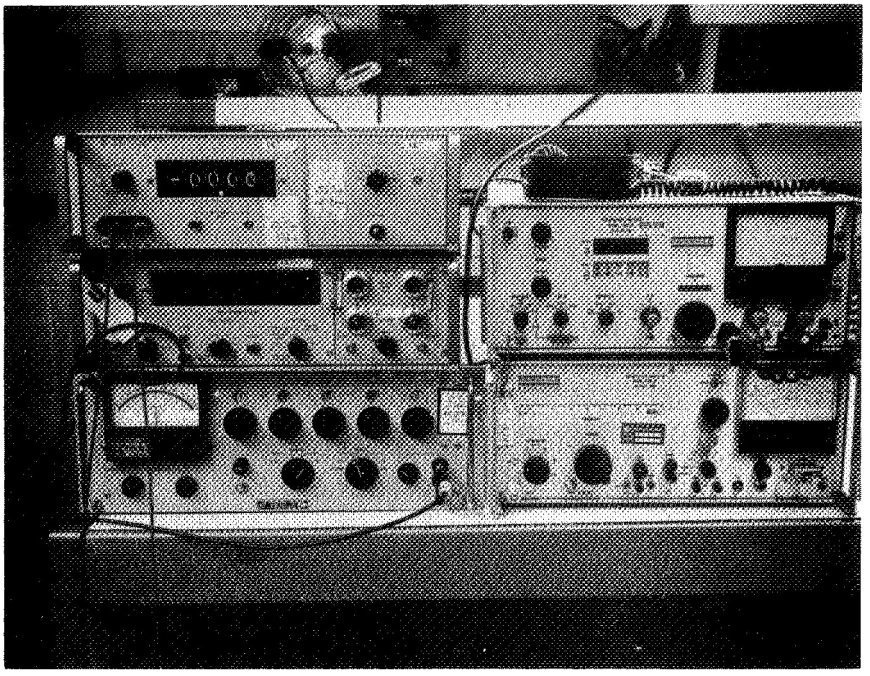

Figure 20. Noise Measurement Equipment

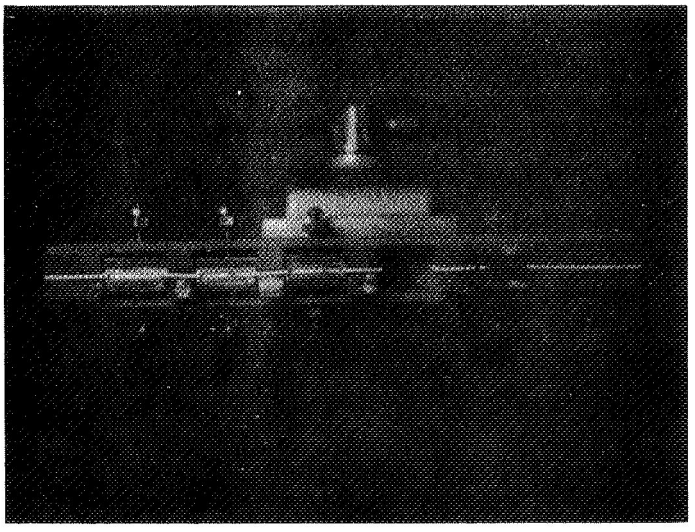

Figure 21. Stability of Oxide Test Rack

During the test period no change in contact angle between the gallium and the electrode surface was observed, and there was no tendency for the gallium to spill out from between the electrode plates even though the rack was subjected to a slight vibration (due to the vacuum pump operation) during the total test time.

It is therefore concluded that the non-wetting conditions of tungsten, tantalum, molybdenum, and graphite due to the oxide are not effected by vacuum at $80^{o}C$.

5.0 ENGINEERING TEST MODEL DESIGN AND FABRICATION

The Engineering Test Model (ETM) (See Figure 22) consists of ten, vertically-stacked rings. Five different electrode materials--graphite, beryllium, molybdenum, tungsten, and tantalum--are represented, but the basic electrode configuration is maintained throughout. Each ring is made up of a non-rotating electrode having a gallium-filled cavity on its upper surface and a rotating electrode, essentially a thin circular disk, that rotates within the non-rotating cavity. A nominal gap of 0.050" is maintained between the rotating electrode and both sides of the cavity. The depth of the cavity is established by the requirement to maintain current flow after loss of 50% of the gallium. The ETM design fully meets the requirement.

For the graphite and beryllium non-rotating electrodes, the cavity is machined from a solid piece of material (see Figure 23) and bonded to a Delrin housing. These electrodes were never tested since it was decided that graphite had excessively high resistance and beryllium is not a suitable material because of gallium attack. For molybdenum, tungsten, and tantalum, the cavity is formed by three 120^{o} inner segments and three 120^{o} outer segments bonded to the sides of a slightly wider cavity in the Delrin housing. This method was chosen to reduce manufacturing costs. Since the segments can be rolled from sheet metal, there was less wasted material and less fabrication time involved. Segmented electrodes that have been wetted are shown in Figure 24.

Prior to final assembly of the ETM, a sample ring was assembled using Epon 815 adhesive and a teta catalyst to bond the electrode segments to the Delrin. The sample ring was then exposed to $125^{o}C$ for two hours. At the conclusion of testing, small gaps had appeared between the electrodes and the Delrin. The following factors contributed to this problem:

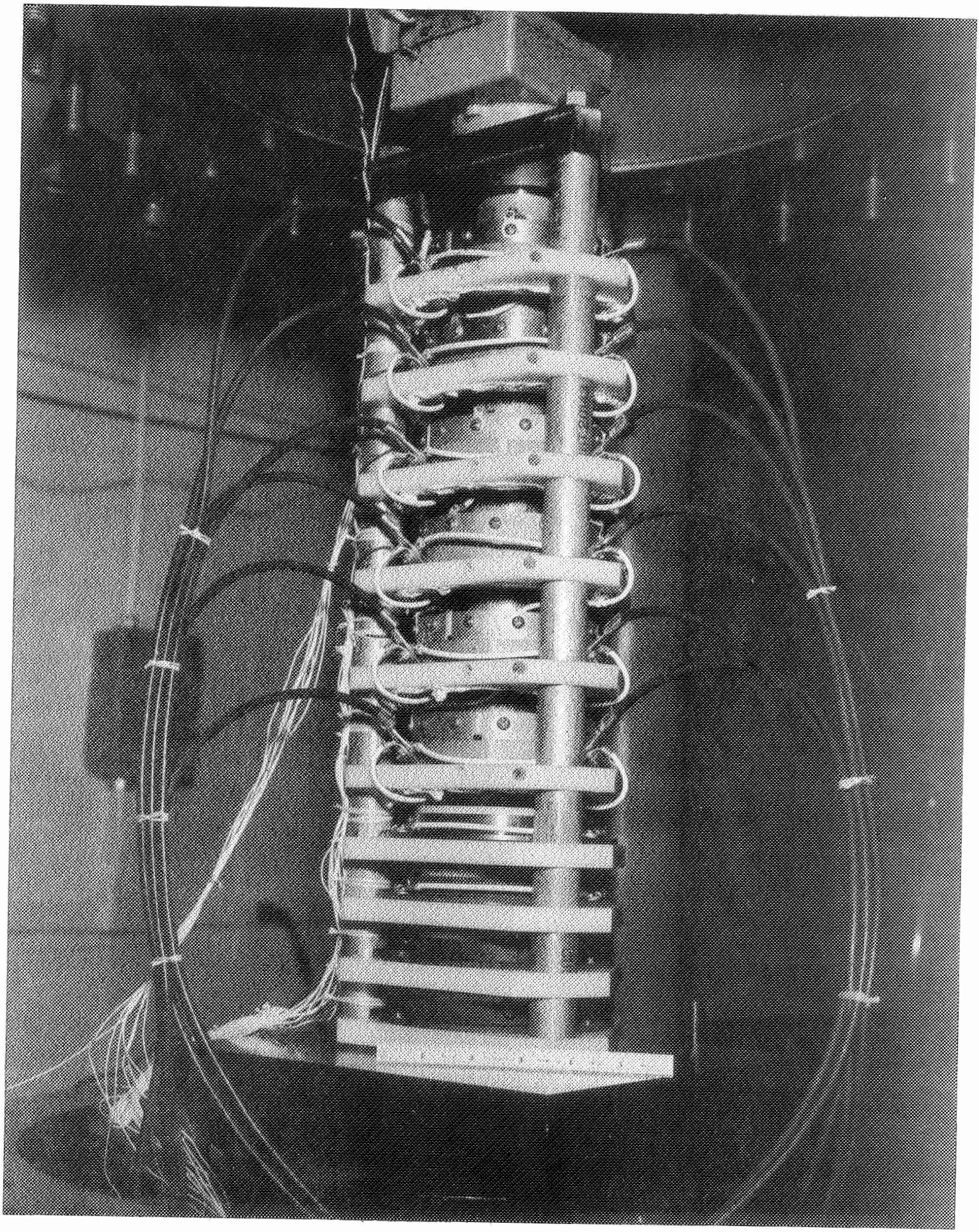

Figure 22. Engineering Test Model Assembly

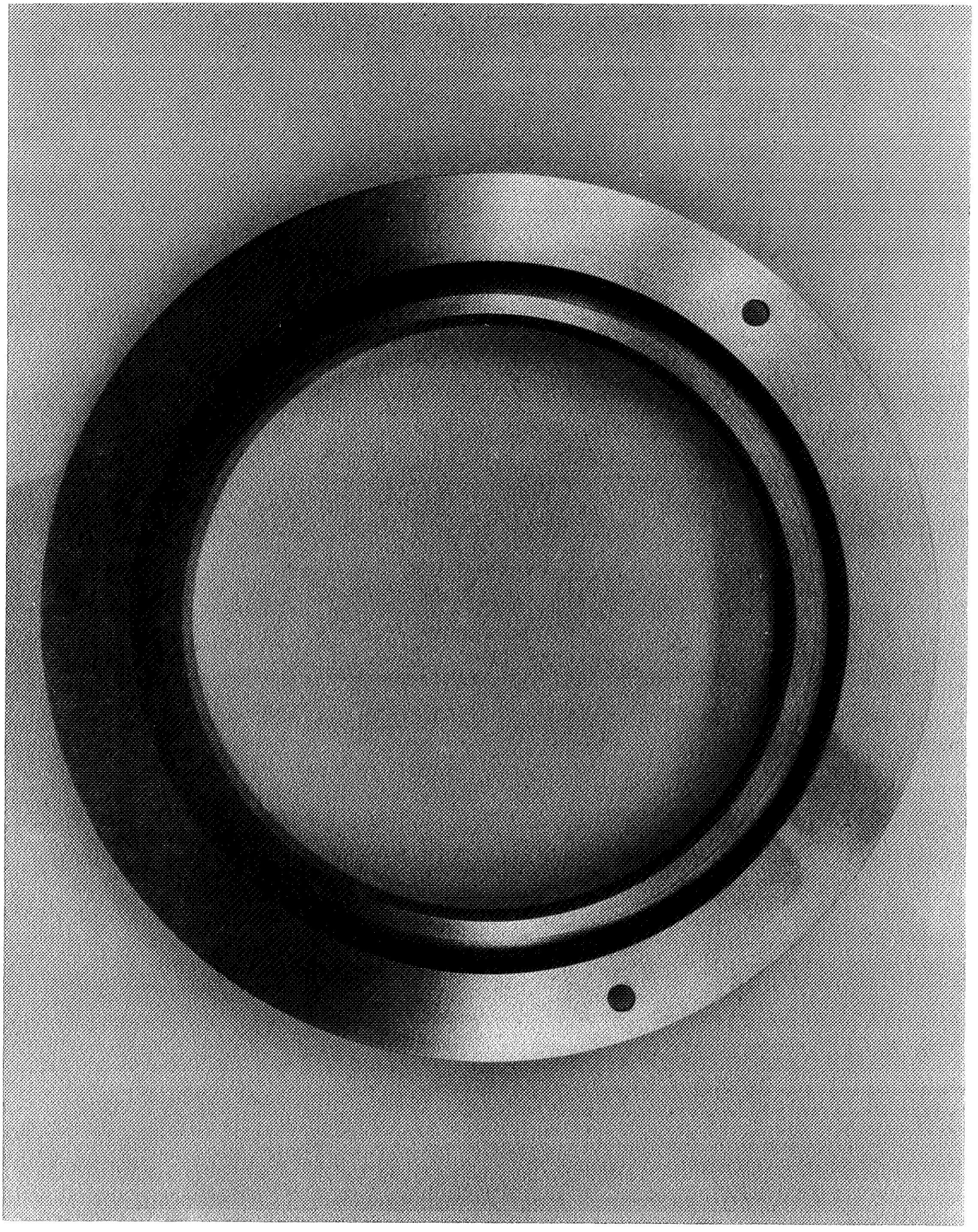

Figure 23. Beryllium Non-Rotating Electrode

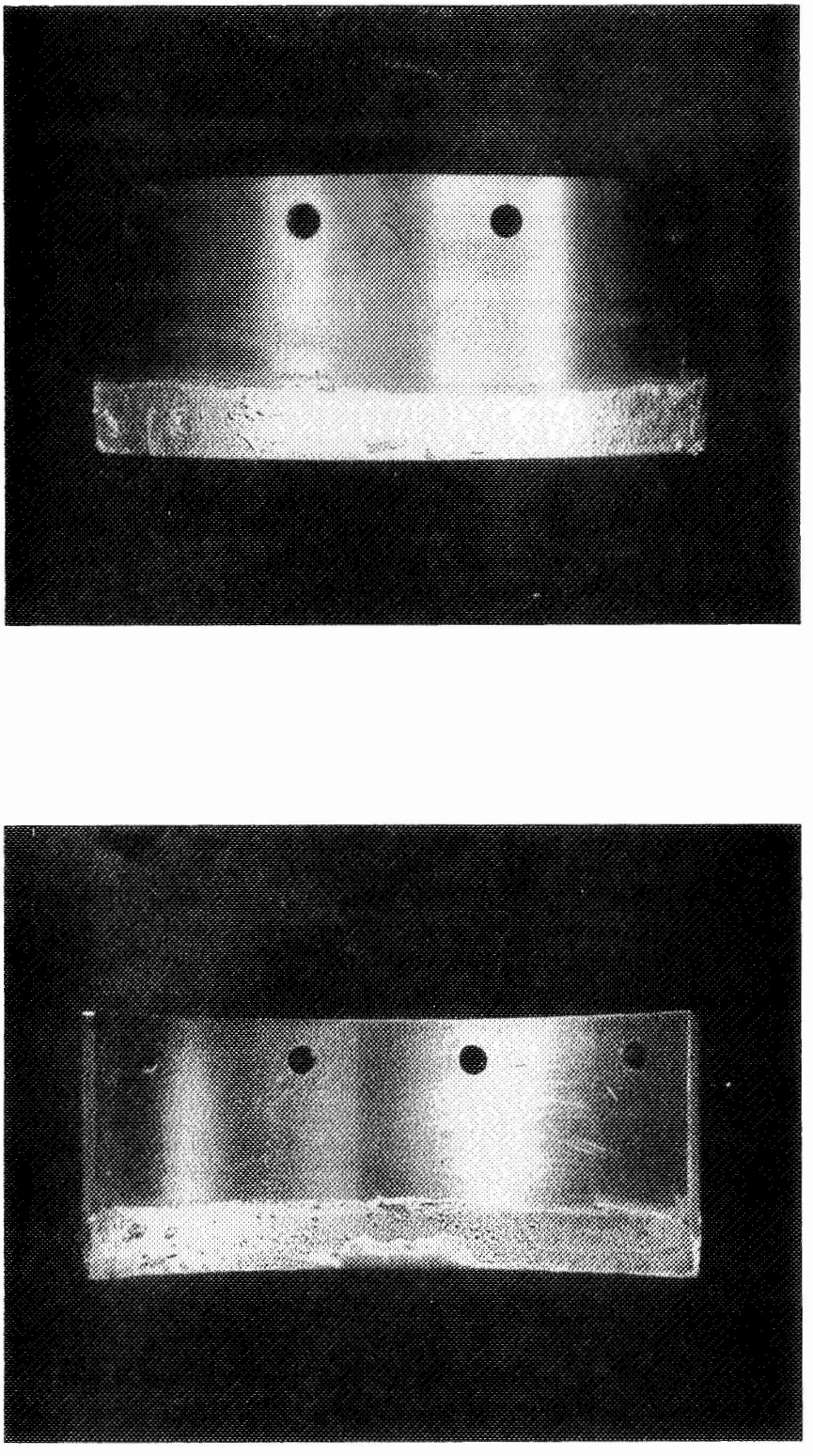

Figure 24. Wetted Segmented Electrodes

(1) Delrin is an extremely difficult material to bond.

(2) The electrodes were slightly out-of-round.

(3) Temperature extremes and dissimilar materials caused high loads due to thermal expansion.

The design solution was to use bolts as well as adhesive to attach the electrodes to the Delrin. Another problem discovered during assembly was the leakage of gallium from the cavity. In order to simplify fabrication, the Delrin housing was made in two pieces with a joint at the cavity. It was felt that a close fit between the two parts would retain the gallium; in fact, the gallium leaked through the joint. The design fix was to bond at the joint with RTV 102, and this remedy did stop the leakage.

Delrin was selected as the insulating material after an extensive investigation of available insulating materials. An initial screening of insulating materials was performed early in the program. This screening produced the following list of materials:

Lexan	Polycarbonate
Noryl	Mod. polyphenylene oxide
Zytel 101	Polyamide
Teflon TFE	Fluorocarbon
Delrin 150	Polyacetal
Teflon FEP	Fluorocarbon
PPO	Polyphenylene oxide
Zytel 31	Polyamide

In addition to the above materials, Vespel polyamide was also considered because of its excellent vacuum and thermal properties. In selecting the

insulating material for the ETM, all of the properties in para. 3.4 were considered, but the heaviest emphasis was placed on:

(1) Dimensional stability

(2) Manufacturability

(3) Cost

As a result, the list of candidates was narrowed to three: Vespel, Delrin, and Lexan. In the final selection, Lexan and Vespel were eliminated.

For the rotating electrodes, a similar design rationale was utilized; the graphite and beryllium electrodes are machined as one-piece disks (see Figure 25) whereas the others consist of three 120^{o} segments bolted to Delrin housings. The ends of the rotating electrodes are provided with a 10^{o} included angle taper (see Figure 26). This taper helps to contain the gallium within the cavity by capillary forces.

The baseplate and three rods are pre-assembled and accurately aligned. The non-rotating electrodes are stacked on the three rods, which then hold the position of the cavity. The rotating electrodes are stacked on a shaft which rotates in two bearings, one mounted in the base and the second mounted in the top plate. The bearings selected for the ETM are Fafnir type 9108 lubricated with a few drops of SF 1147, methyl alkyl silicone fluid. This lubricant was selected for its lubricating and outgassing properties. The top plate also serves to secure the non-rotating electrodes on the three rods. A Nimbus rotary actuator is mounted to the top plate and drives the shaft at a very slow speed (approximately 12 revolutions per day).

In order to avoid twisting of the power leads, the rings are wired in pairs. The input lead goes to the non-rotating electrode of one ring. The output lead from the rotating electrode of that ring goes to the rotating electrodes of an adjacent ring rather than going directly to the output.

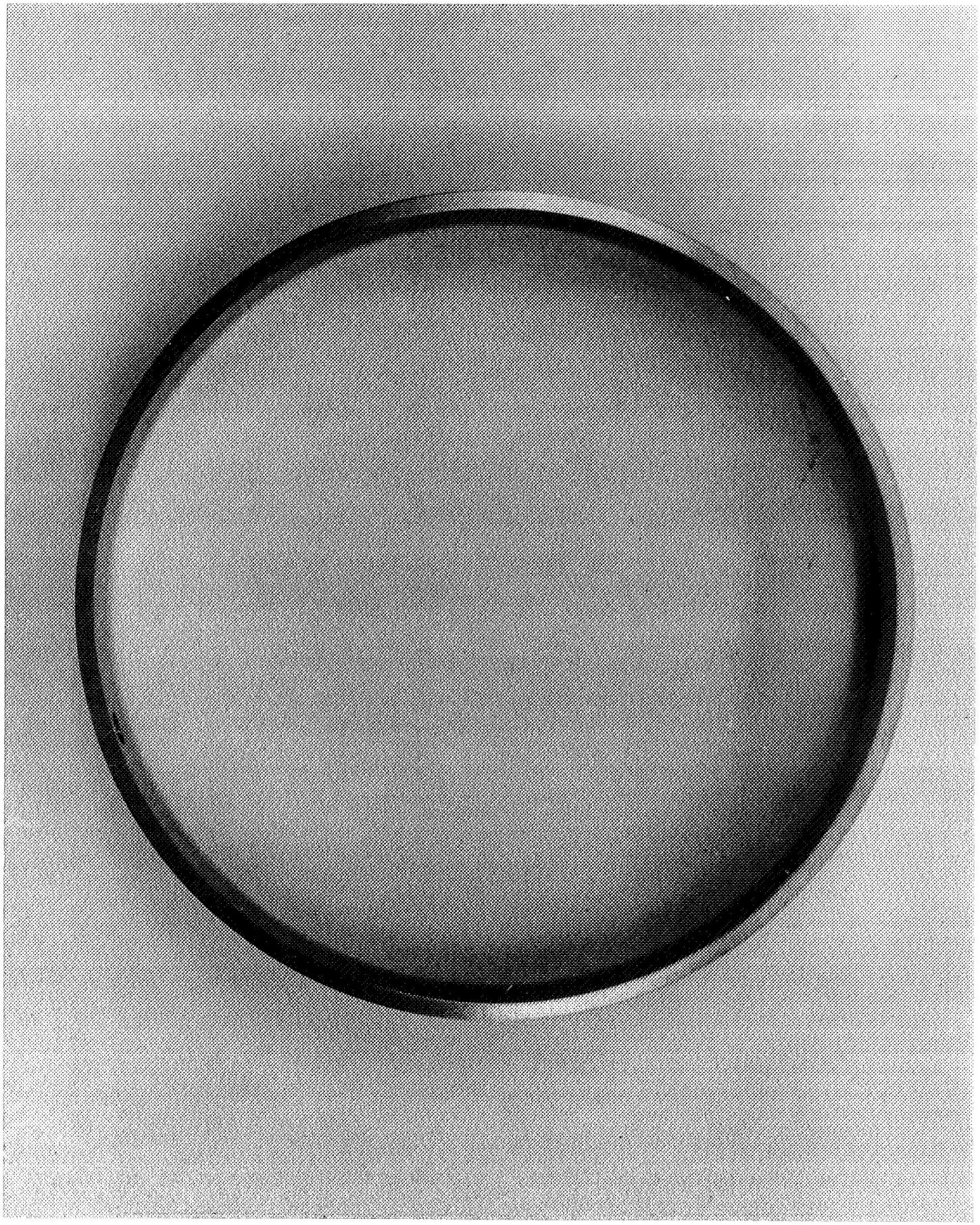

Figure 25. Beryllium Rotating Electrode

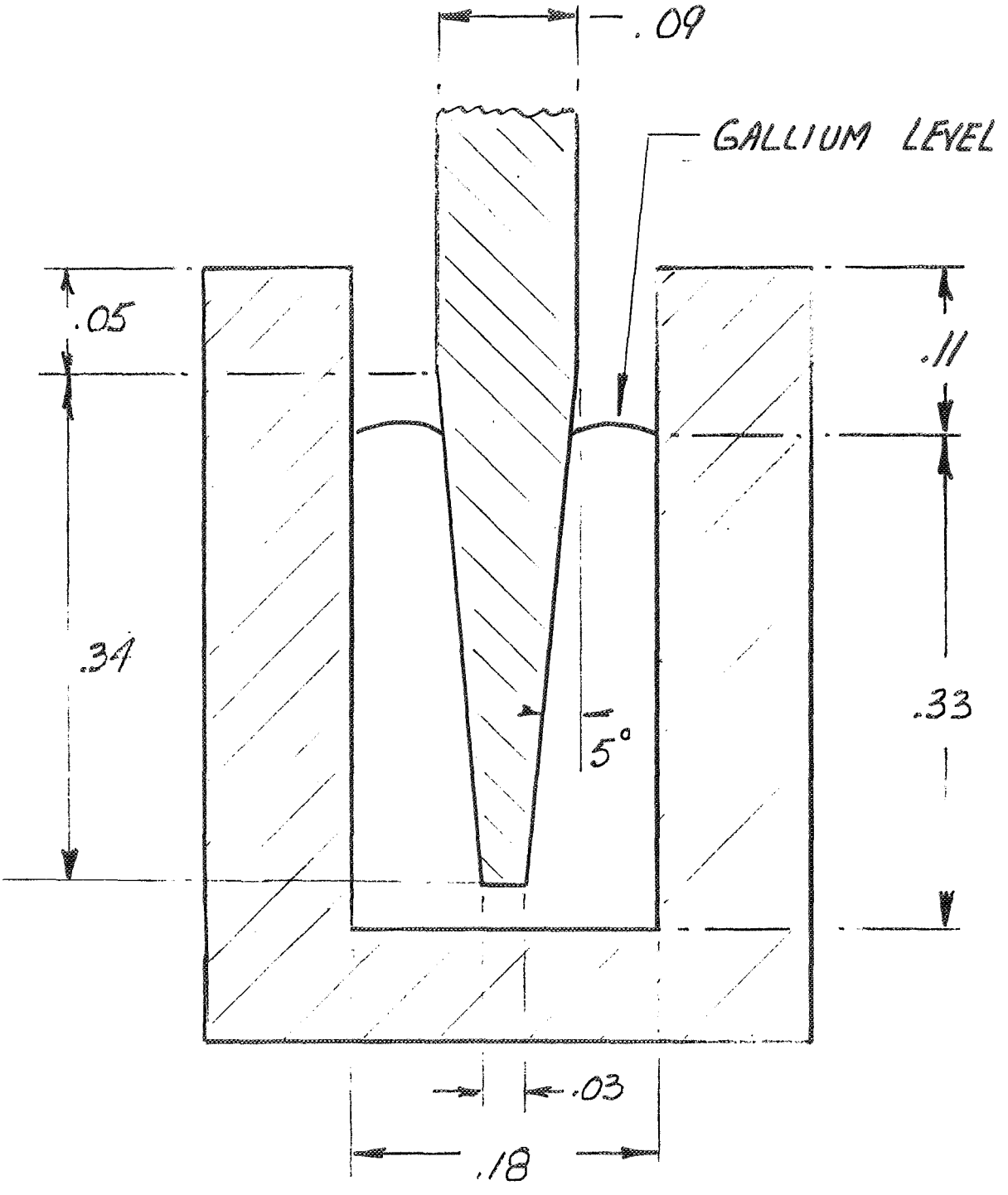

Figure 26. Cavity Geometry

This pattern is repeated for all five pairs. Separate sets of leads are provided for each pair of electrodes so that any pair can be removed from test without affecting any other pair of rings. In the event that one electrode or pair of electrodes fails open while in the vacuum chamber, testing of the remaining rings can continue by removing the faulty pair. Lead wire sizes were selected so that the resistance contribution would be small compared to the resistance of the slip ring. The initial sizing of these lead wires and the relative value of their resistance is shown in Table 12.

TABLE 12.

INITIAL ESTIMATE OF OVERALL "ETM" RESISTANCE

	Resistance (ohms)
Input lead (#8)	.00262
Internal lead (#14) - .00009/pair	.00045
Non-rotating electrode joints - .00010/pair	.0050
Gallium - .0001 to .001/pair	.00050 to .00500
Rotating electrode joints - .00020/pair	.00100
Internal lead (#12) - .00017/pair	.00085
Rotating electrode joints - .00020/pair	.00100
Gallium - .0001 to .001/pair	.00050 to .00500
Non-rotating electrode joints - .0001/pair	.00050
Internal lead (#14) - .00009/pair	.00045
Input lead (#8)	.00262
TOTAL	.0110 to .0200

Each 120° segment of the segmented electrodes is provided with a tab for attachment of a power lead. Each one-piece electrode has three machined tabs for leads. An electrical connection failing during operation at one or two tabs would raise the resistance but would not prevent operation due to the built-in redundancy. Due to the size of the power leads, it is necessary to provide support for them. This is accomplished by tying them to the three rods at frequent intervals. Mechanical means are used to attach leads to the electrodes. Lugs are crimped to the wire leads, and the lug is then bolted to the tab of the electrode. The resistance of the resultant joint is sufficiently low for our application. Brazing of the leads to the refractory metals was considered but ruled out due to development risk.

The assembly was made as large as possible within the space limitations of the vacuum chamber (maximum assembly height 36", maximum assembly diameter 17"). Large rings are desirable to optimize machining tolerances and to simplify assembly. One assembly procedure that was made significantly easier by the increased size was the filling of the cavity with gallium. In order to assure proper gallium depth, a sample ring was filled to the desired depth and the volume of gallium required was measured. In subsequent filling of the ETM rings, equal volumes of gallium were inserted into each ring.

In order to reduce the resistance between the gallium and the electrodes, it is necessary to wet the electrodes with gallium before an oxide film can be formed. This is accomplished by heating the electrodes in a controlled atmosphere furnace to 1000°F to remove the existing oxide. The furnace is then cooled and filled with argon gas. While still in the argon environment, the electrodes are wetted with gallium as previously described.

Capillary forces are utilized to retain the gallium in the electrode cavity. There are a number of parameters which influence the capillary force; these include surface rough, cavity geometry, oxides on the gallium surface, and oxides and water vapor on the solid electrodes. The cavity geometry is shown in Figure 26.

For two parallel plates, the capillary depression if the fluid is non-wetting is:

$$h = \frac{2 \sigma \cos \theta}{\rho g r}$$

For gallium assuming a .05" electrode separation:

σ = 735 dynes/cm

ρ = 6.1 grams/cc

θ = 135 degrees (based on tests with refractory metals)

g = 980 cm/sec/sec

r = (.05/2) (2.54) cm

$$h = \frac{2 \ (735) \ (.707)}{980 \ (6.1) \ (.025 \times 2.54)}$$

$$= 2.74 \text{ cm}$$

For a gallium depth of 0.3" and a length of one cm, the retaining force in g's in the longitudinal direction is:

$$f = \frac{h}{h_g}$$

where h = capillary depression, cm

h_g = physical height of gallium, cm

$$f = \frac{2.74}{.3 \times 2.54} = 3.6 \text{ g's}$$

In the lateral direction, the effective height is the diameter of the electrodes, 4". In this direction, the retaining force is:

$$f = \frac{2.74}{4 \times 2.54} = .26 \text{ g's}$$

Thus, there is no problem of retaining the liquid metal in any direction in a zero gravity environment. In cases where large g-forces are expected, the liquid metal would be frozen to preclude spillage.

In order to verify the electrical integrity of the electrode assemblies, electrical resistance data was taken of each assembly. This data would show if there were any areas of excessive resistance. There are two areas of special concern: the mechanical joint between the lead and electrode, and the electrode-to-electrode resistance through the gallium. A mechanical joint was used between leads and electrodes because of the potential problems of brazing or welding to the refractory metals. Preliminary tests indicated that relatively low joint resistances of less than a milli-ohm could be expected even though the contact area is small and the electrode surface is oxidized. The electrode-to-electrode resistance through the gallium should be checked in order to verify that the oxide has been properly removed from the electrode surfaces. The resistance was determined by circulating 20 amps dc through the assembly and measuring voltage drops with a digital voltmeter. This technique gives the overall resistance between the electrodes

and is not an indication of the effectiveness of the wetting of the entire electrode surface. Localized resistance readings which would show the degree to which the electrode surface is wetted could be determined by having a small bubble of gallium placed between the electrodes, placing the electrodes on their periphery, with their axis horizontal and rotating them slowly about this axis, noting any variations in voltage drop.

The results of these tests are summarized in Table 13 and the location of the points for resistance readings is shown schematically in Figure 27 . The major conclusions that can be drawn from these tests are as follows:

(1) The leads are the single major source of resistance.

(2) The joint resistance is generally small.

(3) The electrode-to-electrode resistances are somewhat higher than expected.

As was expected from the calculations performed in the design above, the lead resistance is a significant portion of the entire electrode assembly resistance. Lead resistance could be reduced by either using heavier lead wire or putting additional leads in parallel. Heavier lead wire than #8 AWG which is presently used will present difficulties in handling and attachment; therefore, an additional lead in parallel might be preferable.

The joint resistance was the next most significant resistance, being about an order of magnitude less than that of the leads. The magnitude of the joint resistance was highly variable varying from .00008 ohms for

tungsten #2 to .001 ohms for molybdenum #1. This variation is probably the result of many factors, such as electrode oxide thickness, tightness of connection, and localized pressure.

TABLE 13.

Resistance* (ohms)

Electrode Assembly	Terminal to Terminal 1-6	Lead 1-2	Joint 2-3	Electrode -Gallium -Electrode 3-4	Joint 4-5	Lead 5-6
Molybdenum						
#1	.011	.0013	.001	.000025	-----	.01 **
#2	.0031	.0013	.00005	.000015	.0007	.001
Tantalum						
#1	.0032	.0013	.00015	.000015	.0006	.001
#2	.013	.0015	.00017	.000015	-----	.012**
Tungsten						
#1	.0033	.0014	.00015	.0001	.0005	.0023
#2	.004	.0015	.00008	.0008	.00007	.0016

* See Figure 27 for physical locations of test points for resistance readings.

** Clip leads used during resistance measurement test.

The electrode-to-electrode resistance is higher than expected based on the resistance of the test cells. For the tantalum and molybdenum electrodes, the resistance was approximately 15×10^{-6} ohms for a surface area of about 6 square inches. The same materials in a test cell had a resistance of approximately 10×10^{-6} ohms for 1/2 square inch surface area. The net difference is about one order of magnitude. In addition, the tungsten electrode resistance was at least an order of magnitude greater than either the tantalum and molybdenum. A possible explanation of this

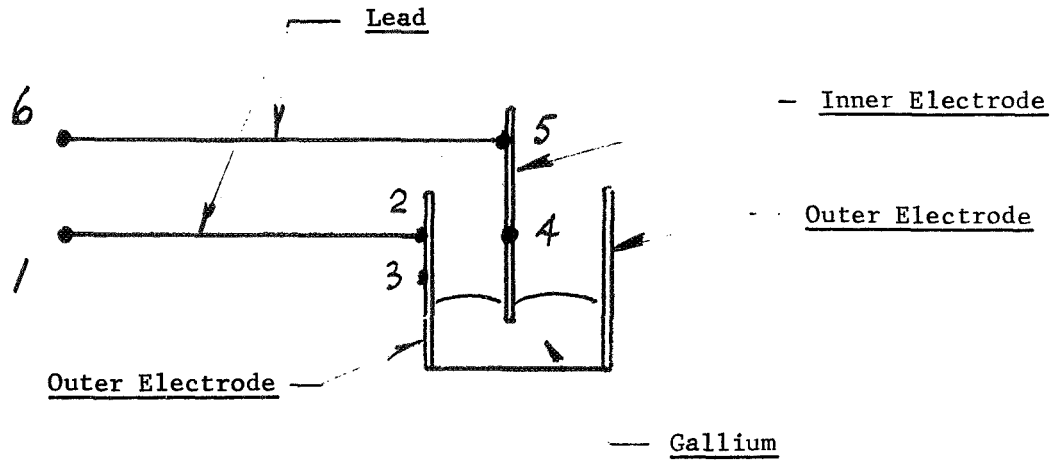

Figure 27. Test Point Locations for Resistance Readings

Designations:

1-6	Terminal to terminal
1-2	Lead
2-3	Joint, outer electrode
3-4	Outer electrode to inner electrode through gallium
4-5	Joint, inner electrode
5-6	Lead - tungsten #1 and #2
	Clip lead - molybdenum #1
	tantalum #2

higher electrode-to-electrode resistance in the engineering test model lies in the method of electrode preparation. The test cell electrodes were first polished with emery cloth to an 8 micro-inch finish prior to having the oxide removed by the heating technique. The engineering test model electrodes did not go through this procedure prior to having the oxide removed. The polishing might have been effective in removing a tenacious portion of the oxide which was not completely removed by the heating procedure.

6.0 ENGINEERING TEST MODEL TESTS

Tests were run on the engineering test model in order to determine the operational characteristics and to demonstrate the validity of the design configuration concept. A test plan was prepared which defined the tests to be run, the test procedure to be followed, the test sequence, and the required test apparatus. The test program for the engineering model consisted of the following major parts:

(1) Pre-test examination and check-out

(2) Air tests

(3) Test evaluation

(4) Vacuum tests

(5) Post-test evaluation

The basic test philosophy was to run the engineering test model in steps of progressively additive operating conditions. This was done to continuously monitor and assess the model's performance so that any incipient failure could be detected with ample opportunity to take remedial action.

6.1 PRE-TEST EXAMINATION AND CHECK-OUT

After final assembly of the engineering test model, a pre-test examination and check-out was conducted including clearances, electrode-to-insulation bonds, hand rotation, motor rotation, inspection of power leads, instrumentation wiring, and gallium level.

During this check-out, it was noted that when hand rotated some semi-solid material was being ejected from the beryllium and from one of the graphite electrodes. Since these electrodes would not be functioning electrically in the engineering test model, as much gallium as possible was removed from the electrodes to preclude any additional formation of this contamination.

Very small quantities of this semi-solid comtamination were observed in some of the other electrodes. It was decided that since the rate of formation of the material on the other electrodes was so small that the tests should be continued to determine whether the contamination formation continued or not. It was postulated that the material was probably an oxide of gallium in the tantalum, molybdenum and tungsten electrodes. It was also theorized that the reason for the large quantity of contamination in the beryllium electrodes was the result of a beryllium-gallium reaction. In the case of the graphite electrodes, it was theorized that the large volume of contamination was perhaps due to particles of graphite which had not been removed from the electrode cavity physically mixing with the gallium and gallium oxide.

In all the electrodes, the gallium level appeared unchanged. Upon a close examination, the top of the gallium appeared covered by a grey film similar to that previously observed on top of gallium in the test cells.

6.2 AIR TESTS

Air tests were the first actual operational tests of the engineering test model. The purpose of these tests was to verify the operational integrity of the unit so that its function would be known and verified prior to the vacuum tests. During the vacuum tests, it would be impossible to visually observe the operation of the unit. Accessibility would be poor since this would entail breaking the vacuum and removing the bell jar cover from the chamber. During vacuum tests, the only real information available from the engineering test model would be current, temperature and voltage readings from the electrodes together with voltage and position indications from the drive motor.

As part of the air tests, visual inspection, dielectric strength, application of current and rotation were performed. The visual inspection was a determination of the mechanical and electrical integrity of the ETM. The following items were checked: clearance, hand and motor rotation, leads, wiring, wire connections, gallium level, gallium leakage. Upon completion of the visual inspection, a dielectric test was run.

6.2.1 Dielectric Strength Test

In order to verify the electrical integrity of insulation system on the engineering test model, a dielectric strength test was run. No attempt was made to determine the ultimate dielectric breakdown voltage of the unit because of the concern that an electrical breakdown might cause permanent damage which would necessitate repair in order to be able to run any further electrical tests. The test procedure consisted of applying the test input voltage between input line and ground with a maximum current limitation set on the test instrument. The voltage was then increased in steps to a pre-determined maximum voltage and held at this voltage for two minutes; an AC voltage was used even though the engineering model is basically a DC device, an AC dielectric test being somewhat more severe than a DC test for the same peak voltage conditions. The dielectric tests were run in air at room temperature and humidity conditions with the engineering model mounted in the vacuum chamber but with the bell jar off.

Specifically, the AC voltage between line and ground was increased in 250 volt steps starting at 500 volts peak. The dielectric tester circuit breaker was set to trip at 20 microamps leakage current. It was decided that the upper limit of test voltage that would be applied to the

model would be 3000 volts peak and that the maximum allowable leakage current would be 20 microamps. The test was successfully run with the voltage on the unit taken up to 3000 volts peak and held there for two minutes with the leakage current less than 20 microamps. There did not appear to be any tendency to breakdown. The resistance to ground at 3000 volts is, therefore, at least 150×10^6 ohms.

6.2.2 Engineering Test Model Checkout

Current was applied to the engineering test model. Initially, a small current was applied to the ETM, approximately 10 amps, for a period of several hours. Electrode voltages, temperatures and the gallium level was monitored. Since the ETM appeared to be functioning properly at 10 amps, the current was subsequently increased in steps to 25, 50 and 100 amps. The current was held at the 25 and 50 amp level for about two hours and then at the 100 amp level for eight hours. No adverse effects were observed in the ETM.

With the engineering test model carrying current at the 100 amp level, the drive motor was energized. Motor rotation tests were run to determine the motor speed and to verify the limits of rotation in either direction. It was critical that the angular rotation of the drive motor be limited to approximately $\pm$ 2 revolutions from the center position so that the voltage sensor leads attached to the electrodes would not be sheared off. Motor rotation was limited to less than $\pm$ 2 revolutions by using a timer which reversed the polarity of motor at set intervals. This timer was set to reverse the rotation every 1½ hours.

Rotational tests were run for five days in air and with 100 amps electrode current. No additional contamination was observed being ejected from the electrodes and temperatures and voltages remained stable.

After the completion of the air tests, the ETM was visually examined to verify the electrical and mechanical integrity. No mechanical or electrical changes were noted. The gallium level was checked and the inter-electrode space was examined for contamination build-up. The gallium level in all electrodes did not change and no significant additional contamination build-up was observed in the electrode cavities.

6.3 VACUUM TESTS

Prior to running the long-term vacuum tests, a preliminary test was run in vacuum on the engineering test model. Figure 28 shows the functioning of the unit and its inaccessability when it was in the vacuum chamber. Any anomaly that might occur under these conditions could go undetected until the completion of the test and the removal of the bell jar. The ETM was mounted in the vacuum chamber, baked-out, and pumped down to approximately 10^{-6} torr for 24 hours. A current of 10 amps was applied to the slip rings, the drive motor was energized and the unit run for 5 days. During this period, the electrode resistance and temperature were monitored with no unusual or inconsistent results noted. At the completion of this preliminary test, the vacuum was broken, the bell jar removed and the ETM examined. There was no evidence of contamination being ejected from the electrodes and there did not appear to be any additional contamination on the surface of the gallium or in the electrode cavity. There was no change in the appearance of the contamination floating on the gallium. A slight leakage of gallium was noted on one electrode assembly, apparently occurring through one Delrin joint. This leakage was unexpected since there had been no evidence of gallium leakage throughout the entire previous history of assembly, checkout and air testing.

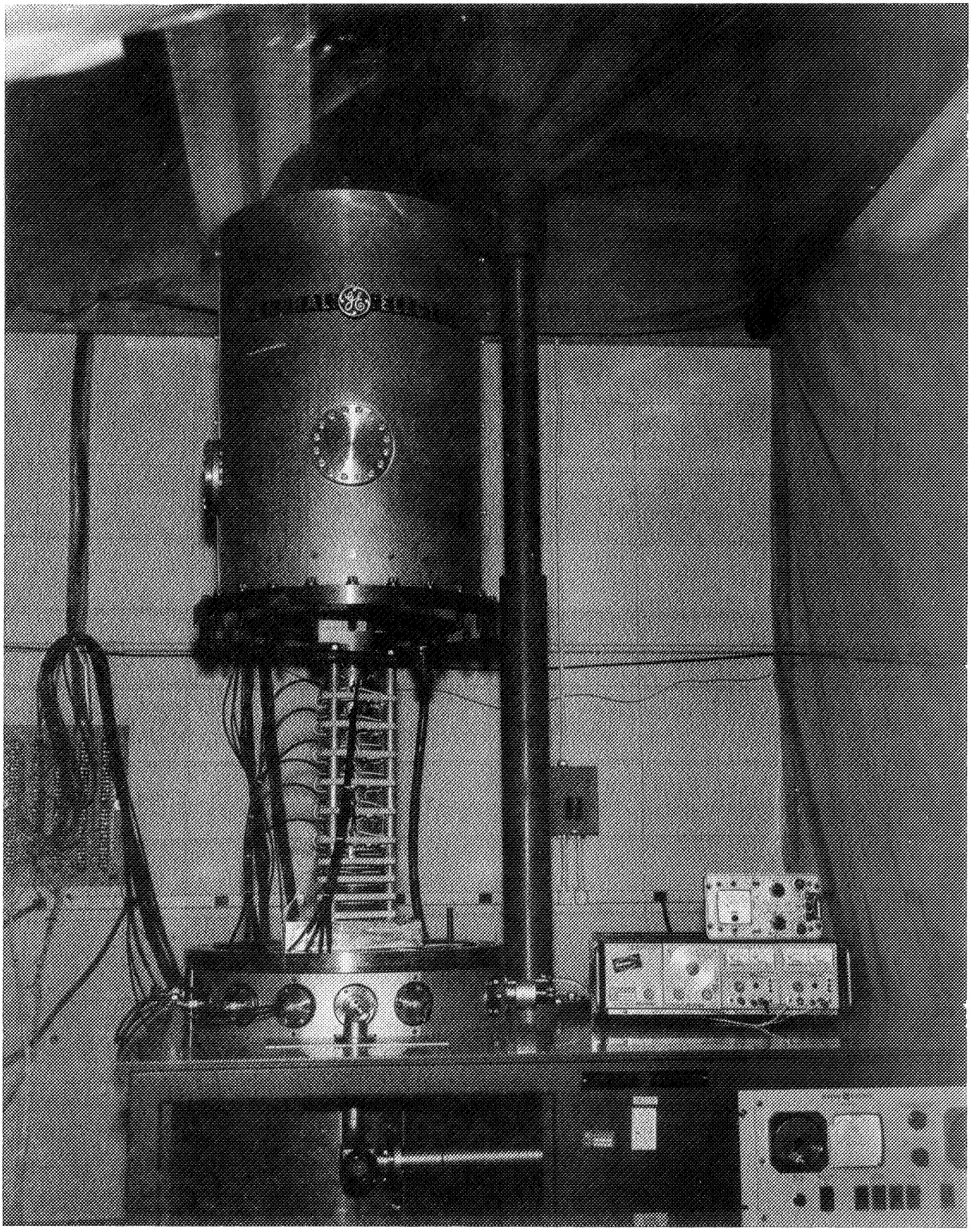

Figure 28. Engineering Test Model, Liquid Metal Slip Ring, Prior to Vacuum Test

There is no obvious explanation for this occurrence since the Delrin is non-wetted by gallium and the Delrin parts are bolted together minimizing the possible size of the joints. A possible explanation for this leakage is that since it occurred only under vacuum conditions, the gallium was forced out through the joint by outgassing due to the vacuum environment. In order to prevent the reoccurrence of the leakage, all joints on the bottom of the Delrin were sealed with RTV. A checkout was made by putting the test model under vacuum for two days. After this period under vacuum, the ETM was re-examined and there was no evidence of any gallium leakage.

After the completion of the preliminary vacuum tests, the long term vacuum tests were started. The initial vacuum runs were at 25 amps. This current level was maintained for five days so as to complete the outgassing of the engineering model and to monitor the temperature rise. After attaining a vacuum of 10^{-7} torr, the current was increased to 50 amps. Although the temperatures measured in the slip rings were not excessive, the maximum being $145^{o}F$, it was decided not to increase the magnitude of current any further. It was felt that it was of more importance to obtain data at 50 amps than to risk a possible failure at 100 amps before meaningful data could be obtained. Another consideration was that most of the losses and heating in the slip ring occurred in the power leads rather than in the electrodes or in the liquid metal. Therefore, tests at higher current levels would be a test of the leads and would not necessarily be significant from the standpoint of the engineering test model design concept. It was also deemed important to be able to run the engineering model for as long as possible to determine what happens to the gallium contamination under the conditions of high vacuum.

The test results of the vacuum tests are given in Table 14. The electrode resistance as measured in the slip ring is higher than that of the electrode assembly (see Table 13, Section 5.0). There is no apparent reason for this except that perhaps some of the gallium wetting the electrodes was inadvertently wiped off during the handling necessary to bond and bolt the electrodes to the Delrin insulation. It does not appear that the resistances were not measured accurately since there is a correlation between the high resistance and temperature. The tungsten rings which had the largest resistance had the highest temperature. The significant resistance in the engineering test model is the lead resistance. The terminal-to-terminal resistance is approximately 0.01 ohms while the total electrode to gallium slip ring resistance is probably less than 0.003 ohms of the total slip ring resistance, approximately one-half occurring in a single tungsten electrode; typical electrode resistance is approximately 0.0003 ohms.

The temperature rise of the engineering test model was quite small, about $10^{o}F$ at 25 amps and $40^{o}F$ at 50 amps. Extrapolating this data, the temperature rise at 100 amps would be $160^{o}F$, most of this temperature rise being the result of lead resistance.

The stability of the resistance and temperature over the period of testing was very good. There did not appear to be any consistent long term drift in either resistance or temperature that would indicate an increase of electrode resistance.

TABLE 14

TEST RESULTS VACUUM TESTS

Time	Current (amps)	Input Voltage (volts)	Resistance and Temperature						Base
			Tungsten Electrodes		Molybdenum Electrodes		Tantalum Electrodes		
			#1	#2	#1	#2	#1	#2	
Initial run	25	.234	.00052 Ω 95°F	.00041 Ω 95°F	* 90°F	.000124 Ω 90°F	.000116 Ω 90°F	.000328 Ω 90°F	-- 90°F
Final (+5 days)	25	.229	.00054 Ω 90°F	.0004 Ω 90°F	* 90°F	.000232 Ω 90°F	.000112 Ω 90°F	.000324 Ω 90°F	90°F
Initial run	50	.522	.00064 Ω 142°F	.00041 Ω 135°F	* 125°F	.00017 Ω 125°F	.000156 Ω 125°F	.000340 Ω 125°F	125°F
+ 3 Weeks	50	.504	.00078 Ω 145°F	.00041 Ω 135°F	* 125°F	* 125°F	.000148 Ω 125°F	.000334 Ω 125°F	125°F
+ 6 Weeks	50	.486	.00092 Ω 140°F	.000394 Ω 130°F	* 125°F	* 125°F	.000142 Ω 125°F	.000350 Ω 125°F	125°F

* INSTRUMENTATION LOST, OPEN CIRCUIT.

6.4 POST-TEST EXAMINATION

After the completion of the long-term vacuum tests, a post-test evaluation was made of the engineering test model. The bell jar was removed and the ETM was examined for mechanical and electrical integrity and to determine whether there was any physical degradation as a result of operation. There was no observable evidence of deterioration mechanically, electrically, or structurally, except for one molybdenum electrode which appeared to have the gallium wiped off as if there were mechanical rubbing (see Figure 29). This electrode had been completely wetted, both inside and outside, prior to assembly. Although the outside appeared to have the gallium wiped off, the inside diameter was still completely wetted. There were certain significant changes in the gallium. Figure 30 shows the electrode cavity of tantalum electrode #1; a mottled grey contamination on the gallium can be observed.

Although not electrically energized, there was evidence of externally ejected contamination from the beryllium electrodes, this contamination being grey in color. The gallium in the other electrodes had contamination floating on it. Regardless of electrode material, tungsten, tantalum, or molybdenum, the contaminant had the same appearance; light and darker grey floating contamination with some particles of very dark grey material (see Figure 31). There was no evidence of gallium leakage or spillage. There also was no evidence of any of the gallium having been vaporized or condensing anywhere. After the post-test examination, a gallium surface contamination study was conducted.

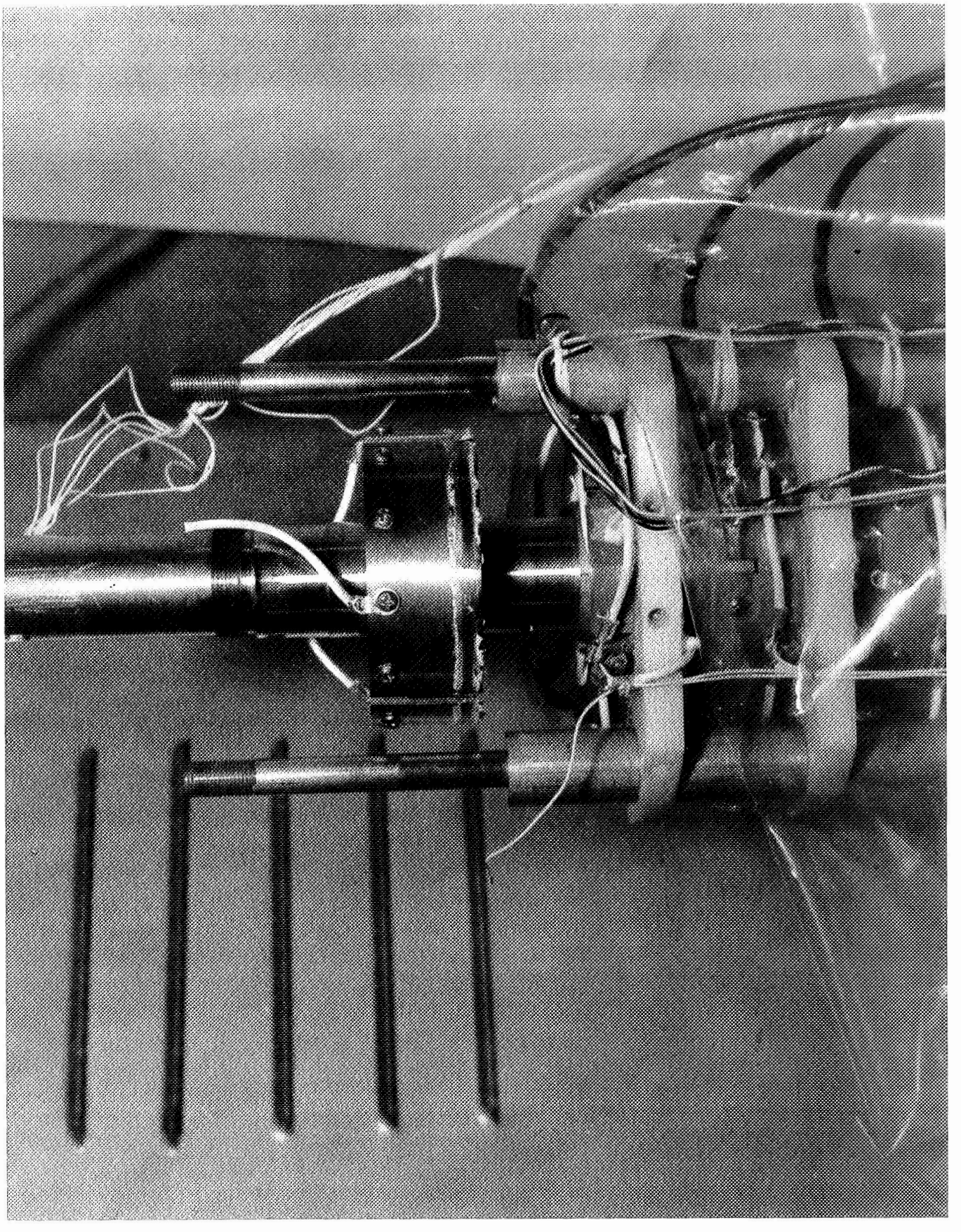

Figure 29. Molybdenum Electrode

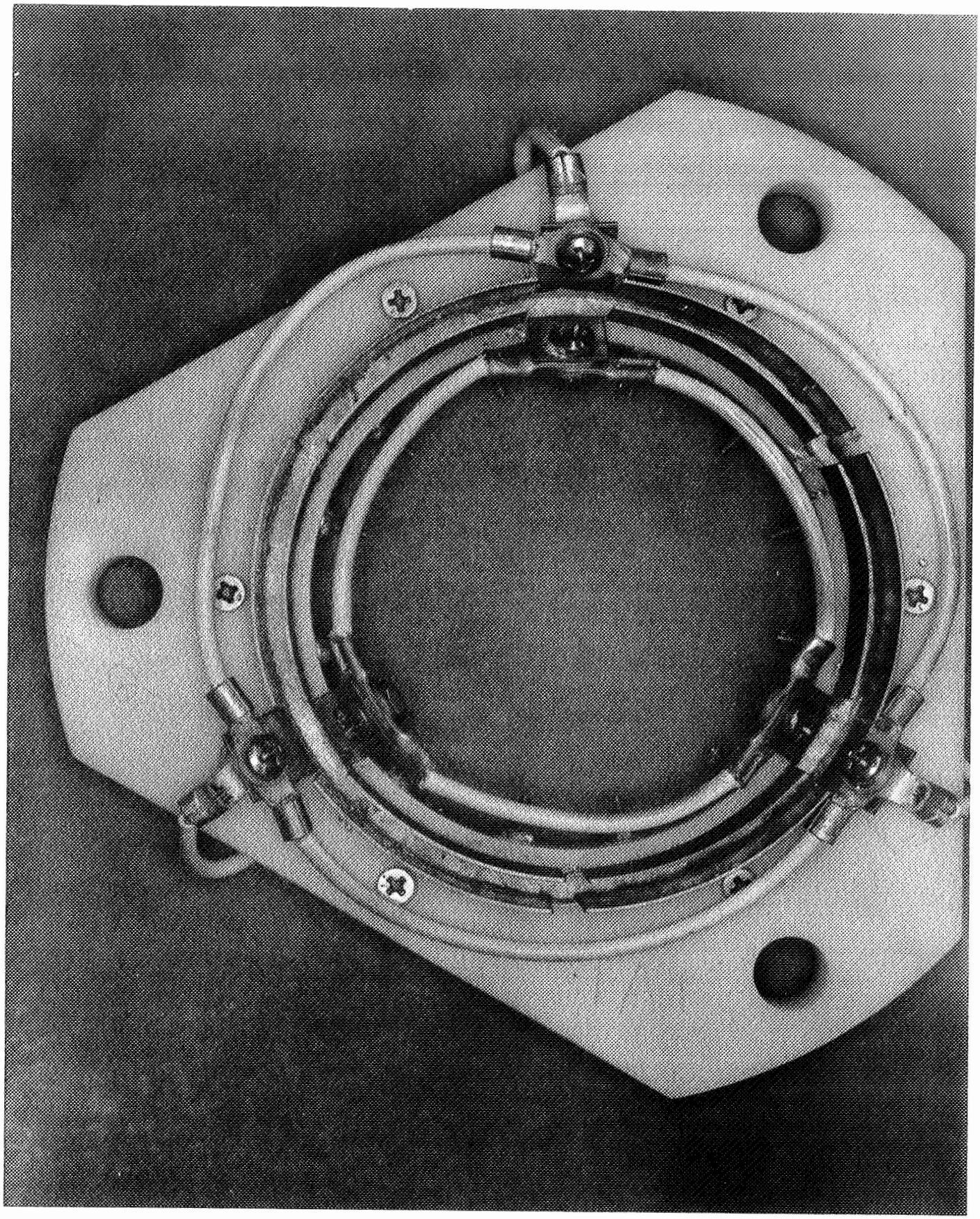

Figure 30. Tantalum Electrode

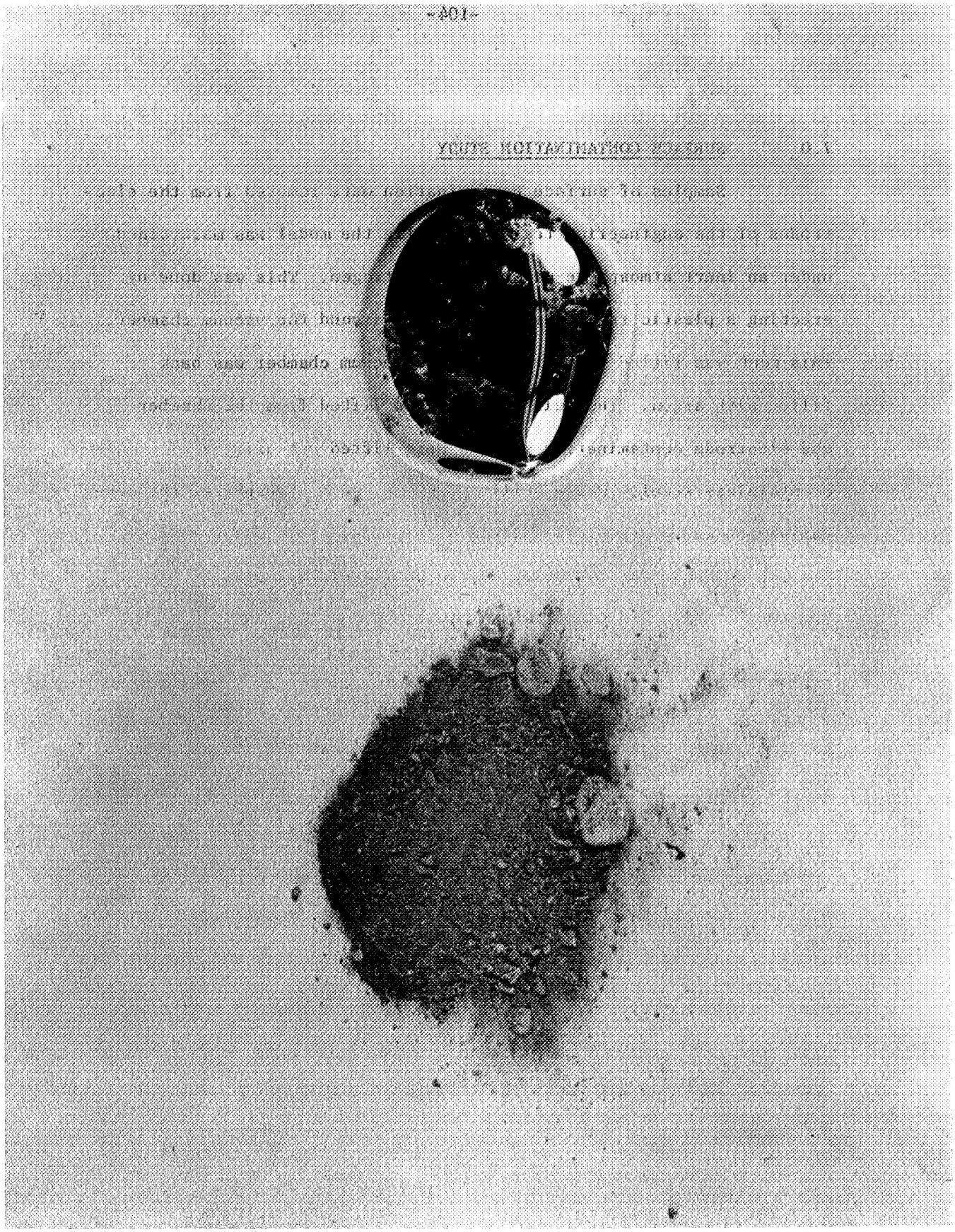

Figure 31. **Gallium Contamination**; Dark Grey **Contamination from Bottom of Tantalum** Electrode #1 (on left). On right, **Gallium from** Electrode.

7.0 SURFACE CONTAMINATION STUDY

Samples of surface contamination were removed from the electrodes of the engineering test model while the model was maintained under an inert atmosphere of argon and nitrogen. This was done by erecting a plastic tent having hand ports around the vacuum chamber. This tent was filled with argon and the vacuum chamber was back filled with argon. The bell jar was then lifted from the chamber and electrode contamination samples were lifted out using a wire loop of stainless steel. While still under the inert atmosphere, the contamination was placed into individual bottles. This was done to prevent oxidation or hydration of the sample contaminants by the atmosphere after the vacuum environment.

Emission spectroscopy was initially performed on the contamination from the molybdenum electrode cavity, electrode #4. Then, emission tests were run on the contamination from all the electrodes. The results of these tests are given in Table 15. From the results of the emission tests, there are very strong indications that the electrode materials have not passed into solution and absorbed by the gallium. The only indication of electrode material in the contamination is a trace of molybdenum in the gallium from molybdenum electrode #3. Traces of other elements were recorded; these included copper, the strongest, aluminum, iron, magnesium, manganese, and silicon. It is believed that contamination by these materials took place during either the fabrication or assembly cycle.

X-ray diffraction tests were run on a number of samples in order to determine the presence of oxides, hydrated oxides, or hydroxides of gallium. The results of the diffraction tests are given in Table 16.

TABLE 15

EMISSION TESTS ON CONTAMINATION

Emission Spectroscopy

A. Contamination from molybdenum electrode cavity, electrode #4

Strong indication - Ga
Trace indications - Sn, Cu, Mo, Al, Fe, Mg, Mn, Si

B. Contamination from all electrodes

Electrode No.	Electrode Material	Elements Present							
		Ga	Cu	Al	Fe	Mg	Mn	Si	Other
1	Ta	S	M	T	T	T	T	T	--
2	Ta	S	M	T	T	T	T	T	--
3	Mo	S	M	T	T	T	T	M	Mo
4	Mo	--- Insufficient Sample ----------							
5	W	S	M	T	T	T	T	T	--
6	W	S	M	T	T	T	T	M	Ca
99.9999% Ga	--	S	T	--	--	--	--	--	--

S = Strong Indication
M = Moderate Indication
T = Trace Indication
-- = No Indication

TABLE 16

EMISSION TEST RESULTS

Sample	Results
A. Air-exposed gallium	Amorphous
B. Contamination from tungsten electrode cavity	Amorphous
C. Contamination from tantalum electrode cavity (dark grey powder)	Amorphous

All samples show a diffraction pattern indicative of amorphous materials. In order to obtain diffraction patterns, it is necessary to have a crystal at least 100 angstroms in size. Since the surface oxidation of gallium has been estimated to be about 10 angstroms thick, it is likely that the oxide crystal in the ETM is less than 100 angstroms.

Gallium oxide, Ga_2O_3, displays two characteristic absorption bands in the infrared region, a moderate absorption at 13.5 microns and a high absorption at 14.35 microns. An infrared absorption test was run in order to determine the presence of gallium oxide. This was done first by mixing some air-exposed gallium contamination with potassium bromide to make a pellet for exposure to the infrared. Potassium bromide is used as a standard matrix because of its transparency to infrared. When the gallium contaminant was mixed with the KBr, even in successively smaller concentrations, the resulting pellet darkened and was completely opaque to infrared. It is theorized that there may have been a reaction between the bromine and gallium in the pellet which caused the darkening. Another approach was taken by spreading the contamination on the surface of a salt crystal. The infrared test showed no absorption up to approximately 16 microns wavelength. There was no indication of absorption at the 13.5 and 14.35 micron wavelength which would be an indication of Ga_2O_3.

The engineering test model was partially disassembled for examination. The contamination of all electrodes consisted of a floating portion which had a mottled appearance, being light and darker grey in color, and was quite thin being of gossamer thickness. Three electrodes were disassembled. There was no evidence of gallium attack and they were all well wetted. A contamination was observed at the bottom of the electrode cavity apparently adhering very slightly to the Delrin insulation. This contamination was very dark grey in color and powdery in appearance.

The powder was examined microscopically and found to consist of very small droplets of gallium covered with a dark grey powder. The sample appeared to be mostly gallium, perhaps 95% to 99% by volume, with only a small amount of the dark grey powder covering it. The sample was centrifuged in an attempt to separate the powder from the gallium. This was not successful, indicating that the density of the powder and gallium probably were identical. X-ray diffraction was performed on the powder. The diffraction pattern indicated an amorphous structure to the powder.

Emission tests were run on the floating contamination (dross), the powder and gallium from the electrode, and as a control, pure gallium. The results were as follows:

	Ga	Cu	Mo	Al	Sn	Fe	Mg	Mn	Si	Other (Trace)
Powder	X	T	T	T	T	T	T	T	T	In, W (?)
Dross	X	T	T	T	T	T	T	T	T	Ni, Ag, K (?)
Gallium	X	M	-	M	T	-	T	-	-	-
Pure Gallium (99.9999%)	X	T	-	T	-	-	T	-	-	-

X = Strong Indication
M = Moderate Indication
T = Trace Indication
- = No Indication

Because of the difficulty being experienced in identifying the contamination by x-ray diffraction, it was decided to run a gravimetric thermal analysis (GTA), and if this was successful, a differential thermal analysis (DTA). A gravimetric thermal analysis is a means of determining water of hydration and differential thermal analysis determines change of state. In the GTA, a sample of the unknown is heated slowly at a fixed rate to about 1200°C. During this heating, the weight and temperature of the unknown are continuously monitored. When the sample loses the water of hydration, there will be accompanying weight change. By knowing the weight change and the temperature at which it takes place, the composition of the unknown can be determined by either comparison with a known or from published data. In the DTA, the unknown is subjected to a constant heat input and the temperature monitored continuously. A change in state of the sample will be accompanied by an endothermic or exothermic reaction which will be determined by a relatively sudden temperature change. The composition of the sample can then be found by the comparison with a known or from published data.

A GTA was performed on the floating portion of the contaminant to determine if it was a hydrated form of an oxide of gallium (see Figure 32). A weight change was observed at 750°C. However, after disassembly and examination of the GTA test equipment, there appeared to be some attack by some gallium in the contaminant upon the wire holding the test sample. Upon further analysis, it was decided that because of the highly reactive nature of gallium at elevated temperatures and the relatively small percentage quantity of oxide in the sample, that it would be difficult to obtain meaningful data within the constraints of the program direction. Similarly, a DTA, although feasible to run, would be extremely difficult to implement because of the reactive characteristics of the gallium.

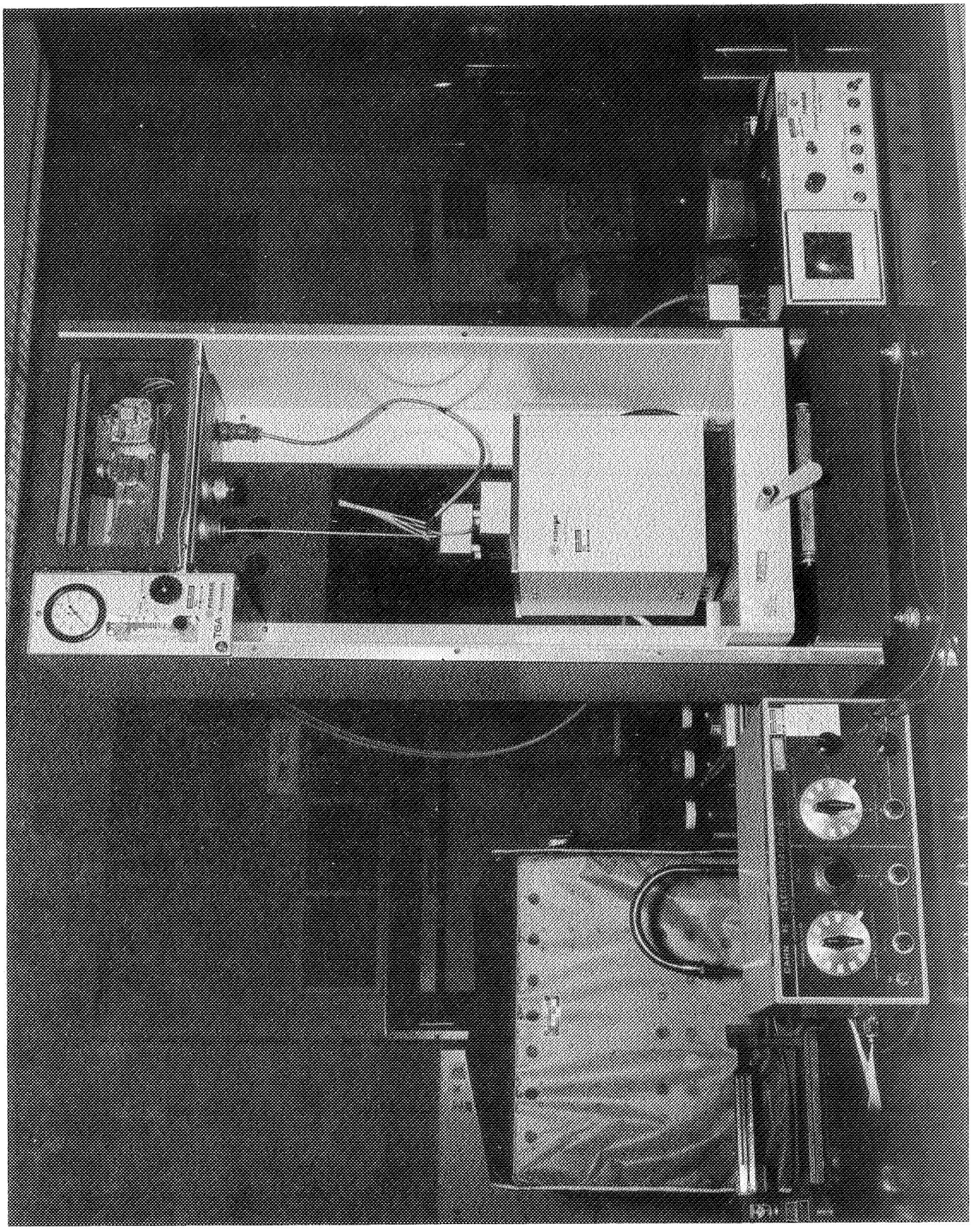

Figure 32. Gravimetric Thermal Analysis Apparatus

True determination of the composition of the gallium contamination by literature search, analysis or by test is not amenable to easy solution. The chemistry of gallium has not been widely studied, especially from an engineering point of view, and the simple determination of the presence of oxygen compounds is difficult to achieve.

In order to obtain qualitative effects of water vapor and oxygen on gallium, a bubbling test was set up and run in which dry and saturated air and nitrogen was passed through a column of gallium. The gas flow rate was at the rate of approximately 2 cubic feet per hour and the test was run for a period of one month for the nitrogen and two weeks for the air (see Figure 33).

During the test, nothing was observed occurring in the gallium columns having the dry and saturated air and the dry nitrogen passing through them. However, the gallium having the saturated nitrogen bubbled through it appeared to contain both a very dark grey contamination and a very light grey or even white contamination. Upon completion of the tests, the gallium was removed from the tubes and visually examined. The appearance of the contamination was as follows:

Gas	Appearance of Contamination
Dry air	Light grey
Wet air	Light grey
Dry nitrogen	Light grey and dark grey
Wet nitrogen	Light grey and very dark grey white contamination on tube

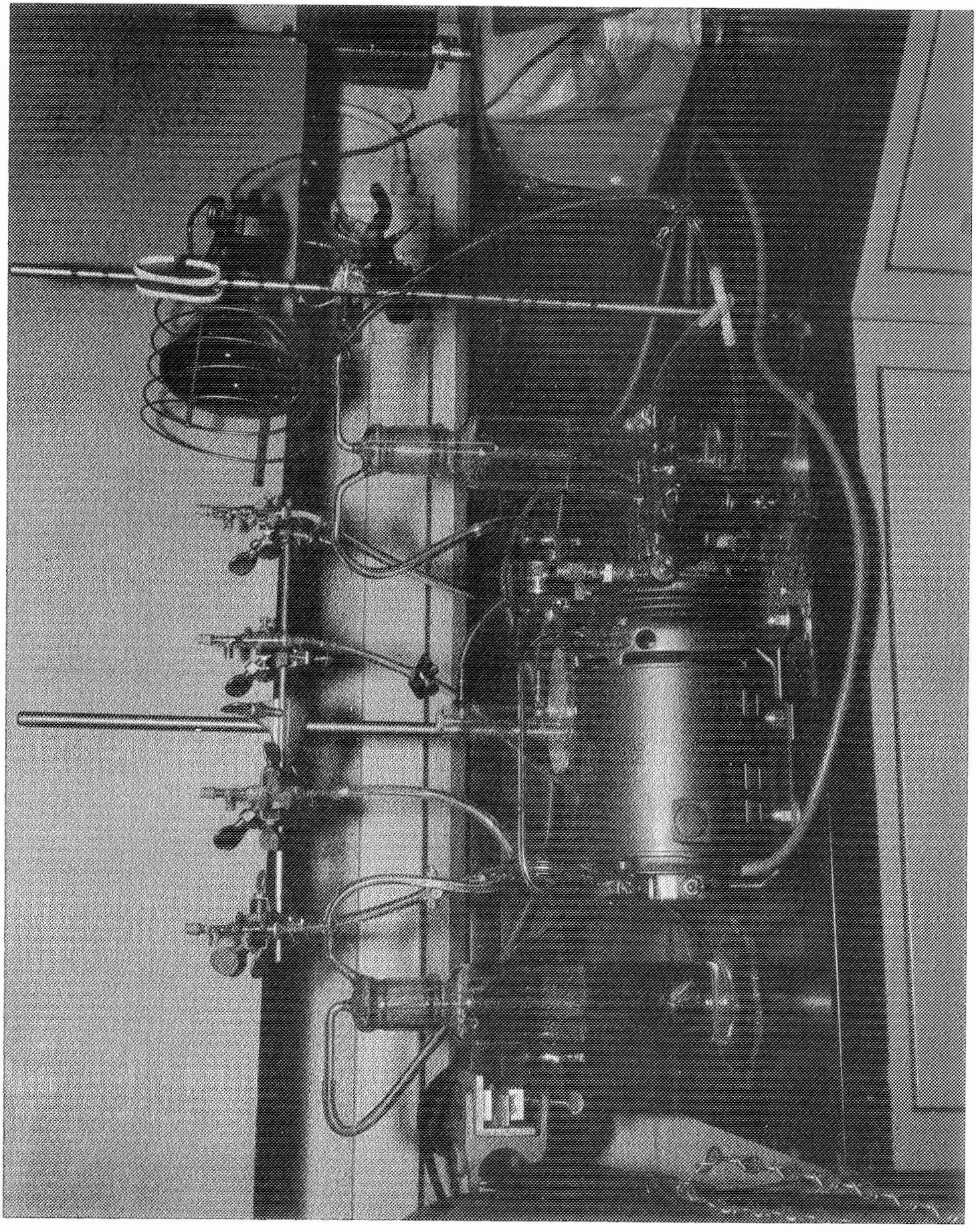

Figure 33. Bubbling Test

8.0 CONCLUDING REMARKS

Based on the work done on this program, the following can be stated:

(1) Tungsten, tantalum, and molybdenum having surface oxides removed are compatible with gallium and are satisfactory for use in a liquid metal slip ring. Graphite has too high an electrical resistance to have general application.

(2) Delrin and Teflon are compatible with gallium.

(3) A liquid metal slip ring capable of carrying 100 amps at 3000 volts in a vacuum is feasible.

(4) Further studies must be undertaken to determine the composition and to control gallium contamination.

REFERENCES

1. Solubility of Non-Electrolytes, Hildebrand and Scott.

2. Liquid Metals Handbook.

3. (a) Gallium (Reprinted from Journal of Chemical Education, Vol. 29, p. 162, 1952), ALCOA.

   (b) Gallium and Gallium Compounds, 1963 ALCOA Publication.

4. Zelikman, A. N., Krein, O. E., and Samsonov, G. V., Metallurgy of Rare Metals, available from U.S. Department of Commerce, Clearinghouse for Federal Scientific and Technical Information, Springfield, Va. 22151.

5. Properties of Gallium, ANL 4109, W. D. Wilkinson, Argonne National Laboratory.

6. Proceedings of the NASA-AEC Liquid-Metals Corrosion Meeting Vol. I and II, NASA SP-41 and 42.

7. Epstein, L. F., "Notes on Liquid Metal Studies in France and Great Britain."

8. Stang, J. H., et al, Compatibility of Liquid and Vapor Alkali Metals with Construction Materials, DMIC Report 227, April 15, 1966, Battelle Memorial Institute.

9. Wilkinson, W. D., Effects of Gallium on Materials at Elevated Temperatures, Argonne National Laboratory, Aug. 1953.

10. Murphy, H. J., Physical Properties of Gallium, Department of Physics, John Carroll University, Cleveland, Ohio, Dec. 15, 1959.

11. Edwards, R. K. and Wahlbeck, P. G., Chemical Thermodynamics of Materials at High Temperatures, Illinois Institute of Technology, June 30, 1961.

12. Kuczkowdki, T. J. and Buckley, D. H., Friction and Wear of Low-Melting Binary and Ternary Gallium Alloy Films in Argon and in Vacuum, NASA TN D-2721, March 1965.

13. Speiser, R. and Johnston, H. L., Vapor Pressures of Inorganic Substances XI Gallium, Ohio State University, 4 December 1952.

14. Finniston, H. M. and Howe, J. P., Metallurgy and Fuels, Vol. 2, Series V in Progress in Nuclear Energy, Pergamon Press 1959.

15. Compatibility of Liquid and Vapor Alkali Metals with Construction Materials, DMIC Report 227, April 1966.

16. Grosse, A. V., "The Relationship Between the Surface Tensions and Energies of Liquid Metals and their Critical Temperatures," Journal of Inorganic and Nuclear Chemistry, 1962, Vol. 24, pp. 147 to 156.

17. Jackson, D. A., The Accelerated Corrosion of Metals, AD-237775, Virginia Institute for Scientific Research.

18. Mayer, S. W., "Calculation of Metal Surface Tensions, Ionic-Salt and Monatomic Methods for Liquid Metals," Journal of Chemical Physics 35, 1513-14 (Oct. 1961).

19. Physical Chemistry of Metallic Solutions and Intermetallic Compounds Symposium, Vol. 1, Chemical Publishing Co., Inc., 1960.

20. Electrons, Atoms, Metals and Alloys, William Hume-Rothery.

21. Current Collectors - Liquid Metals, General Electric TIS Report DG 62SL103, 1962, J. F. Quinlan, Schenectady, N. Y.

22. NASA AEC Liquid Metals Corrosion Meeting, TID 7626, Brookhaven National Laboratory, Dec. 1961.

23. Compatibility of Liquid Cesium with Containment Materials, Report P62-26, Flight Propulsion Department, General Electric, Cincinnati.

24. Evaluation of a High Strength Columbium Alloy for Alkali Metal Containment, NASA Contract 3-2140 (1962), General Electric, Flight Propulsion Dept., Cincinnati.

25. Solubility of Refractory Metals and Alloys in Potassium and Lithium, NASA CR 1371, May 1969, R. L. Eichelberger, R.L. McKisson, B.G. Johnson.

26. An Exploratory Study of Refractory Alloy Corrosion in Sodium and Potassium, General Electric DM 60-224 (60 ADM-3).

27. The Encyclopedia of the Chemical Elements, Clifford A. Hampel, P223, 1968, Reinhold.

28. de In Breteque, Gallium Proprietes Principales Bibliographie, Pour l'Industrie de L'Aluminum a Marseille, Marseille - June 1962.

    This is a bibliography of articles on Gallium, primarily European. It includes tables of properties. It has been supplemented each year through September 1968, and is available in this country from:

    Alusuisse Metals, Inc.
    2460 Lemoine Avenue
    Fort Lee, New Jersey 07024

29. Brennecke, M. W., Gallium Bibliography 1950-1959, Alcoa Research Laboratories, New Kensington, Pa.

DISTRIBUTION LIST

National Aeronautics & Space Administration
Headquarters
Washington, D. C. 20546

Attention:	SA/L. Jaffe	1 Copy
	SAC/A.M.G. Andrus	10 Copies
	SC/R. B. Marsten	1 Copy
	RN/W. H. Woodward	1 Copy

NASA Lewis Research Center
21000 Brookpark Road
Cleveland, Ohio 44135

Attention:	S. C. Himmel (M.S. 3-3)	1 Copy
	C. C. Conger (M. S. 54-1)	1 Copy
	R. E. Alexovich (M. S. 54-5)	1 Copy
	Technology Utilization Officer (M.S. 3-19)	1 Copy
	Library (M.S. 60-3)	2 Copies
	Report Control Office (M.S. 5-5)	1 Copy
	N. T. Musial (M.S. 501-3)	1 Copy
	R. R. Lovell (M.S. 54-5)	50 Copies
	Spacecraft & Support Proc. Section (M.S.500-110)	1 Copy
	J. S. Przybyszewski (M.S. 23-2)	1 Copy
	A. F. Forestieri (M.S. 302-1)	1 Copy

NASA George C. Marshall Space Flight Center
Huntsville, Alabama 35812

Attention:	Library	1 Copy

NASA Goddard Space Flight Center
Greenbelt, Maryland 20771

Attention:	Library	1 Copy

NASA Ames Research Center
Moffett Field, California 94035

Attention:	Library	1 Copy

NASA Langley Research Center
Langley Station
Hampton, Virginia 23365

Attention:	Library (M.S. 185)	1 Copy

NASA Manned Spacecraft Center
Houston, Texas 7001

Attention:		
	Library	1 Copy
	F. E. Eastman (EB8)	3 Copies
	C. Robinson (EP52)	1 Copy

Jet Propulsion Laboratory
4800 Oak Grove Drive
Pasadena, California 91103

Attention:		
	Library	1 Copy
	W. Hasbach	1 Copy

NASA Scientific and Technical Information Facility
Box 7500
Bethesda, Maryland 20740

Attention:	NASA Representative	3 Copies

General Dynamics, Convair Division
P. O. Box 1128
San Diego, California 92112

Attention:	F. J. Dore/Advanced Programs Lab.	1 Copy

Air Force - Aero Propulsion Laboratory
Wright-Patterson Air Force Base
Ohio 45433

Attention:	L. D. Massie (APIP-2)	1 Copy

Hughes Aircraft Company
Space Systems Division
Los Angeles, California 90009

Attention:	R. B. Clark	3 Copies

Federal Communications Commission
521 Twelfth Street
Washington, D. C. 20554

Attention:	M. Fine	1 Copy

U. S. Information Agency
25M St. S.W.
Washington, D. C. 20547

Attention:	IBS/EF/G. Jacobs	1 Copy

Naval Electronic Systems Command
PME 116
Washington, D. C.

Attention: Lt. Commander L. Wardel — 1 Copy

McDonnell Douglas Corporation
5301 Bolsa
Huntington Beach, California 92647

Attention: J. Chester (A-3-BBDO-830) — 2 Copies

Poly Scientific Division
Litton Industries
1111 N. Main Street
Blacksburg, Virginia 24060

Attention: W. O'Brian — 2 Copies

Spar Aerospace Products
825 Caladonia Road
Toronto, Ontario 315
Canada

Attention: T. Usher — 2 Copies